DISS. ETH NO. 27249

DIRECT AND INDIRECT HARNESSING OF CYTOTOXIC CD8+ T LYMPHOCYTES FOR CANCER THERAPY: ADOPTIVE CELL THERAPY VERSUS IMMUNOCYTOKINES

A thesis submitted to attain the degree of

DOCTOR OF SCIENCES of ETH ZURICH

(Dr. sc. ETH Zurich)

Presented by

Marco Stringhini

MSc ETH Pharmaceutical Sciences, ETH Zürich

Born on 11.03.1990

Citizen of Caslano (TI)

Accepted on the recommendation of

Prof. Dr. Dario Neri, examiner

Prof. Dr. Cornelia Halin-Winter, co-examiner

Dedicato a mio nonno, Franco.
Mi ha chiamato “dottore” per una vita.

Table of contents

1 Summary

The birth of immunotherapy dates back to the beginning of the twentieth century, when an American surgeon named William Coley started to treat cancer patients with inactivated bacteria to stimulate the "body's defense mechanism". Today we call this mechanism "immune system", and strategies to activate it and get it to fight cancer "immunotherapies".

The development of immunotherapy started off slowly. However, advances in research techniques and growing knowledge about the immune system allowed to start understanding the complex interactions between the tumor and the immune cells and to come up with more and more approaches to stimulate an anti-tumor immune reaction. To date, immune-checkpoint inhibitors and adoptive cell therapies (ACTs) constitute the backbone of immunotherapy. The firsts are therapeutic agents, which release the power of tumor-infiltrating cytotoxic T cells by blocking inhibitory signals directed to them. The seconds are treatments involving living lymphocytes, which are isolated from a patient, boosted in the laboratory, and then re-infused into the same patient. Together these strategies have contributed to improving therapeutic outcomes in patients with metastatic melanoma, various hematological malignancies, and in a subgroup of patients with other solid epithelial cancers.

According to the American Cancer Society, one out of 2-3 Americans will develop invasive cancer during their lifetime and about 30% of them will die in the five years following diagnosis. Despite advances in treatments and early diagnosis have resulted in a dramatic improvement since the early 1960s, when average 5-year survival rates were around 30-40%, cancer still accounts for about 600000 deaths every year in the United States alone, which highlights the need for new treatment modalities.

Current immunotherapy with immune-checkpoint inhibitors generally fails in patients with "cold" tumors characterized by low CD8+ T cell infiltration. The cytokine LIGHT, when overexpressed in the tumor, has been shown to mediate a massive CD8+ T cell infiltration followed by tumor clearance in different murine models of cancer and may represent an ideal candidate to turn "cold" tumors into "hot". To avoid systemic exposure and related toxicity, typical of cytokines, various methods to selectively deliver LIGHT into the tumor have been investigated in animal models. We decided to work on a novel antibody-LIGHT fusion protein

to target LIGHT to the tumor extracellular matrix. To do that we employed the antibody F8, specific to the extra domain A of Fibronectin, an antigen expressed in the majority of tumors in both humans and mice but absent in normal healthy tissues. After obtaining a functional fusion protein, we tested its activity in two syngeneic murine models of cancer. F8-LIGHT was able to delay tumor progression, however, analysis of the tumor immune infiltrate suggested that Natural Killer cells (NK cells), and not CD8+ T cells, were responsible for the anti-tumor activity.

Most cancer-related deaths are caused by solid epithelial cancers, against which current immunotherapies struggle to demonstrate consistent activity. For tumors, which fail to respond to immune-checkpoint blockade, ACT with tumor-infiltrating lymphocytes may represent the most promising treatment option. This approach has shown remarkable response rates in patients with melanoma during the last thirty years. Recently, thanks to the introduction of new procedures for the selection of tumor neoantigen-specific T cells, it has been employed with success also in other solid tumors. Treatment with neoantigen-specific enriched T cells has so far lead to durable complete responses only in a handful of cases, but neoantigen-specific, tumor infiltrating T cells can be identified in most patients with epithelial cancers. Unfortunately, these cells are extremely rare, and expanding them ex vivo to a sufficient number is not trivial. Implementing this type of treatment may be the key to reducing death rates in these difficult-to-treat tumors.

In an attempt to demonstrate that a pure population of CD8+ T cells specific to the rejection antigen AH1 (derived from an endogenous retroviral protein expressed in several murine tumors but not in healthy organs) could mediate complete tumor rejections in mice, we indirectly come across issues related to dealing with rare tumor-specific T cells. We developed a reproducible protocol for the selective expansion of AH1-specific CD8+ T cells both from tumors and from secondary lymphoid organs, which may represent an alternative source of tumor-specific T cells. We were able to achieve 100-500-fold expansions starting from a low number of cells (i.e. down to few thousands), with purities consistently closer to 100%. Expanded T cells were highly cytotoxic *in vitro*, caused moderate tumor growth retardation when administered to tumor-bearing immunocompetent mice, but failed to induce tumor regression, due to their poor engraftment ability. With this work, we confirmed that methods for improving fitness and *in vivo* persistence of these extensively expanded T cells are needed and should be the focus of future research.

2 Riassunto

La nascita dell'immunoterapia si può far risalire ai primi anni del novecento, quando un chirurgo americano, tale William Coley, cominciò a trattare pazienti malati di cancro con estratti di batteri inattivati, con l'intento di stimolare un cosiddetto "meccanismo di difesa del corpo". Oggigiorno tale meccanismo viene chiamato "sistema immunitario" e con il termine "immunoterapia" si intende l'insieme di strategie usate per attivarlo.

Lo sviluppo dell'immunoterapia è stato un processo inizialmente lento. Tuttavia, nuove tecniche di ricerca e una crescente conoscenza del sistema immunitario hanno permesso di cominciare a capire le complesse interazioni tra cellule del sistema immunitario e cellule tumorali, e hanno portato allo sviluppo di diversi approcci atti a stimolare una reazione immunitaria contro il tumore. Oggi, due tipi di trattamento rappresentano la spina dorsale dell'immunoterapia: gli inibitori dei checkpoint immunitari e le terapie cellulari adottive.
I primi sono agenti terapeutici che, bloccando determinati segnali inibitori diretti ai linfociti T citotossici presenti nel tumore, ne rilasciano il potenziale. Le terapie cellulari adottive, invece, prevedono l'uso di linfociti viventi, che dopo essere stati isolati dal paziente, vengono potenziati in laboratorio e successivamente re-infusi nel paziente stesso. Collettivamente questi due approcci hanno contributo a migliorare il successo terapeutico in pazienti con melanoma metastatico, varie malignità ematologiche, e in un ristretto gruppo di pazienti con altri tumori epiteliali.

Malgrado ciò, secondo i dati riportati dall' "American Cancer Society", un americano su due sarà colpito da un tumore invasivo durante l'arco della sua vita e circa un terzo dei pazienti colpiti soccomberà al tumore nei primi cinque anni dopo la diagnosi. Nonostante ci siano stati miglioramenti sostanziali grazie a nuovi trattamenti e diagnosi precoci (basti pensare che nei primi anni '60 la speranza di vita a 5 anni dalla diagnosi si aggirava attorno al 30-40%), tutt'oggi, solo negli Stati Uniti, attorno a 600000 morti all'anno vengono attribuite al cancro. Persiste pertanto il bisogno di sviluppare trattamenti più efficaci.

L'impiego di inibitori di checkpoint immunitari non è generalmente efficace in tumori definiti "freddi", ovvero con poca infiltrazione di linfociti T CD8-positivi. È stato dimostrato da studi in diversi modelli tumorali pre-clinici, che la sovra espressione della citochina LIGHT nel tumore porta ad una infiltrazione massiva di linfociti T CD8-positivi, e all'eliminazione del

tumore. La citochina LIGHT, pertanto, potrebbe rappresentare un candidato promettente per trasformare un tumore "freddo" in uno infiammato. Per evitare un'esposizione sistemica alla citochina, che generalmente causa tossicità, vari metodi sono stati studiati in laboratorio, che permettano di far accumulare la citochina LIGHT selettivamente nel tumore. Noi abbiamo deciso di provare a legare LIGHT ad un anticorpo monoclonale in grado di portare la citochina nella matrice extracellulare del tumore. Per fare ciò, ci siamo serviti dell'anticorpo F8, specifico per il dominio-extra A della proteina Fibronectina, un antigene espresso nella maggior parte dei tumori sia nel topo che nell'uomo, ma non negli organi sani. Dopo aver ottenuto una proteina ricombinante funzionale, ne abbiamo testato l'attività in due diversi modelli tumorali murini. F8-LIGHT era in grado di ritardare la progressione del tumore. Tuttavia, come suggerito da un'analisi delle cellule del sistema immunitario presenti nel tumore dopo il trattamento, questa attività sembrava essere dovuta all'azione di cellule natural killer, e non di linfociti T citotossici come ci saremmo aspettati.

La maggior parte delle morti in pazienti oncologici sono da attribuire a tumori epiteliali solidi, contro i quali le attuali immunoterapie faticano a dimostrare un'efficacia riproducibile. Nel caso di tumori che non rispondono al trattamento con inibitori dei checkpoint immunitari, l'alternativa più promettente è probabilmente l'impiego di linfociti T isolati dal tumore come terapia cellulare adottiva. Questo approccio negli ultimi 30 anni ha portato a tassi di risposte rimarchevoli in pazienti affetti da melanoma. Recentemente, grazie all'introduzione di nuove procedure per selezionare linfociti T specifici contro neo-antigeni tumorali, è stato usato con successo anche in altri tumori solidi. Il trattamento con linfociti T specifici contro neo-antigeni tumorali ha indotto risposte complete solamente in pochi casi isolati fino ad ora. Nonostante ciò, linfociti T reattivi contro neo-antigeni tumorali possono essere identificati con successo nella maggior parte dei pazienti con tumori epiteliali. Sfortunatamente queste cellule sono estremamente rare ed espanderle in laboratorio per raggiungere una dose terapeutica non è scontato. Un implemento di questo approccio potrebbe comunque rappresentare una svolta nel ridurre il tasso di mortalità in tumori difficili da trattare come i tumori epiteliali.

Nel tentativo di dimostrare che una popolazione formata esclusivamente da linfociti T CD8-positivi specifici contro l'antigene di rigetto AH1 (un peptide derivante da una proteina retrovirale endogena nel topo, espressa in vari modelli tumorali, ma assente in organi sani), potesse curare determinati tumori nel topo, ci siamo indirettamente imbattuti nelle difficoltà di aver a che fare con popolazioni rare di linfociti specifici contro il tumore. Abbiamo sviluppato

un protocollo per l'espansione selettiva di linfociti T CD8-positivi specifici per AH1, ottenuti sia dal tumore, che da organi linfoidi secondari, i quali potrebbero rappresentare una fonte alternative di linfociti T specifici contro il tumore. Partendo da numeri di cellule T nell'ordine di migliaia fino a centinaia di migliaia, siamo stati capaci di espanderle fino a 100-500 volte, ottenendo una purezza vicina al 100%. Dopo l'espansione, i linfociti dimostravano di poter uccidere con efficienza cellule tumorali esprimenti l'antigene AH1 *in vitro*, e di poter indurre un moderato ritardamento della crescita del tumore, senza tuttavia mai causarne una regressione. Questa mancanza di efficacia può essere spiegata dall'impossibilità di questi linfociti di sopravvivere dopo essere stati amministrati *in vivo*. Questo lavoro ribadisce ancora una volta l'importanza di trovare nuovi metodi per ottenere linfociti T robusti e in grado di persistere nel paziente una volta somministrati.

3 Introduction

3.1 Cancer

Cancer is a general term used to define a multitude of pathologies characterized by an abnormal, uncontrolled proliferation of a patient's own cells. Different cancers are broadly classified according to the type of tissue they arise from. For example, the term carcinoma includes all the cancers arising from the skin or epithelial tissue lining around internal organs, sarcoma indicates cancers originating from connective or supportive tissues like bones, muscles, fat, etc., whereas glioblastoma refers to cancers that occur in the brain or spinal cord. By proliferating in an uncontrolled way, malignant cells alter the physiology of the tissue they arise from, leading to organ failure. Moreover, they can spread and invade other tissues, forming metastasis. When this happens, cancer is referred to as "late-stage", it is more difficult to treat and prognosis is generally poor.

At a molecular level, cancer is caused by alterations in the genome of the cell, which results in either gain- or loss-of-function of genes involved in survival and proliferative processes[1]. These alterations can be the result of inherited genetic defects or defects acquired by aging, or can be caused by extrinsic factors, like UV- or ionizing-radiation, exposure to carcinogenic substances, or chronic infections[2]. Major extrinsic risk factors for cancer are the use of tobacco and alcohol, unhealthy diet, and limited physical activity. Chronic infections including Hepatitis B and C, Human Papilloma Virus, Epstein-Barr Virus, and Helicobacter pylori, represent a relevant source of risk especially in low- and middle-income countries, where treatments against these pathogens are not readily available[2].

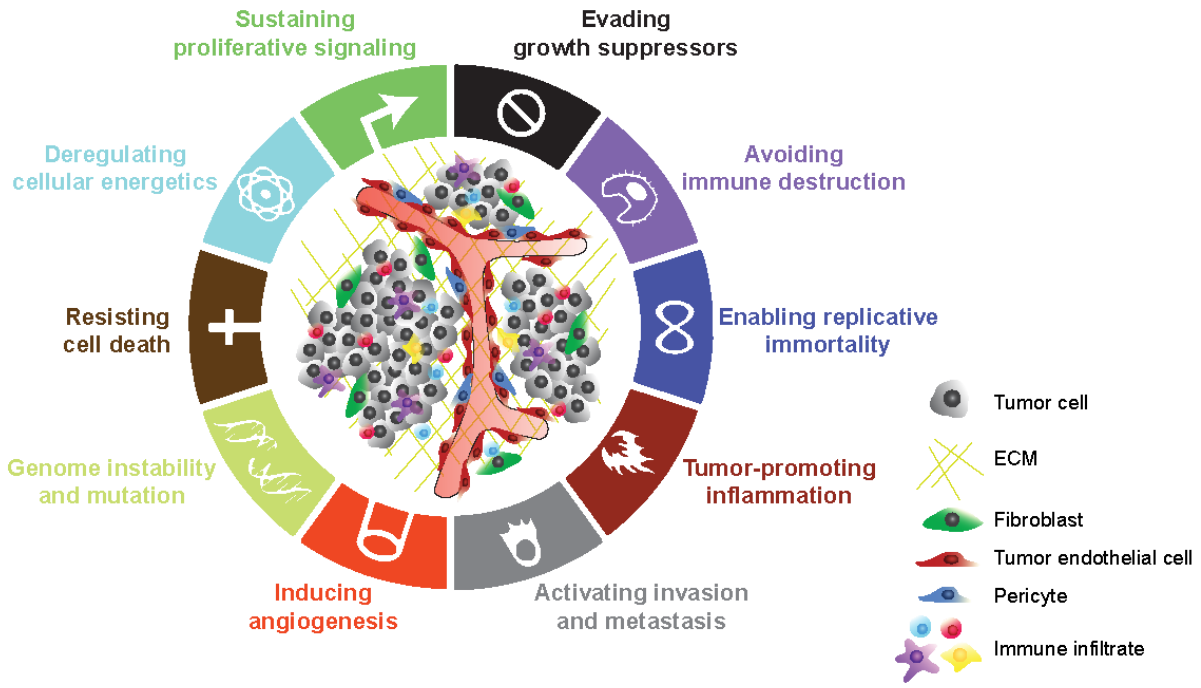

*Figure 1: **The hallmarks of cancer**. Schematic representation of the acquired capabilities necessary for tumor progression. In the middle of the circle, the principal components of the tumor microenvironment are depicted. ECM stands for Extracellular matrix. Image adapted from[1].*

As of 2018, cancer represented the second leading cause of death worldwide, accounting for approximately one out of six deaths, with an estimated 9.6 million total deceases[2]. The five most common cancers in all age groups and both sexes were lung (2.09 million), breast (2.09 million), colorectal (1.85 million), prostate (1.28 million), and stomach cancer (1.03 million)[2]. The types of cancer, which accounted for more deaths were, in order, lung (1.76 million), colorectal (0.88 million), stomach (0.78 million), liver (0.78 million), and breast cancer (0.63 million)[2].

Each type of cancer is usually divided into different stages according to size and localization[3]. Small and localized lesions are included in low stages (0 to 2). If malignant cells have spread in adjacent tissues or lymph nodes, the cancer is classified as stage 3. Finally, stage 4 is reserved for cancers that have metastasized to distant organs. The different stages have strong prognostic value, for example, according to data from the World Health Organization on colon cancer cases between 2010 and 2014, the 5-year-survival rate was around 91-96% for localized lesions, 63-78% for regional lesions, and only 8-17% for distant lesions[2]. Stage classification, together with tumor type and age of the patient, is also an important determinant for the choice of treatment[3].

There are four main types of treatment for cancer patients. Surgery, radiation, and chemotherapy have been traditionally employed, alone or in combination, for decades. The last one, immunotherapy, represents a more recent approach and will be treated in a separate section.

Surgery aims to remove cancerous tissue from the body, by resecting it. Despite its simplicity, it comes with some limitations. It is only applicable if the tumor mass is accessible. Moreover, since it is not trivial to discriminate between malignant and normal tissue, parts of adjacent healthy tissue are often removed together with the tumor. This minimizes the risk of leaving malignant cells behind, which could lead to recurrence of cancer, but further restricts the employment of surgery to (parts of) organs, which the patient can survive without.

Radiotherapy aims to employ high doses of ionizing radiation to kill malignant cells. Depending on whether the source of radiation energy is located inside or outside the body, radiation therapy can be divided into two types: external and internal. External radiation therapy is the most common and utilizes external beams directed against tumor tissue. Radiotherapy is used in approximately 50% of cancer patients, often before, during, or after surgery[4]. The main limitation of this treatment is the high toxicity associated with bystander irradiation of normal tissue.

Chemotherapy is based on the systemic administration of cytostatic or cytotoxic molecules to the patient, which preferentially target rapidly dividing cells, including tumor cells[5]. Many chemotherapeutic agents have been approved for the treatment of cancer, which act by different mechanisms. For example, alkylating agents like oxaliplatin or cyclophosphamide bind to DNA molecules and inhibits DNA replication and/or transcription, whereas plant alkaloids like paclitaxel or vincristine stabilize polymeric resp. monomeric forms of microtubules, inhibiting chromosome segregation and causing cell cycle to arrest[5]. Besides still being widely prescribed, the efficacy of chemotherapeutic drugs is limited by systemic toxicity.

3.2 Immunotherapy

3.2.1 The role of the immune system in cancer

That there must have been a body's natural anti-tumor defense mechanism, had been already postulated by P. Ehrlich in 1909, based on the logic that mutant cells may continuously arise during such a complex process as the development of an organism from a single cell[6]. At the time, however, limited knowledge of the immune system and lack of experimental models and techniques did not allow the theory of the German scientist to be scientifically proven. Nearly 50 years later, independent animal experiments performed by M.R. Lewis, L. Gross, and E.J. Foley, demonstrated that tumors could be immunogenic in both rats and mice, supporting the existence of a defense mechanism against neoplastic cells[7-9]. It soon became clear that the immune system was responsible for this anti-tumor defense. L. Thomas and F.M. Burnet hypothesized that newly arising malignant cells could be specifically recognized and eliminated early on by immune cells and formulated the theory of immune surveillance[10, 11]. Extensive research in the late part of the century allowed the immune surveillance theory to be revised and finally refined by G.P. Dunn and R.D. Schreiber, who included it in the concept of "cancer immunoediting"[12]. This new hypothesis implicated a role of the immune system not only in cancer inhibition, but also in cancer development and progression.

The theory of cancer immunoediting describes tumor development as a process characterized by three subsequent distinct phases: elimination, equilibrium, and escape (the "three Es")[12]. During the first phase, as already proposed in the immune surveillance theory, innate and adaptive immune cells patrolling the body recognize and eliminate transformed cells. Various mechanisms involving different immune cells and molecules have been shown to contribute to the elimination of early tumor cells, which had escaped cell-intrinsic tumor-suppressor mechanisms. For example, expression of stress-induced molecules like MIC-A/B, or other NKG2D ligands on transformed cells can induce secretion of IFN-γ and other effector functions in natural killer cells. Release of Type I IFN can act on CD8+ conventional dendritic cells to enhance cross-presentation and activation of CD8+ T cells. Surface calreticulin can serve as "eat-me" signal for macrophages and other antigen-presenting cells and finally, activated CD4+ and CD8+ T cells can recognize transformed cells via neo-epitope presented on MHC molecules, or via Fas/Fas-ligand interaction[13]. If newly transformed cells are successfully eliminated by the immune system, the host may remain tumor-free.

Some tumor cells, however, may resist elimination and enter the equilibrium phase, where they are held in a dormant state by the immune system and are unable to proliferate. Compared to the elimination phase, the equilibrium phase has been traditionally difficult to model in mice[14]. As a consequence, the molecular mechanisms defining this phase are not so well understood. Effector molecules like IL12 and IL23 have been shown to have an opposing effect on tumor growth and their balance in the tumor microenvironment is thought to be important to keep tumor cells in the dormant state[15]. Similarly, immune cell composition of the tumor microenvironment seems to be determinant to maintain this phase, where a high proportion of CD8+ T cells, NK cells, or γ:δ T cells opposed to low NKT cells, myeloid-derived suppressor cells (MDSCs) or Tregs has been associated with maintenance of equilibrium[14]. Experimental evidence also suggests a coordinated role of TNF and IFNγ in maintaining dormancy by inducing senescence of transformed cells[14].

During the equilibrium phase, tumor cells are held under constant pressure by the immune system. Under these conditions, genetically unstable transformed cells may accumulate mutations that eventually allow them to elude the defenses and escape immune control[13]. When the immune brake is released, tumor cells may begin to proliferate uncontrollably and disease may become clinically apparent. There are multiple strategies tumor cells employ to elude the immune system. Reduced presentation of antigen, either through reduced expression of MHC or co-stimulatory molecules, loss of antigen, or reduced antigen processing, may allow tumor cells to hide from T cells[13, 14]. Increased expression or constitutive activation of molecules associated with proliferation and survival, like the phosphorylated form of STAT3 or the anti-apoptotic molecule bcl2 may lead to resistance to immune effector functions[14]. Alternatively, tumor cells may dampen immune response directly, by up-regulating inhibitory molecules like PD-L1 or secreting indoleamine 2 3-dioxygenase [16], or indirectly, by progressively creating an immune-suppressive microenvironment rich in inhibitory cytokines (TGFβ, IL10 among others) and immune-suppressor cells like regulatory T cells, MDSCs or M2 macrophages[14].

With their cancer immunosurveillance hypothesis, Burnet and Thomas originally envisioned tumor development as a binary system, where either immunity worked in eradicating nascent tumors, or it did not[13]. This may imply a rather pessimistic vision, where little can be done to stop cancer progression, once natural immune defense had failed. The expansion of this first concept in the cancer immunoediting theory, which describes tumor development as a gradual

process characterized by mutual and continuous interactions between tumor and immunity, and the understanding of the various molecular mechanisms involved in this complex relationship, allowed to come up with new strategies to potentiate anti-tumor immunity. Efforts in this sense are collectively defined as immunotherapies.

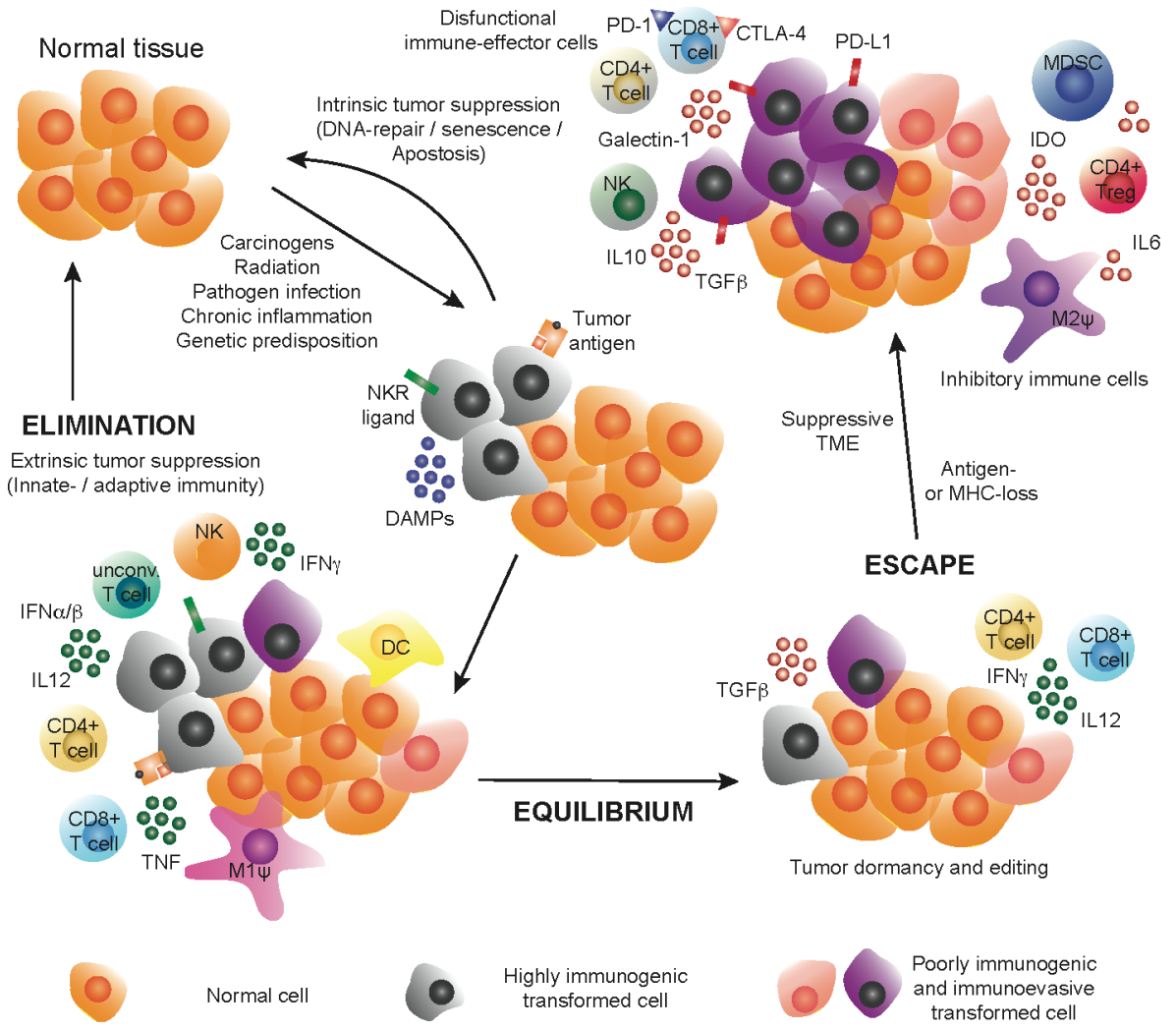

Figure 2: ***Cancer immunoediting****. When cell-intrinsic mechanisms for tumor suppression fail, early neoplastic cells may be recognized and eliminated by cells of both innate and adaptive immunity in a process called elimination. If malignant cells are not completely cleared by the immune system, the tumor may enter into the equilibrium phase, where tumor cells are held into a dormancy state by the immune system. Equilibrium may be preserved for a long period of time and may be the final stage of tumor progression in certain cases. During this phase, genetic-unstable tumor cells are kept under constant pressure from the immune system. Under these conditions some mutant may evolve, which are not sensitive to immune effector functions. Such cells may start to outgrow resulting in a clinical apparent disease (escape phase). NKR: Natural Killer cell receptor, DAMPs: Damage-associated molecular patterns, NK: Natural Killer cell, DC: Dendritic cell, MΨ: Macrophages, unconv. T cell: unconventional T cell, MDSC: Myeloid-derived suppressor cell, TME: Tumor microenvironment. Image adapted from*[17].

3.2.2 History of immunotherapy

The concept of immunotherapy was introduced way before the cancer immunoediting theory. Already at the end of the nineteenth century, two German physicians, W. Busch and F. Fehleisen reported cases of spontaneous tumor regressions in patients with erysipelas, a skin infection caused by *Streptococcus pyogenes*[18, 19]. American surgeon W.B. Coley formerly demonstrated the correlation between bacterial infection and regression of tumors, by starting to treat patients with different tumors using inactivated extracts of *S. pyogenes* and *S. marcescens*, (now known under the name of Coley's toxin)[20]. His treatment consisted of daily administration of the toxin for weeks or even months and although causing frequent and severe side effects, it could induce complete tumor regression in selected patients. A retrospective analysis of the work of Coley showed he was able to achieve cures in more than 10% of the treated patients[21]. At the time, however, toxicity and lack of reproducibility, together with the introduction of radio- and chemotherapy, lead to the abandonment of this strategy after Coley's death in 1936.

The concept was revisited about 30 years later, when D.L. Morton started to use living Bacillus Calmette-Guérin (BCG), an attenuated version of *Mycobacterium bovis* used as a vaccine for tuberculosis, to treat patient with metastatic melanoma[22]. Despite BCG being used to these days as a first-line treatment for nonmuscle-invasive bladder cancer, however, no similar approaches have been established in clinical practice.

Around the same time, G. Köhler and C. Milstein came up with an effective way to produce murine monoclonal antibodies with predefined specificity: they invented the hybridoma technology[23]. Antibodies (or immunoglobulins) are immune effector molecules produced by B lymphocytes, which can bind with high affinity and specificity to target antigens and help to protect the host from infections. Upon binding to target antigens on the surface of viruses, bacteria, or infected cells, antibodies can exert a number of effector functions depending on their class and isotype. For example, they can prevent viruses to infect new cells, they can block and inactivate toxins released by bacteria and they can mediate activation of complement system or immune effector cells[24]. Because of their characteristics, antibodies (in particular of the IgG class) were soon recognized as being particularly suited for pharmaceutical applications and the first therapeutic monoclonal antibody, OKT3, was approved by the FDA in 1985. The utility of monoclonal antibodies as anti-cancer therapeutics was demonstrated a few years later,

when Rituximab, a monoclonal antibody directed against CD20, was approved for the treatment of refractory non-Hodgkin lymphoma. More than 10 monoclonal antibodies against various tumor-associated antigens are approved to date, including anti-VEGF-A Bevacizumab (Avastin®, Roche), anti-CD20 Rituximab (Rituxan®, Roche) and anti-HER2 Trastuzumab (Herceptin®, Roche), which made it in the list of the top 10 selling drugs in 2019[25, 26]. Many of them are thought to act mainly by decorating target cells and mediating their elimination by effector cells like NK cells or Macrophages, which are activated upon interaction with the antibodies via Fc-Receptors (a process called Antibody-Dependent Cellular Cytotoxicity, or ADCC)[25]. Others, like Avastin® or antibodies targeting Epidermal growth-factor receptor (EGFR), block the biological function of their target by binding to it[25].

Another milestone in the history of immunotherapy has been the discovery of the cytokine IL2. In 1976 D.A. Morgan and colleagues described a method to culture human T lymphocytes from bone marrow using a medium derived from phytohemagglutinin-stimulated T cells[27]. A few years later, IL2 was identified as the key growth factor in the medium and it has been used since then to maintain T cells *ex vivo*, facilitating immunological research. Following demonstration of its ability to stimulate T lymphocytes in patients, recombinant human IL2 (Proleukin®, Novartis) was approved by the FDA, first for the treatment of metastatic renal cell carcinoma, and later for metastatic melanoma, and became the first reproducible effective immunotherapy for human cancer[28].

Metastatic melanoma has been playing a central role in the development of immunotherapies during the last 30 years. Several new treatment strategies have been tested in melanoma patients, sometimes showing impressive efficacy, at least in a part of treated subjects. Immune checkpoint inhibitors were part of these new strategies and their success in the clinic arguably represented a turning point in oncology practice. Immune inhibitory receptors play a crucial role in the induction and maintenance of self-tolerance or in preventing excessive activation and proliferation of effector T cells, which would arm the host[29]. In the context of cancer, however, limiting the T cell response could result in tumor progression and inhibition of these immune checkpoints was proposed as an anti-cancer strategy[29]. The first immune inhibitory co-receptor, CTLA-4, was identified in the nineties by Allison and colleagues[30, 31]. CTLA-4 is induced in activated T cells and works by sequestering B7 molecules on antigen-presenting cells, thus preventing their interaction with T cells co-stimulatory molecule CD28[31]. Blocking

CTLA-4 using the monoclonal antibody Ipilimumab resulted in improved survival of patients with advanced metastatic melanoma, which served as a basis for approval by the FDA in 2011[32, 33]. The success of Ipilimumab represented a formal validation of the concept that T cells could serve as effective fighters against cancer. Following its approval, many other immune-checkpoints inhibitors have been (and are being) investigating, and improving T cell reactivity against tumor cells has become the main and ultimate goal of immunotherapy[34].

3.3 Different types of immunotherapy

3.3.1 Immune-checkpoint inhibitors

Besides the already mentioned recombinant IL2 (Proleukin®, Novartis), the various TAA-targeted monoclonal antibodies and the CTLA-4-blocking antibody Ipilimumab (Yervoy®, Bristol-Myers Squibb), many other immunotherapeutic agents have been developed in the last 30 years. One important category of immunotherapeutic drugs is represented by immune-checkpoint inhibitors.

CTLA-4 was the first co-inhibitory receptors identified on T cells and lead to the development of the first immune-checkpoint inhibitor Ipilimumab, but another checkpoint pathway has gained particular attention in cancer research: the one involving the programmed death-1 (PD-1) and its ligands (PD-L1 and, to a minor extent, PD-L2). PD-1 expression is induced in T cells upon repeated TCR stimulation and PD-1 signaling can suppress T cell activity in multiple ways, influencing proliferation, survival, metabolism, and effector function[35]. Compared to CTLA-4, PD-1 is thought to act more on maintenance, rather than on induction of tolerance. Experiments in knockout mice showed that, while lack of CTLA-4 was associated with rapid and fatal development of systemic inflammation, lack of PD-1 or its ligands did not result in spontaneous autoimmunity, which suggested blocking the PD-1 pathway may result in lower toxicity compared to blocking CTLA-4[35]. Pembrolizumab (Keytruda®, Merck & Co.) and Nivolumab (Optdivo®, Bristol-Myers Squibb) were the first PD-1 inhibitors to be approved by the FDA for metastatic melanoma in 2014. Since then, targeting of the PD-1/PD-L1 axis has shown remarkable clinical activity in a multitude of clinical trials and three PD-1 resp. three PD-L1 inhibitors are approved today for a number of different malignancies. Moreover, following the success of this first generation of immune checkpoint inhibitors, many other immune-checkpoints modulators are currently under investigation[35-37].

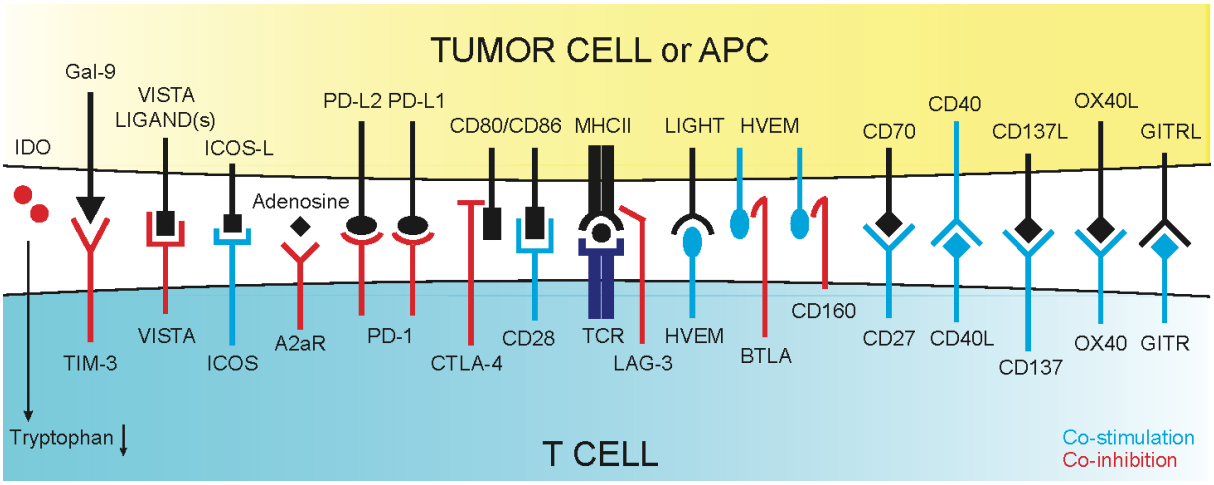

*Figure 3: **Immune checkpoints**. Examples of co-stimulatory and co-inhibitory molecules expressed by T cells, which may serve as targets for immunotherapy. APC: Antigen-presenting cell.*

Although immune checkpoint inhibitors have revolutionized cancer therapy, demonstrating activity in many different types of cancers and inducing durable responses, curative responses have only been observed in a subset of patients and many patients do not benefit from monotherapy with these agents. Current efforts to improve therapy with immune checkpoint inhibitors include the identification of better prognostic markers associated with therapeutic activity, which would allow selecting for responders[38]. Moreover, therapeutic combinations with synergistically active agents are being evaluated both in preclinical models and in the clinic[39].

3.3.2 Bispecific antibodies

Bispecific antibodies represent a second category of promising immunotherapeutic drugs. They are antibodies or antibody fragments engineered to bear two different specificities, which allows them to simultaneously bind two different targets. One part of the molecule is directed against a TAA, while the second binds and activates immune effector cells[40]. The first bispecific antibodies were tested in the clinic in the early nineties but were all discontinued for two main reasons: lack of efficient manufacturing technologies and limited effect[40]. They were obtained either using hybridoma technology adapted to produce bispecific IgGs (quadroma) or by chemical conjugation of two F(ab')2 fragments generated by pepsin digestion of IgGs[41, 42]. Murine antibodies produced by Quadroma technology were immunogenic in patients and neither method could generate good yields of homogenous products. Moreover, $F(ab')_2$-based bispecific were initially designed to recruit macrophages and neutrophils via CD64, which was proven to be a poor strategy. Targeting CD16 expressed on NK cells and macrophages (together

with the TAA CD30), resulted in objective response in 6 out of 30 patients with Hodgkin's Lymphoma, but immunogenicity and low production yields precluded further studies[40]. Advances in protein engineering and production eventually allowed to obtain bispecific products suitable for therapeutic applications[40]. To date, two bispecific antibodies have reached the market, Blinatumomab (Blincyto®, Amgen), and Catumaxomab (Removab®, Fresenius Biotech). The first one, in a Bi-specific T-cell Engager [16] format, targets CD3 on T cells and CD19 on B cell blasts and is approved as an intravenous infusion product for Acute Lymphocytic Leukemia (ALL)[43]. The second is a hybrid of a mouse/rat IgG targeting CD3 and EpCAM, which was approved in Europe for the treatment of malignant ascites in ovarian cancer but was withdrawn in 2017 for commercial reasons[43]. Additionally, more than 40 bispecific antibodies in different formats are in clinical development[43]. Remarkably, the vast majority of the new-generation of bispecific products are equipped with an anti-CD3 for targeting of T cells, highlighting their central role in immunotherapy. Challenges in the field of bispecific antibodies are mainly related to toxicity. Suffice it to say that Blincyto® is administered at a dose not to exceed 28 μg/day and about 10% of patients experience grade 3 or higher toxicity (cytokine-release syndrome or neurological events)[44]. Moreover, although bispecific antibodies have been proven to be active in a variety of hematological malignancies, their efficacy in solid tumors is still limited[40].

Monoclonal antibodies have been exploited in at least two additional promising immunotherapeutic strategies, namely immunocytokines and chimeric antigen receptor T cells (CAR-T cells), which will be described in detail below. If we exclude other conjugated-antibody therapeutics (e.g. antibody-drug-conjugates, which may not be primarily regarded as immunotherapeutics because of their mechanism of action), adoptive cell therapies (ACTs) other than CAR-T, cancer vaccines and oncolytic viruses complete the plethora of clinically relevant immunotherapies. Analogously to immunocytokines, ACTs are particularly relevant to this thesis and will be discussed in separate chapters.

3.3.3 Cancer vaccines

Vaccination against cancer has been proposed already by W.B. Coley, with his Coley's toxin[20], and has been pursued since the realization that the immune system was able to detect and kill nascent malignant cells. Unfortunately, the development of an efficacious anti-cancer vaccine

has been hindered by many factors, which are only now starting to be understood thanks to a deeper understanding of tumor immunology and accumulated clinical experience[45].
Early work on vaccination against cancer was based on experience with prophylactic vaccines against infectious agents. There are however three main differences between vaccines for infectious disease and cancer. First, viruses and bacteria are foreign pathogens, whereas malignant cells arise from the patient's own cells. Our immune system is trained to recognize invading pathogens and thus viral and bacterial-derived proteins are highly immunogenic. TAA traditionally targeted with vaccination strategies, instead, are self-proteins against which patient T and B cell underwent negative selection, and are minimally, if at all, immunogenic[24, 45]. Second, while vaccines for infectious diseases are given to healthy individuals to preventively train the immune system, cancer vaccine have to act on patients with established disease. Third, while viruses and bacteria effectively alert and activate innate immunity via pathogen-associated molecular patterns (PAMPs), which is required for mounting an adaptive immune response, the tumor microenvironment is immunosuppressive[24, 45]. As a result, cancer vaccine efficacy in the clinic has been limited so far.

Cancer vaccine development starts with the choice of the target antigen (or antigens). TAAs are weakly immunogenic and are not exclusively expressed in tumor cells, which in case of an effective vaccination may lead to the development of autoimmunity[45]. Tumor-specific neoantigens (antigenic peptides resulting from mutated proteins) have been proposed as an alternative. Two recent early phase studies with neoantigens vaccines showed promising results in melanoma patients[46, 47]. Nevertheless, immunogenic neoantigens are generally rare, especially in tumors with low mutational burden, and challenging to identify. Moreover, they are specific for each individual, which only allows highly personalized therapy.

A second important step in vaccine development is the choice of the vector types. There are three main vaccination platforms: molecular vaccines (peptides, DNA or RNA), viral-based vaccines, and cellular vaccines (DCs, tumor cells, other), each coming with specific advantages and challenges[45]. Especially in the case of peptide vaccines (or the less popular tumor cell vaccines), the choice of a suitable adjuvant, capable of alerting antigen presenting cells (APCs), may also be determinant for efficacy[48]. In fact, antigen presented by immature APCs may lead to tolerance, instead of activation[24]. DCs for cellular vaccines can be easily activated *in vitro* before administration, while viral components and foreign DNA or RNA can be recognized by

Toll-like receptors (TLRs) or other Pattern-recognition-receptors (PRRs) expressed by APCs, but cancer-derived peptides are not recognized as non-self by innate immune cells[45, 48].

To date, excluding the prophylactic vaccines for Hepatitis B and Human Papilloma Virus (two oncogenic viruses, which can cause liver, resp. cervical cancer), there are only two cancer vaccines available on the market[45]. The first is BCG for nonmuscle-invasive bladder cancer (already mentioned in 3.2.2). The second, sipuleucel-T (Provenge®, Dendreon Pharmaceuticals), is approved for metastatic hormone-refractory prostate cancer and consists of autologous DCs pulsed *ex vivo* with a fusion protein comprising the TAA prostatic acid phosphatase, and granulocyte-macrophage colony-stimulating factor (GM-CSF)[49].
Many others have failed to demonstrate consistent efficacy at various stages of clinical trials, mostly because of inability to induce a sustained immune response[45].
Nevertheless, advances in choice of the target antigens (e.g. neoantigens instead of TAAs), together with development of new vaccine vectors, have recently resulted in vaccines, which showed promising activity in early-phase clinical trials[50-52].

3.3.4 Oncolytic viruses

Oncolytic viruses are yet another immunotherapy approach with high potential, but which have so far failed to meet the expectations. By definition, oncolytic viruses are viruses that are able to preferentially infect and lyse tumor cells. Different mechanisms are used by different virus families to achieve tumor selectivity, mainly based on altered metabolism or defect in signaling pathways specific to malignant cells[53]. In the context of immunotherapy, oncolytic viruses can exert a dual effect. On one side, they may directly eliminate malignant cells (and self-replicate at the same time), on the other, they can modify the suppressive tumor microenvironment and stimulate anti-tumor immunity[53, 54].

An attractive feature of using viruses to target tumor cells is that their genome can be easily manipulated with current genetic engineering techniques, allowing to enhance their selectivity toward tumor cells, their lytic potential, and their immuno-stimulating properties[54]. Strategies to enhance virus tropism for malignant cells include for example the genetic modification of components of the viral capsid (e.g. with antibody fragments targeting TAAs), the insertion of tumor-specific promoters that control viral gene expression, or the deletion of viral genes,

which are essential for replication in normal host cells, but not in tumor cells (e.g. the adenoviral protein E1a)[55, 56].

Killing potential has been potentiated in Herpes Simplex Virus-1 (HSV-1)-based oncolytic viruses by equipping them with fusogenic membrane glycoprotein of the GALV (gibbon ape leukemia virus) or measles virus, or with prodrug-converting enzymes[57]. Fusogenic proteins cause neighboring tumor cells to fuse, creating multinucleated syncytia, which leads to cell death, while prodrug-converting enzymes specifically expressed at the site of disease can activate administered cytotoxic prodrugs *in situ*[57]. Moreover, oncolytic viruses expressing a multitude of genes coding for pro-inflammatory cytokines or chemokines, immune-checkpoint inhibitors, and BiTEs, among others, have been investigated[58-60].

The limited efficacy of oncolytic viruses observed so far may be due to a number of reasons. Oncolytic viruses may be neutralized or cleared rapidly by pre-existing or *de novo* induced immune response *in vivo*, or may not reach the tumor when administered systemically, because of trapping in organs like liver and spleen or due to intrinsic physical barriers in the tumor mass (e.g. high hydrostatic pressure, dense extracellular matrix)[54]. Engineering the virus for selectivity may reduce virulence and lytic potential. Arming it with additional killing ability may be toxic, or may result in rapid debulking, which may prevent the induction of an anti-tumor immune response. On the other hand, favoring immune activation may lead to a premature clearance of the virus[54]. Direct injection in the tumor may help circumvent some targeting challenges, but restricts the use to accessible lesions and may not be effective in a metastatic setting[61].

Nevertheless, one oncolytic virus has gained approval from the FDA. Talimogene laherparepvec, or T-VEC (Imlygic®, Amgen), is a GM-CSF-expressing HVS-1, which has been modified to enhance selectivity to tumor cells. It has been approved as intratumoral injection for the treatment of unresectable recurrent melanoma, based on a phase III clinical trial, where it demonstrated superiority to GM-CSF (durable response rate in 16.3% v. 2.1% of the patients)[62].

3.4 Adoptive cell therapy

Broadly speaking, adoptive cell therapy refers to any treatment involving the transfer of living immune effector cells to patients. In general, however, this term is used to describe therapies with autologous T cells or NK cells, which have been expanded and eventually enhanced before transfer. Although not exclusively, most immunotherapy approaches have been focusing on the enhancement of CD8+ T cells, which have been identified as the most powerful type of effector cells for cancer therapy. ACTs are no exceptions and although employment of NK cells is gaining interest[63], and CD4+ T cells have been shown to play a critical role in both development and sustenance of effective anti-tumor responses[64], the vast majority of studies in this field are based on CD8+ T cells.

3.4.1 Biology of CD8+ T cells

Conventional T lymphocytes are adaptive immune cells expressing a characteristic receptor, the α:β T cell receptor (TCR), which enables them to recognize antigenic peptides presented on major histocompatibility complex (MHC) molecules. They arise from common lymphoid progenitor cells in the bone marrow, which also give rise to B and NK cells. Unlike B and NK cells, however, T cells develop from lymphocyte precursors that migrated to the thymus. In the thymus, they gradually rearrange and express a specific TCR and undergo positive and negative selection to ensure their TCRs are able to bind self MHC molecules but do not strongly recognize self-peptides[24]. The process of genetic rearrangement, together with the combinatorial pairing of the two subunits that constitute the complete α:β TCR, generates a very high number of different TCRs (theoretically around 10^{18}), which allow an individual's T-cell repertoire to recognize a variety of different peptides[24]. This allows T cells to carry out their primary functions: to protect the host from pathogens like viruses, bacteria, and parasites, or, as discussed above, from nascent tumor cells.

Commitment to the CD8+ lineage takes place during the final stages of thymic development, when CD4/CD8 double-positive immature T cells expressing a functional TCR start to interact with thymic cortical epithelial cells[24]. T cells interacting with MHC class I develop into mature, CD8+ naïve T cells and leave the thymus. After leaving the thymus, mature naïve T cells migrate to secondary lymphoid organs via the bloodstream. In secondary lymphoid organs, naïve T cells are provided with survival stimuli for homeostatic maintenance by resident APCs,

in particular DCs. Short-lived naïve T cells need interaction with self-peptide:MHC complexes and homeostatic cytokines like IL7 to survive[24].

Secondary lymphoid organs are also the sites where adaptive immune responses are initiated. When DCs sense the presence of a pathogen or a danger signal, they get activated, eventually migrate to the closest secondary lymphoid organ, and express a number of co-stimulatory molecules, cytokines, and chemokines needed to attract and activate naïve T cells (a process called maturation)[24]. Naïve T cells recognizing antigenic peptides presented by mature DCs, temporarily lose the ability to leave secondary lymphoid organs and start to clonally expand, generating a high number of effector T cells with the same specificity[24]. Effector CD8+ T cells migrate to the site of disease to specifically kill host cells infected with the pathogen. Similarly, tumor-specific T cells may be primed by mature DCs presenting tumor-derived antigenic peptides.

Engagement with antigenic-peptide:MHC complexes is essential, but not sufficient to prime a naïve T cell. In fact, naïve T cells recognizing peptides without proper co-stimulation either differentiate into FoxP3-expressing regulatory T cells, die, or enter into an anergic state[24]. Because negative selection in the thymus (named central tolerance) is not 100% effective, this mechanism (named peripheral tolerance) reduces the risk of autoreactive T cells to become active and cause damages to the host own tissues. Understanding peripheral tolerance is particularly relevant for cancer vaccine development. Two additional types of signals must be provided by DCs to effectively prime naïve T cells. Co-stimulatory molecules, in particular the interaction between B7 on DCs and CD28 on T cells, promote survival and proliferation, while different cytokines drive differentiation into specific subtypes with distinct effector functions[24]. The quality, intensity, and duration of each signal delivered during priming may also influence the generation of memory subtypes[65]. While effector T cells are efficient killers, but relatively short-lived, memory T cells persist after clearance of disease and can mediate a rapid and more vigorous response by subsequent encounter of the same antigen[24].

Based on expression of specific phenotypic markers, five main subsets of CD8+ T cells can be identified: naïve T cells (T_N), T memory stem cells (T_{SCM}), central memory T cells (T_{CM}), effector memory T cells (T_{EM}), and terminally differentiated effector T cells (T_{TE})[66]. Additionally, a phenotypically distinct subset of T cells called resident memory (T_{RM}) has been

described, which reside in peripheral tissues and has been shown to play an important role in anti-tumor immunity[67, 68].

Three different models have been proposed to describe memory T cell formation, which is still an intense matter of debate[69-71]. In the first and perhaps most widely accepted, memory T cells derive from few surviving effector T cells at the end of the contraction phase of the immune response. A second model suggests that asymmetric division of T_N during priming results in both precursors of T_{CM} and T_{EM}. More and more experimental evidence, however, supports a third theory (first proposed by Lanzavecchia and Sallusto), claiming that T_N progressively differentiates into T_{SCM}, T_{CM}, T_{EM}, and finally to T_{TE}[72, 73]. Accordingly, telomere length and telomerase activity are progressively reduced in further differentiated T cell subsets and T cells of a particular subset can give rise to progeny including following, but not preceding T cell subsets[74, 75].

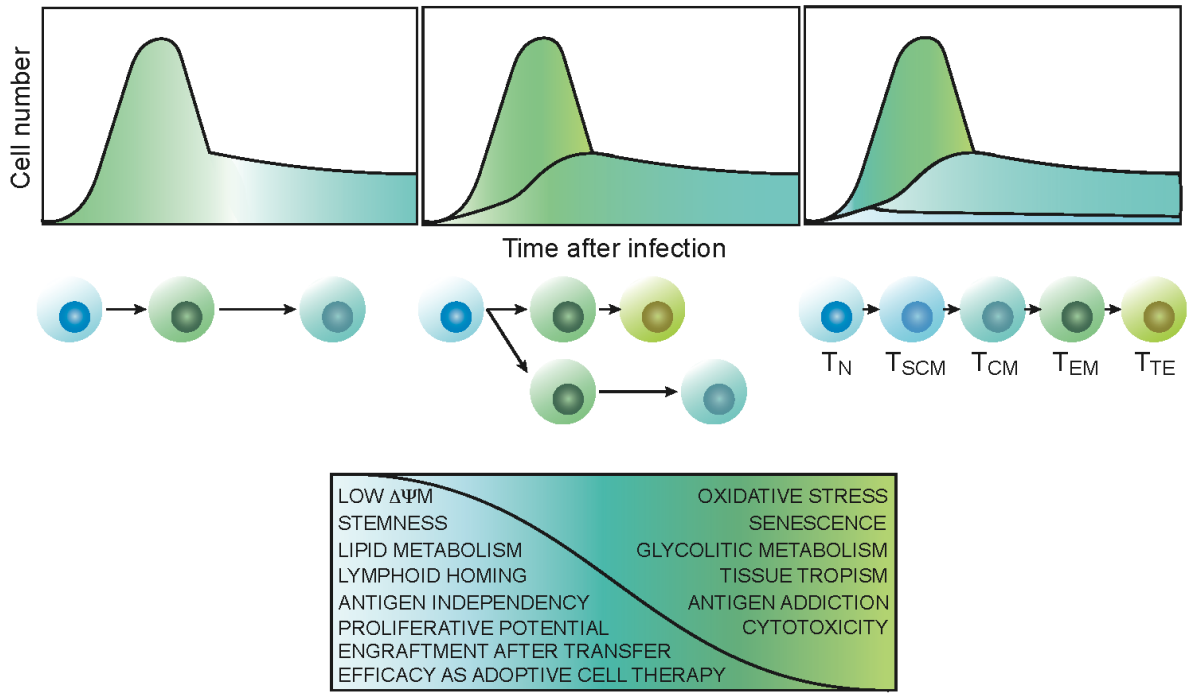

*Figure 4: **T cell memory formation**. Schematic representation of an adaptive immune response, based on the three different theories explaining memory formation. Left: Upon priming, naïve T cells start to proliferate and develop into effector T cells, which migrate to the site of disease. After disease resolution, most effector cells die, whereat 5-10% survive as memory T cells. Middle: Primed naïve T cells asymmetrically divide into effector- and memory-precursors. Effectors cells extensively proliferate and fight the disease, before becoming terminally differentiated and dying, while memory-precursors develop into long lived memory T cells. Right: Naïve T cells gradually mature into stem cell-like memory T cells, central memory T cells, effector memory T cells and finally terminally differentiated effector cells. Keys characteristics related to different T cell phenotypes are listed in the lower panel. T_N: naïve T cell, T_{SCM}: stem cell-like memory T cell, T_{CM}: central memory T cell, T_{EM}: effector memory T cell, T_{TE}: terminally differentiated effector T cell.*

Cytotoxic CD8+ T cells recognize their target cells via TCR-peptide:MHC complex interaction and are activated to kill target cells without the need for additional co-stimulation[24]. After TCR

engagement and synapsis formation, CD8+ T cells release into the synaptic cleft granules containing perforin and granzymes, which synergize to induce apoptosis of the target cell[76]. Additionally, activated CD8+ T cells secrete interferon-gamma (IFNγ) and tumor-necrosis-factor-alpha (TNFα) and may induce death of target cells via Fas-FasL interaction[24]. Upon activation, the expression of a multitude of molecules is induced in CD8+ T cells, which may modulate their activity by interacting with cognate ligands. Examples are inhibitory checkpoint molecules as CTLA-4 (which however acts more during priming), PD-1, LAG-3, TIM-3 among others, or stimulatory checkpoint molecules like CD137, OX40, ICOS, or GITR[37]. Signals from inhibitory checkpoints are important to contain the T cell-mediated immune response and avoid excessive activation of CD8+ T cells, which could cause damages in healthy tissues. For an adaptive immune response to be successful, naïve CD8+ T cells must be properly primed, they must proliferate, migrate to the site of disease, clear the pathogen/the transformed cells, and persist as memory T cells.

3.4.2 Development of ACT with tumor-infiltrating lymphocytes

In the first half of the 20th century, immunological studies mostly focused on antibodies and humoral immunity, neglecting lymphocytes and cellular immunity[28]. The realization that lymphocytes played a direct role in delayed hypersensitivity reactions and rejection of heterologous tissue-transplants, sparked the interest of immunologist in these cells and their possible role in anti-tumor immunity[77]. Initial research on lymphocytes was hampered by the inability to maintain this cell population *ex vivo* and only started to flourish after the discovery of IL2[27]. IL2 allowed to grow and study T lymphocytes *in vitro* and even showed remarkable anti-tumor activity in patients when used as a therapy[28].

Parallel to the clinical development of recombinant IL2, Steven A. Rosenberg started to administer IL2-cultured splenocytes called "Lymphokine-activated killer cells" (LAKs) as a treatment in murine tumor models of metastasis[78]. Soon afterward, he realized that lymphocytes extracted from murine tumors (TILs) and cultured in a similar way were more effective than LAKs in reducing metastasis in mice and that combination with recombinant IL2 further improve their efficacy[79]. The culture method was later applied to grow TILs from human melanoma tumor samples and the first results of therapy with TILs in combination with IL2 were reported in a landmark publication in 1988[80].

In the following 4 years, treatment of a total of 86 patients with metastatic melanoma with ACT and IL2, performed at Surgery Branch of the National Cancer Institute (NCI, Bethesda, USA), resulted in an overall response rate of 34%, with 6% of the patients experiencing complete tumor regression[81]. Unfortunately, however, responses were mostly of short duration, reflecting the fact that administered T cells were rarely detected in circulation just days after transfer[82].

A first substantial improvement was seen in 2002, with the introduction of a non-myeloablative lymphodepleting chemotherapy regimen consisting of fludarabine (25mg/m^2 for 5 consecutive days) and cyclophosphamide (60mg/kg in addition to fludarabine for the first 2 days)[83]. T cells transferred after preparative lymphodepletion were shown to persist and proliferate *in vivo*, resulting in a higher incidence of long-lasting responses. Attempts were made to further optimize the lymphodepletion regimen, for example, the effect of additional total body irradiation was investigated in a pilot trial, resulting in objective responses in 72% of the patients, with complete regression in 40%[84, 85]. The addition of total body irradiation, however, resulted in increased toxicity and failed to demonstrate superiority compared to the standard chemotherapy regimen. A recent meta-analysis of clinical studies on metastatic melanoma patients performed in various cancer centers from 1988 to 2016, reported pooled overall response rates of 41% and complete response rates of 12%, the majority of which were durable[86].

The standard protocol for TILs generation starts with the excision of the tumor biopsies from patients (diameter at least 2cm). The tumors are then dissected into small fragments of about 2mm^2 and each fragment is plated individually in medium supplemented with human serum, HEPES buffer, antibiotic and antimycotic, L-Glutamine, beta-mercaptoethanol, and high dose IL2 (usually 6000IU/mL). In a certain variation of the protocol, individual TIL cultures are started from aliquots of single-cell suspensions generated by enzymatic digestion of the tumor. During the following 2-4 weeks of incubation, tumor cells slowly die off, while TILs may proliferate to about $3x10^7$ cells and are tested for reactivity against primary tumor (if available) or HLA-matched tumor cell lines. Cultures showing tumor recognition by IFNγ secretion are then individually expanded for 14 days using agonistic antibodies against CD3, IL2, and an excess of irradiated allogeneic feeder cells: a procedure referred to as rapid expansion protocol (REP)[87]. Up to 10^{11} cells may be obtained within 6 weeks from tumor resection and, to date, TILs can be generated from the majority of melanoma patients[88].

In vitro TILs cultures have been generated for a multitude of different epithelial cancers, however, cancers other than melanoma have generally failed to consistently yield tumor-reactive TILs[89]. The success of ACT with TILs and other immunotherapies (recombinant IL2, immune-checkpoint blockade) in melanoma was hypothesized to rely on the high incidence of mutations in coding genes of melanoma tumors, which could be recognized by T lymphocytes[82]. An important study published in nature in 2013 identified melanoma as the tumor with the highest mutational burden[90]. Moreover, already in 1995, TILs specific for a mutated version of the protein cyclin-dependent kinase 4 were identified in a patient[91]. In early studies, two TAAs (namely gp100 and MART-1) were found to be often recognized by TILs grown from melanoma lesions. Both gp100 and MART-1 are expressed by normal melanocytes in the skin, eyes, and ears, however, successful eradication of melanoma after TILs therapy was not accompanied by toxicity in these organs in the majority of patients, which spoke against a prominent role of these antigens in tumor rejection[82]. Efforts aimed at identifying melanoma antigens, which could drive an effective tumor rejection, resulted in an optimized protocol for the selection of neoantigen-specific TILs for ACT[82, 92].

The optimized protocol included whole-exome sequencing of tumor and matched healthy tissue to identify amino acid mutations in the tumor. RNA sequences containing the identified mutations were assembled into tandem mini-genes and used to force presentation of all mutated peptides on patient autologous DCs. Instead of using tumor cells, reactivity of cultured TILs was tested by co-incubation with DCs, and neoantigen-specific TILs were isolated for rapid expansion based on expression of early activation markers like CD137 or OX40[82, 92]. Using this approach, TILs preparations containing relatively high proportions of neoantigen-specific TILs were successfully employed to treat malignancies including cervical cancer, bile duct cancer, colorectal cancer, and breast cancer[93-96].

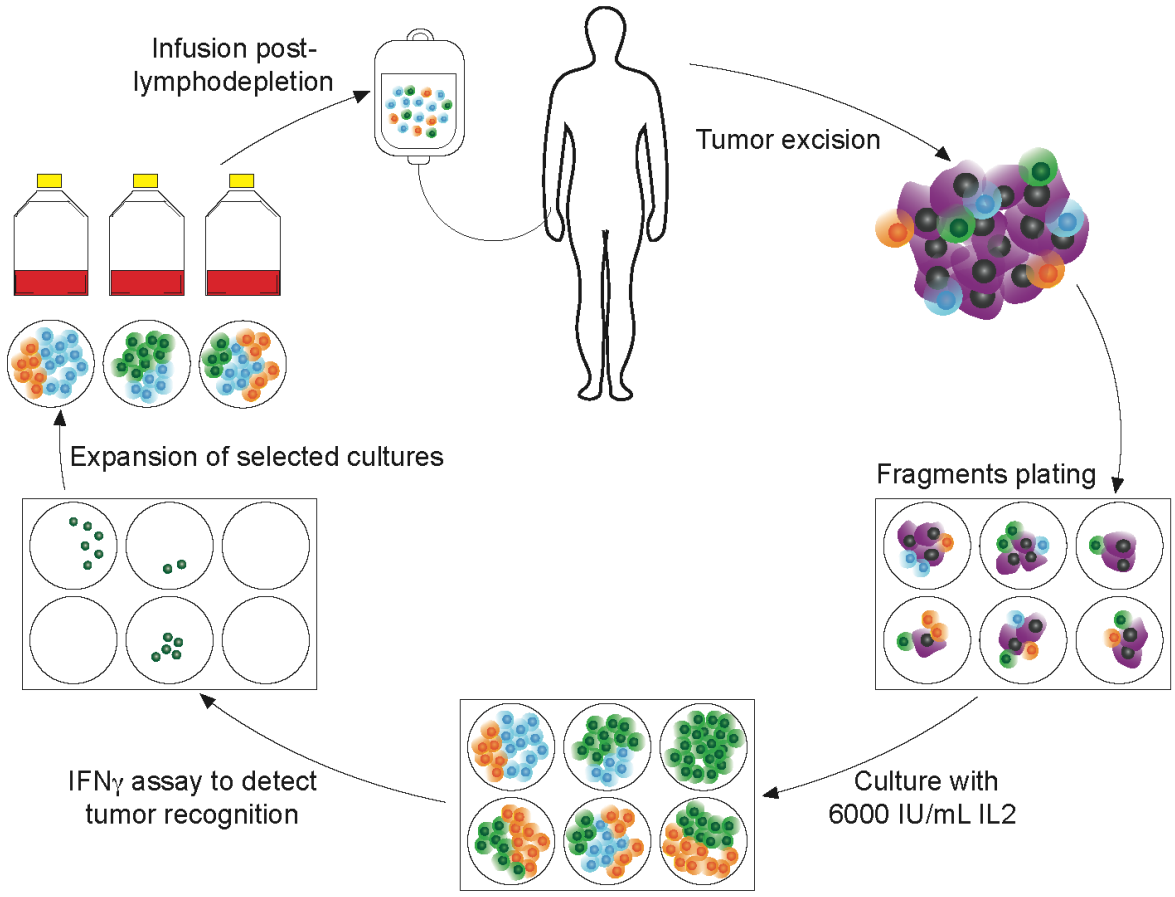

*Figure 5: **Adoptive cell therapy with tumor-infiltrating lymphocytes**. Schematic representation of the principal steps involved in generating tumor-infiltrating T cell products for adoptive therapy. Tumor is initially resected from the patient and cut into small fragment, which are individually plated in medium containing high-dose IL2. Under these culture conditions, tumor cells slowly die out or are killed by expanding T cells. Individual cultures of preliminary-expanded T cells are co-incubated with tumor cells to test their tumor reactivity. Cultures showing tumor recognition are expanded using a rapid expansion protocol, before pooling and re-infusion into the pre-conditioned patient. The whole process usually lasts 4-6 weeks. After T cell transfer, patients receive high dose IL2. Image adapted from[82].*

3.4.3 Other types of ACT

Although immunotherapy with TILs has demonstrated to be a valid option for patients with metastatic melanoma and, in some anecdotal cases, with other epithelial cancers, there are still several limitations related to the use of these tumor-infiltrating cells[89].

First of all, although it is reasonable to assume that tumor-specific T cells may concentrate at the tumor site, where the concentration of their cognate antigen is highest, the proportion of tumor-specific T cells among the lymphocytes infiltrating human tumor is variable and generally low[97]. T cells found in tumors are mainly dysfunctional effector cells[98]. *Ex vivo* culturing is thought to help restore effector functions of TILs, but repetitive *in vitro* stimulation, necessary to expand populations of tumor-specific TILs to a number suitable for therapy, may

drive them toward a terminally differentiated, exhausted phenotype with poor survival *in vivo*[99]. Moreover, it may not be possible to generate TILs cultures from cold tumors, which are poorly infiltrated per definition, and from tumors that are not surgically resectable.

Chimeric-antigen receptor (CAR) T cells and T cell receptor-transgenic (TCR-transgenic) T cells have been proposed as strategies to generate high numbers of fitter tumor-specific T cells for ACT.

CAR-T cells are genetically-engineered T cells expressing a chimeric receptor featuring an extracellular single-chain variable fragment (scFv) linked to an intracellular signaling domain[100]. The scFv provides specificity against a tumor surface antigen, while the signaling domain is responsible for T cell activation upon engagement of the receptor. CAR-T are generated by transduction of activated, patient autologous peripheral blood mononuclear cells (PBMCs)[101, 102]. PBMCs are readily accessible, they can be easily isolated in high numbers and contain T cells, which are mostly naïve. Leukapheresis typically yield between 10^8-10^9 cells[103], which are then activated by CD3/CD28 stimulation before lentiviral (or retroviral) transduction with the CAR construct. CAR-expressing cells are then expanded for about 10 days before administration (or cryopreservation)[101, 102]. Administered CAR-T cell dose is based on body weight and typically range between 10^7-10^{10} cells per patient[104]. During the 10 days of ex-vivo culture, CAR-T cells typically undergo a 20-fold expansion[102]. In comparison, TILs have to be expanded more than 1000-fold over 5-6 weeks before reaching suitable yields[87, 102].

CAR-T cell treatments have shown extraordinary efficacy in multiple hematological malignancies[105]. Of note, two pivotal trials with the CD19-targeting CAR-T cell tisagenlecleucel (Kymriah®, Novartis) in pediatric patients with relapsed or refractory (r/r) B cell acute lymphoblastic leukemia (ALL) and in adult patients with r/r large B cell lymphoma resulted in complete response rates of 82% (at 3 months) and 30% (at 6 months), respectively and lead to FDA approval for these 2 indications[101, 106]. To date, two additional CAR-T cells against CD19 have gained FDA approval in hematological malignancies, namely axicabtagene ciloleucel (Yescarta®, Gilead, former Kite Pharma)[107] and brexucabtagene autoleucel (Tecartus™, Gilead, former Kite Pharma)[108].

Major limitations of CAR-T cell therapies are related to the paucity of good tumor targets. Surface tumor-specific targets are extremely rare and antibody therapeutics are generated against TAAs, which are preferentially, but not exclusively expressed on cancer cells. Since CAR-T cells are formidable killers, the risk of on-target off-tumor toxicity further restricts targetable antigens to molecules present on dispensable healthy cells. Not by chance, CAR-T cells have only been approved for B cell malignancies, where toxicity related to the depletion of B lymphocytes is manageable by Immunoglobulin substitution[109]. Other frequent toxicities associated with CAR-T cell treatments are cytokine-release syndrome (CRS) resulting from massive immune activation and neurological toxicity, which, as recently suggested, may be related to CD19 expression in brain mural cells[109, 110]. New strategies to reduce toxicity include the use of small-molecular-sized bridges between target and CAR-T cells, which allow CAR-T cell to be activated only in the presence of the bridge-molecule (UniCAR or switchable CAR-T technologies)[111, 112], or CAR-T cells, which needs to simultaneously engage with two different targets to be activated[113]. Besides reducing toxicity, an additional current challenge and focus of research in the field of CAR-T cell is augmenting the so far limited activity in solid tumors.

TCR-transgenic T cells represent yet another potential strategy to improve ACT. Similarly to CAR-T cells, also in TCR-transgenic T cells tumor specificity is provided by the genetic insertion of a foreign receptor. In the latter, however, the receptor is a normal TCR[114, 115]. Since peptides from both extra- and intracellular proteins are presented on MHC molecules, the use of a TCR instead of a CAR allows to choose from a substantially enlarged pool of target antigens, including tumor-specific neoantigens. The drawback is the high degree of personalization of this approach, which requires not only the identification of a suitable (neo)antigen to target, but also the identification of a TCR able to bind with high avidity to the patient-specific HLA:peptide complex. In other words, patients need to share both the same immunogenic peptide antigen and the same presenting-HLA molecule to be treated with the same TCR, which is particularly rare especially for neoantigens[116].

Clinical studies with TCR-transgenic T cells have been performed using TCR recognizing TAAs like MART-1, gp100, WT1, and CEA or cancer-testis antigens (CTAs) like NY-ESO-1 and MAGE, mostly presented in the context of the HLA-A*0201 allele (one of the most frequent in the Caucasian population)[116]. None of these antigens is tumor-specific and most studies resulted in significant, sometimes even lethal toxicities related to expression of the

target antigen in healthy organs. Administration of NY-ESO-1-specific TCR-transgenic T cells was well tolerated and, even if mostly short-lasting, produced overall response rates (ORRs) of up to 61% and 55% in patients with synovial sarcoma and melanoma, respectively, demonstrating the feasibility of this approach when targeted antigen expression is more restricted to tumor cells[117, 118]. Of note, for one of these trials was reported that only 10% of the screened patients could be elected for treatment, highlighting the challenge of dealing with HLA-restriction[119].

3.5 Therapy with immunocytokines

3.5.1 Cytokine role in cancer immunology

Cytokines are small proteins involved in cell-to-cell communication. They can be released by several types of cells, usually in response to a stimulus, and exert a multitude of modulatory effects through binding to specific cell surface receptors. They can act locally, on neighboring cells or by autocrine signaling, or systemically[24]. Many cytokines are produced by, and act on, cells of the immune system. Some cytokines create an inflammatory environment and activate immune effector cells, others are involved in inhibiting those same cells and promote tolerance, and there are cytokines, that possess both pro- and anti-inflammatory functions[24]. Different cytokines may act synergistically or antagonistically on the same cell at a given time, leading to different effects depending on relative concentrations and time of exposure.

In the context of cancer, anti-inflammatory cytokines contribute to shape and maintain the suppressive tumor microenvironment characteristic of solid tumors, limiting the anti-tumor activity of immune effector cells and eventually promoting tumor progression and metastasis[120]. Manipulating the tumor microenvironment to favor immune activation has been the aim of many immunotherapeutic approaches and certain cytokines, namely IL2, IL15, IL12, IL21, and IFNγ, may be particularly well suited for the task[121]. However, besides IL2, which has been already discussed above, only three additional recombinant cytokines have been approved so far for cancer treatment. Two subtypes of interferon-alpha (IFNα, Roferon-A®, Hoffmann-La Roche, and Intron-A, Merck & Co.) are currently used worldwide for the treatment of more than 14 types of cancer, including hematological malignancies and solid tumors[122], whereas isolated limb perfusion with recombinant TNFα (Beromun®, Boehringer Ingelheim) in combination with the cytotoxic drug Melphalan has been approved in Europe for the treatment of bulky melanoma metastases and irresectable soft tissue sarcoma of the limbs[123]. Unfortunately, severe toxicity resulting from the systemic administration of cytokines often prevents escalation to therapeutic doses, and remissions after cytokine-treatment have been rarely observed[121].

3.5.2 Immunocytokines in clinical trials

Immunocytokines are a promising class of immunotherapeutics featuring a cytokine genetically fused to a monoclonal antibody[124]. The antibody part of the molecule allows to selectively target

the cytokine payload to the site of disease, potentially increasing its anti-tumor activity and reducing systemic exposure.

Three main features determinate the therapeutic performance of an immunocytokine: the antibody specificity, the antibody format, and the cytokine payload. The choice of an antibody with a high affinity against a good tumor target is the first prerequisite. Suitable target candidates may be expressed in high amounts in the tumor while being virtually undetectable in healthy tissues. Many membrane-associated tumor antigens have been identified over the year, but only a few have been sufficiently validated in the clinic for delivery applications. Examples are carcinoembryonic antigen (CEA)[125], CD44 isoform containing the variable domain 6 (CD44v6)[126], hypoxia marker carbonic anhydrase IX (CAIX)[127], epithelial cell adhesion molecule (EpCAM)[128], the B cell marker CD20[129], human epidermal growth factor receptor 2 (HER2/neu)[130], and disialoganglioside GD2[131], among others. As an alternative, the targeting of tumor necrotic tissue has been achieved using antibodies against histone/DNA complexes[132]. TAAs expressed in the extra-cellular matrix represent another important class of targets for delivery applications[124]. Of note, alternatively-spliced isoforms of fibronectin containing the extra domains EDA or EDB have been detected in the majority of hematological and solid malignancies in both human and mice, while being virtually absent in healthy organs (except for placenta, uterus, and ovary)[133-135].

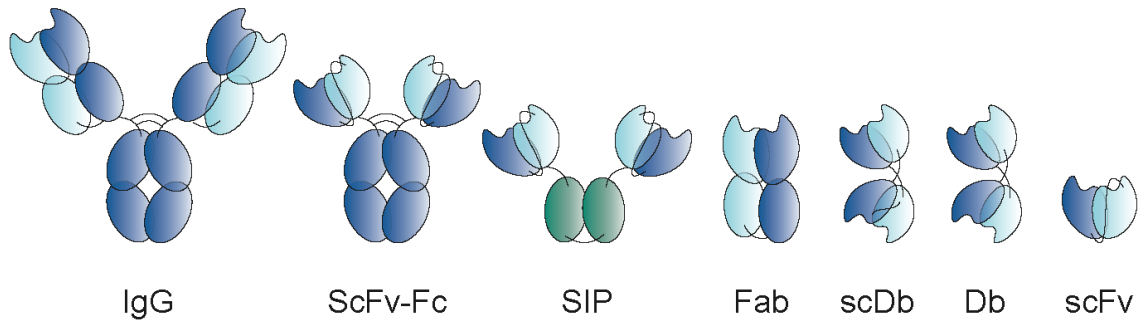

*Figure 6: **Antibody formats**. Schematic illustration of some of the existing antibody formats. IgG: Immunoglobulin G, ScFv-Fc: single-chain variable fragment-constant fragment, SIP: small immunoprotein, Fab: fragment having the antigen-binding site, scDb: single-chain diabody, Db: diabody, scFv: single-chain variable fragment. All fragments are derived from the IgG structure, except for the SIP, which contains the 4th constant heavy domain of the IgE structure (green).*

Different antibody formats have been considered for the delivery of cytokines, with the full IgG and the diabody formats being the most popular[136]. Conjugate stability, pharmacokinetic properties, and tumor accumulation may be influenced by the format of choice[124, 136]. Although both cytokine-conjugated IgGs and diabodies exceed the cut-off size for glomerular filtration,

IgG molecules are stabilized by interchain disulfide bonds and can be recycled through binding of the neonatal Fc receptor via their Fc domain, which results in a longer serum half-life and increased accumulation at the tumor site[137-139]. On the other hand, formats with smaller molecular sizes may extravasate more readily, penetrate deeper in the tumor mass and generally show more selective accumulation at the site of disease[140, 141]. Finally, some immunocytokines may fail to fold properly or loose *in vivo* targeting ability when genetically coupled with an antibody in an unsuitable format[124].

The cytokine payload confers the biological activity but also contributes to molecular stability and targeting performance. Although immune-conjugates based on many different cytokines are being investigated in preclinical models of cancer, only IL2-, IL12-, IL15-[142, 143], TNF-, and CD137L-based[143] products have reached clinical development so far[136].

3.5.3 LIGHT (TNFSF14)

The tumor necrosis factor superfamily is a family of 19 proteins containing the TNF-homology domain and predominantly expressed by immune cells[144]. The majority of TNF-superfamily members are locally active type II transmembrane proteins, however, soluble forms of most members have been identified, which are produced either by alternative-splicing or by proteolytic cleavage of their extracellular domain and act as cytokines[144]. At the cellular level, upon binding to their cognate receptors (29 TNF receptors have been identified so far), they may promote apoptosis, survival, proliferation, or differentiation[144]. TNF superfamily members and their receptors have been implicated in various pathologies including osteoporosis, septic shock, different autoimmune diseases, and cancer progression[144].

Several successful antibody therapeutics act as inhibitors of TNF or TNFR superfamily members, including the best-selling drug adalimumab (Humira®, AbbVie), an anti-TNF monoclonal antibody approved for various autoimmune conditions[145, 146]. Because of their role as inflammatory mediators, their pleiotropic effect on various immune cells, and their cytotoxic ability, various members of the TNF superfamily have been considered as anti-tumor therapeutics.

LIGHT, which stands for homologous to **L**ymphotoxin, exhibits **I**nducible expression and competes with HSV **G**lycoprotein D for binding to **H**erpesvirus entry mediator, a receptor

expressed on **T** lymphocytes, is the member 14 of the TNF superfamily (TNFSF14). It is expressed on monocytes, granulocytes, immature DCs, and mature T cells, and can be cleaved by proteases resulting in a soluble functional form[147]. Like other TNF superfamily members, LIGHT forms a non-covalent homotrimer and signals via trimerization of its cognate receptors[147].

LIGHT can bind to three receptors: the herpes virus entry mediator (HVEM) expressed on immature and memory T cells, NK cells, and DCs, the lymphotoxin-beta receptor (LTβR) expressed mainly in non-lymphoid hematopoietic cells and stromal cells, and the decoy receptor 3 (DcR3), which is a soluble receptor present in humans but not in mice, able to neutralize LIGHT, FasL, and TL1A, and upregulated in various tumors[147, 148]. HVEM has both signal-transducing and signal-eliciting function and together with LIGHT, and the two immune checkpoint molecules BTLA and CD160 form a complex network of signaling involved in both promotion and inhibition of immune functions[147, 149]. In a nutshell, LIGHT delivers a costimulatory signal to HVEM-expressing cells, which can drive T cell differentiation and proliferation, promote secretion of IFNγ by NK cells or expression of co-stimulatory molecules like CD80/86 on DCs. LIGHT-mediated activation of the LTβR, instead, induce expression of a series of adhesion molecules and chemoattractant on target cells and play an important role in lymphoid organs organization and maintenance, and tertiary lymphoid structures (TLSs) formation[150, 151 152].

TLSs are very similar to secondary lymphoid organs like lymph nodes, both in terms of function and organization. They arise in non-lymphoid peripheral tissues, at sites of chronic inflammation, and have been associated with autoimmune tissue destruction[152]. The spontaneous formation of TLSs has been described in several types of cancer and is usually correlated with positive patient outcomes[153].

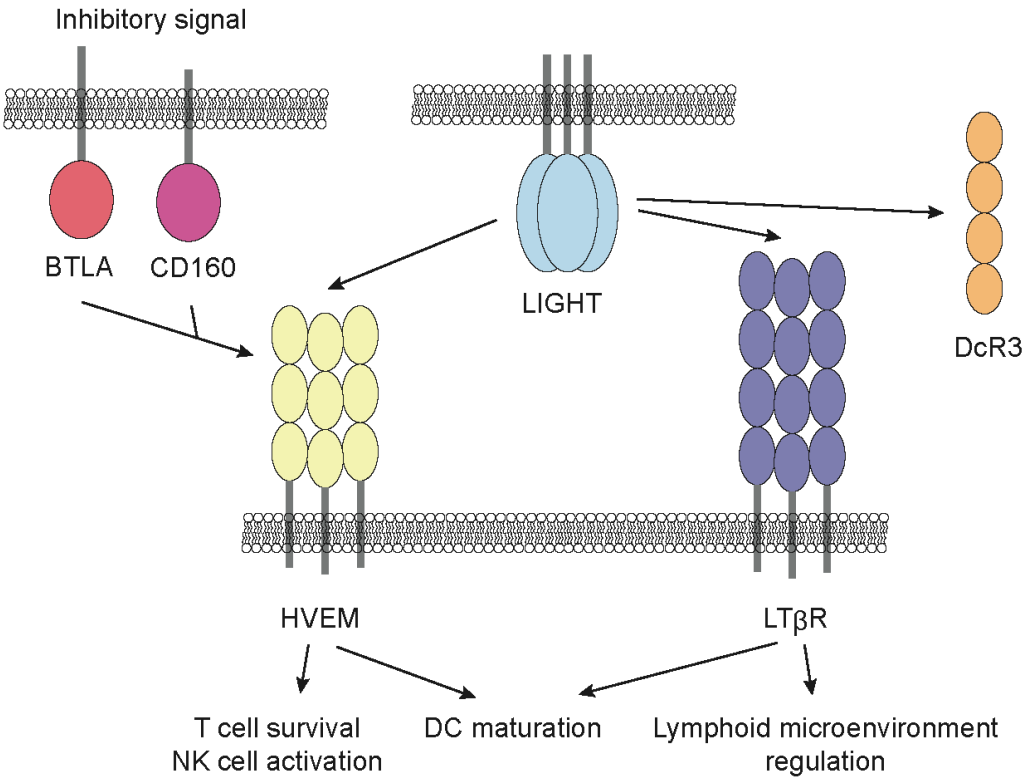

*Figure 7: **LIGHT signaling**. LIGHT can bind and activate both HVEM and LTβR, resulting in pro-inflammatory effects. Humans, but not mice, have an additional soluble receptor for LIGHT, which can prevent LIGHT interaction with its two stimulatory receptors: the decoy receptor 3 (DcR3). BTLA and CD160 are two additional HVEM ligands, which mediate T cell inhibition. Image adapted from[150].*

Shreds of evidence for a potent antitumor effect of LIGHT have arisen from various preclinical studies in the last decade. Two independent studies with engineered tumor expressing LIGHT demonstrated that both constitutive- and inducible expression of LIGHT in the tumor resulted in a massive CD8+ T cell infiltration and rejection of the tumor[154, 155]. T cells were actively recruited into the tumor via expression of adhesion molecules like MadCAM-1 and the chemokines CCL21 and CXCL9, induced by LTβR-signaling on stromal cells, and directly primed *in situ* via TCR activation and HVEM co-stimulation[154]. In other studies, the delivery of recombinant LIGHT using short peptides specific for the aberrant tumor vasculature lead to vasculature normalization, TLSs formation, and reduced tumor burden upon combination with immune-checkpoint blockade[156-158]. Complete tumor eradication was achieved by adenovirus-delivery of LIGHT directly into the tumor[159] and partial tumor regressions were observed in studies employing mesenchymal stem cells or bacteria expressing LIGHT[160, 161].

Despite its anti-tumor potential, the cytokine LIGHT has so far failed to attract the attention of pharmaceutical companies, which have been focusing more on other members of the TNF

superfamily. This may be partly due to the fact that human LIGHT does not cross-react with murine receptors[162], and murine LIGHT, which would be needed to run experiments in immunocompetent mice, is notoriously unstable[162-164]. In fact, the above mentioned preclinical studies employing recombinant LIGHT protein were performed with a peptide-conjugated truncated version of murine LIGHT produced in bacteria (with modest therapeutic activity).
Only one recent study employed an immunocytokine based on LIGHT. The immunocytokine, featuring an engineered version of human LIGHT capable of interacting with murine receptors, was able to recruit CD8+ T cells in poorly-infiltrated tumors resistant to therapy with immune checkpoint blockade, and synergized with anti-PD-L1 to eradicate established tumors[162].

3.6 Aim of the thesis

The recent success of immune-checkpoint inhibitors and adoptive cell therapy has revolutionized cancer treatment. ACT with TILs has shown remarkable efficacy in metastatic melanoma, CAR-T cell therapy allowed to reach unprecedented remission rates in several hematological malignancies, and antibodies blocking PD-1, PD-L1, and CTLA-4 have been successfully employed for different tumor types. All these treatments rely on the effect of tumor-specific CD8+ T cells, which are either directly used as a therapy, or indirectly activated *in vivo*.

Although these approaches have improved the outcome of several patients with cancer, they all still present obvious limitations. CAR-T cells have so far generally failed to show efficacy in solid tumors and their use in cancer treatment is limited by severe toxicity[165, 166].
Tumor-specific TILs have been generated with consistency from melanoma samples but not from other malignancies, except for few isolated cases in which the employment of an elaborate selection protocol allowed to enrich for highly personalized neoantigen-specific TILs[82, 89]. Moreover, the extensive *ex vivo* culturing, necessary to expand tumor-specific T cells to the high numbers needed for therapy, results in terminally differentiated TILs with reduced life-spam and limited engraftment potential[167]. Finally, only a relatively small fraction of patients responds to therapy with immune checkpoint-inhibitors and a key pre-requisite for both TILs and immune-checkpoint blockade therapy is the presence of T cell in the tumor, which cannot be taken for granted[168, 169].

Immunocytokines represent a valid alternative or complement to immune-checkpoint inhibitors. Besides having a direct co-stimulatory effect on CD8+ T cells, certain pro-inflammatory cytokines may influence the immunosuppressive tumor microenvironment more broadly, activating other immune effector cells and contributing to the development of a more sustained immune response[136]. LIGHT elevation in the tumor lead to recruitment and activation of CD8+ T cells in preclinical studies, demonstrating the potential of this cytokine in cancer therapy and in particular in cold tumors – i.e. tumors with little or no CD8+ T cell infiltration, where neither immune-checkpoints inhibitors nor ACT may be of help[170].
One aim of this thesis was to develop a novel immunocytokine to target recombinant LIGHT to the tumor extracellular matrix and investigate its anti-tumor activity in syngeneic murine models of cancer.

Previous work in our group has shown how immunocytokines based on IL2, TNF, and IL12, can eradicate established tumors in mice, either alone or in combination with immune-checkpoint inhibitors, in a process mainly mediated by CD8+ T cells[171-173]. In particular, successful immunotherapy with TNF- or IL12-fusion proteins in multiple syngeneic tumor models of BALB/c origin was accompanied by an expansion of a population of CD8+ T cells specific for the rejection antigen AH1[174, 175]. AH1 is an H-2L^{d}-binding peptide derived from the endogenous murine leukemia virus envelope glycoprotein 70 (gp70)[176]. This retroviral protein is not detected in healthy tissues of BALB/c mice while being expressed in a multitude of murine tumors[174, 176].

Part of this thesis was aimed at better elucidating the role of the AH1 immunogenic peptide in the tumor rejection process, following-up on previous work performed in our laboratory[174, 175, 177]. In particular, we wanted to generate a pure population of AH1-specific CD8+ T cells and see if the transfer of these cells with a single specificity into tumor-bearing hosts could mediate tumor regression *per se*.

4 Immunotherapy of CT26 murine tumors is characterized by an oligoclonal response of tissue-resident memory T cells against the AH1 rejection antigen

This chapter correspond to the published paper: "Immunotherapy of CT26 murine tumors is characterized by an oligoclonal response of tissue-resident memory T cells against the AH1 rejection antigen" by Marco Stringhini, Philipp Probst and Dario Neri, European Journal of Immunology, May 2019.

4.1 Introduction

Successful immunotherapy is able to induce durable complete responses against certain types of tumors, both in animal models of cancer and in patients. For instance, a subset of immunogenic tumors responds to PD-1 blockade and durable complete responses have been described in patients with advanced melanoma [178]. Similarly, a proportion of patients with metastatic melanoma or renal cell carcinoma can be cured using high-dose interleukin-2 treatment [179, 180]. In animal models, cures of CT26 colorectal cancer have been described in mice receiving immune checkpoint inhibitors [171], antibody-cytokine fusions [174, 175] or a combination of these two treatment modalities [171, 175].

$CD8^+$ T cells play a crucial role in the tumor rejection process [181]. Highly-mutated tumors (e.g., melanomas and non-small cell lung cancers) typically respond better to immune checkpoint inhibitors and neo-antigens (i.e., mutated peptides presented on HLA class I molecules) contribute to tumor rejection [182, 183]. Experimental evidence indicates that also aberrantly-expressed antigens (originating from "non-coding regions" in the human genome) may contribute to tumor surveillance and cancer rejection [184]. Recently, Laumont et al. have described that about 90% of targetable tumor specific antigens in two murine cancer cell lines and seven human primary tumors were derived from non-coding regions [184].

AH1 possibly represents the best characterized tumor rejection antigen in mice. It is derived from the gp70 envelope protein of murine leukemia virus (MuLV), which is endogenous in the genome of most laboratory mouse strains [185]. AH1 was first described by Huang et al. [186] as the major rejection antigen of the CT26 colorectal cancer and it has since been used as a model antigen to investigate $CD8^+$ T cell immunity in different mouse tumor cell lines [187]. Rudqvist

and colleagues have recently characterized the TCRβ sequences of AH1-specific clones in BALB/c mice, following radiotherapeutic intervention in combination with CTLA-4 blockade [188].

Our group has previously shown that immunocompetent mice bearing syngeneic tumors could be cured using certain antibody-cytokine fusions with tumor-homing properties. Two antibodies (F8 and L19, specific to the alternatively-spliced EDA and EDB domains of fibronectin, respectively) were found to selectively localize to solid tumors following intravenous administration [189, 190] and were used to deliver various types of cytokine payloads to the tumor environment [191]. Indeed, the F8-mTNF and L19-mIL12 fusion proteins can be used to selectively deliver a proinflammatory cytokine payload to the tumor, helping spare normal tissues [172, 175]. Both products were able to cure BALB/c mice with different types of malignancies [172, 175]. FACS analysis of tumor-infiltrating $CD8^+$ T cells (TILs) had revealed that AH1-specific T cells represented the majority of $CD8^+$ lymphocytes within the neoplastic mass, both at the onset of therapy and after a successful therapeutic intervention.

In this Communication, we have characterized the features of TILs (isolated from tumors of mice which had been treated with F8-mTNF, L19-mIL12 or with saline) using a combination of TCR sequencing and total mRNA sequencing. Our data suggest that successful immunotherapy of CT26 tumors requires an oligoclonal expansion of functional tumor-specific tissue-resident memory $CD8^+$ T cells (T_{RM}) and that a relatively small number of lymphocyte specificities drive the tumor rejection process.

4.2 Results and Discussion

4.2.1 $CD8^+$ T cells response against CT26 is highly clonal

To analyze changes in the TCR repertoire induced by L19-mIL12 and F8-mTNF, tumors and spleens of treated mice were excised 48 h after the second injection of the immunocytokine. 100'000 $CD8^+$ T cells from spleens and tumor cell suspensions of individual mice (n = 3 per group) were sorted, DNA was extracted and used to perform TCR deep sequencing, with a focus on CDR3β. More than 40'000 unique TCR sequences were found, but their relative frequency varied considerably. Indeed, the ten most frequent CD8+ T cell clones accounted for more than 60% of the TCR sequences found within the tumor for the various treatment groups (**Figure 8A-B** and **Supplementary Information**). By contrast, sequences were more evenly distributed within the spleen, where a cumulative frequency of only 3.74% (L19-mIL12 treated mice) – 8.81% (F8-mTNF treated mice) was observed for the ten most frequent $CD8^+$ T cell clones (**Figure 8A**). TCR diversity was further analyzed using the inverse Simpson's index and the Gini coefficient. Both parameters revealed a high clonality of TCR sequences within the CT26 tumor mass and a low clonality of spleen-derived $CD8^+$ T cells, independent of the treatment modality (**Figure 8C-E**). In line with the stochastic nature of the TCR rearrangement process [192], a comparison of TCR sequences from $CD8^+$ T cells found in the tumors of mice treated with different agents (saline, L19-mIL12 and F8-mTNF) revealed that only few sequences where shared among different mice (**Figure 8F** and **Supplementary Table 1**). To analyze the anti-AH1 response, we sorted AH1/H-$2L^d$ tetramer–positive $CD8^+$ T cells from spleens and tumors of pooled mouse samples for each different group and performed single-cell sequencing of their TCR region. Sequence analysis revealed that AH1-specific clones featured consistently among the most frequent lymphocytes within the tumor mass of mice treated with immunocytokines (**Supplementary Table 2**) or saline (**Supplementary Table 3**). Single-cell sequencing results were also used to match AH1-specific TCRβ with their correspondent TCRα sequences, resulting in the identification of 27 unique pairs (**Supplementary Table 4**).

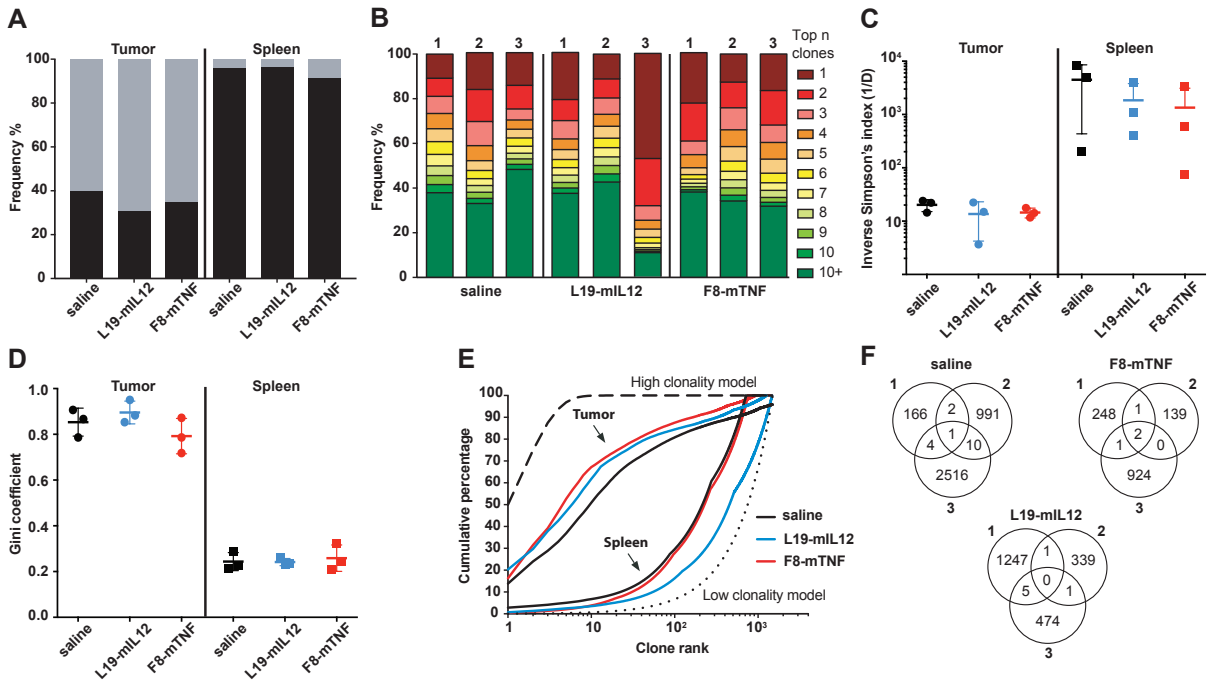

*Figure 8: **Analysis of CD8+ T cell clonotypes within tumor and spleen**. **A-B,** Visualization of clone frequency occupancy by the 10 most frequent CD8$^+$ T cell clones based on CDR3 nucleotide sequence. Columns in A represents the average frequency distribution of the T cell clones within the tumor (left) or within the spleen (right) from animals of the different treatment groups. The Top 10 clones are shown in grey, black represents all the other CD8$^+$ T cell clones. In **B,** each column represents the frequency distribution of the T cell clones within the tumor of each individual animal. Colors represent the clone ranking. **C-D,** Inverse Simpson's index values (C) and Gini index values (D) of CD8$^+$ T cells within the tumor (left) or spleen (right) in mice of the different treatment groups. Individual data are represented with means ± SEM **E,** Average cumulative frequency distribution. CD8$^+$ T cell clones were ranked according to their frequency for each mouse and the average cumulative frequency distribution was calculated for the treatment groups. Two models were included in the graph to illustrate a high and a low clonality distribution. For the low clonality model (dotted line), all clones shared a frequency of 0.069% (100%/1450), whereas in the high clonality model (dashed line) a clone with rank "x" was given a frequency of 50%/2^{x-1}. **F,** Venn diagrams of unique CDR3 nucleotide sequences found in TILs of each individual animal from the respective treatment group. n = 3 mice per experimental group, data are combined from 2 independent therapy experiments.*

Immunocytokine treatment influences the intratumoral TCR repertoire

To gain further insights into the effects of immunocytokine treatment on the TCR repertoire of TILs, we determined the frequency of the TRBJ and TRBV segment usage and the CDR3 length distribution for each animal. This analysis revealed a significant increase in the frequency of the TRBJ 01-03 gene segment (**Figure 9A**) in L19-mIL12 treated mice compared to saline ($p = 0.009$) and F8-mTNF ($p = 0.012$). In contrast, the usage of TRBJ 02-07 was significantly lower ($p = 0.004$ compared to saline and $p < 0.0001$ compared to F8-mTNF treatment). L19-mIL12 treated mice also showed an increased usage of the TRBV 02-01 ($p = 0.001$ compared to F8-mTNF group) and 31-01 gene segments ($p = 0.035$ and $p = 0.011$ compared to saline and F8-mTNF treatment, respectively) (**Figure 9B**). A decreased frequency of the TRBV 13-01 gene was observed in immunocytokine treated mice compared to saline ($p = 0.001$). Analysis of the CDR3 length distribution revealed no significant change between the three groups with a preferential length of 42 base pairs (**Figure 9C**).

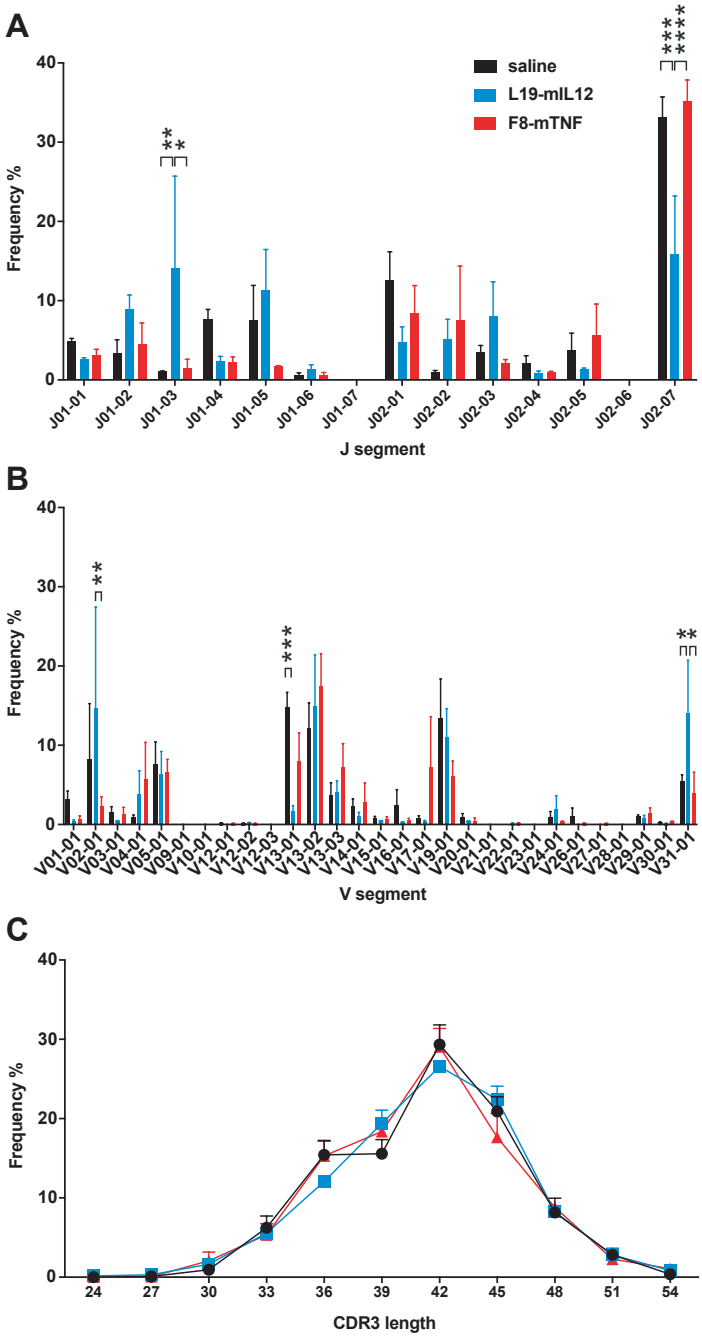

*Figure 9: **TRBJ and TRBV segment usage, CDR3 sequence length**. **A-B,** Bar plot indicating the average usage of the different TRBJ- (A) and TRBV- (B) gene segments in individuals from the different treatment groups. **C,** CDR3 sequence length comparison based on nucleotide sequence. Data represent means + SEM, n = 3 mice per experimental group, data are combined from 2 independent therapy experiments. * = $p < 0.05$, ** = $p < 0.01$, *** $p = < 0.001$, **** = $p < 0.0001$ (two-way ANOVA test with the Bonferroni post-test).*

4.2.2 AH1-specific CD8$^+$ TILs express genes characteristic of tissue-resident memory T-cells

In order to investigate differences in phenotype or activation status between TILs in mice treated with L19-mIL12 or saline, we performed mRNA sequencing of AH1-specific CD8$^+$ T cells isolated from CT26 tumors from the two treatment groups (n = 3 per group). In addition,

we sequenced mRNA from AH1-negative $CD8^+$ T cells isolated from secondary lymphoid organs. AH1-specific cells from tumors of both groups showed a genetic signature typical of tissue-resident memory T cells (T_{RM}), characterized by upregulation of the transcription factors Blimp-1, AhR and NR4A1 and downregulation of Eomes (**Figure 10A**). Compared to $CD8^+$ T cells from lymphoid organs, these cells had very low level of KLF2, TCF1 and of their downstream targets CD62L and S1P1, which are needed to traffic out of tissues and back to secondary lymphoid organs. Moreover, they expressed a number of adhesion molecules associated with retention in non-lymphoid tissues. In keeping with FACS results [193], AH1-specific TILs overexpressed various immune checkpoint receptors, including PD-1, Tim-3, Lag-3, CTLA-4 and CD39. As expected, the cells had an effector phenotype, characterized by elevated mRNA levels of granzyme-B, perforin, TNFα, IFNγ and FasL (**Figure 10A**). The T_{RM} genetic signature was more marked in IL12-exposed cells compared to saline controls. For example, expression of Blimp-1 and of the integrin-α subunit CD49a was significantly upregulate in the L19-mIL12 treatment group, whereas KLF2 and of the lymphoid-tissue homing CCR7 were significantly downregulated (**Figure 10B**).

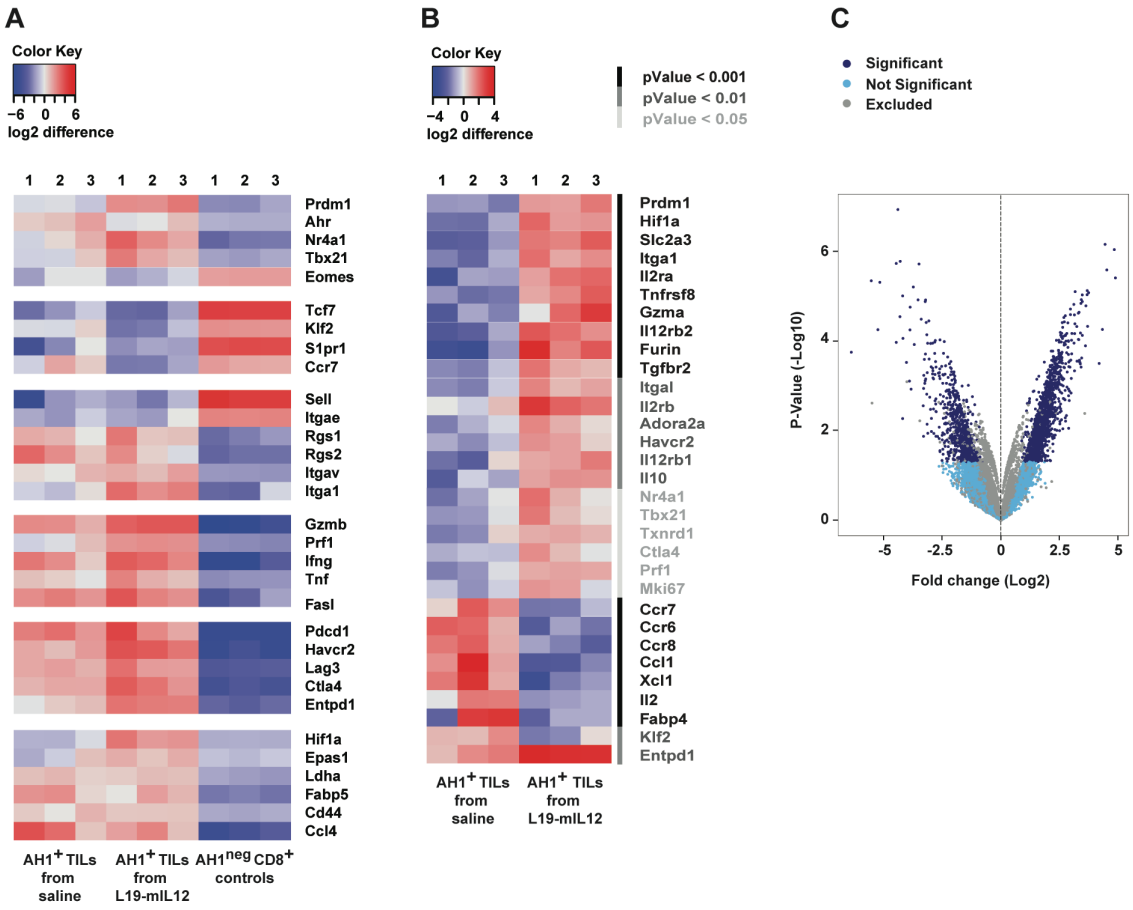

Figure 10: ***Transcriptome analysis of AH1-specific TILs****. **A**, Relative expression of genes characteristic of T_{RM} in AH1-specific TILs from individual mice after different treatments compared to $CD8^+$ AH1-negative T cells isolated from secondary lymphoid organs (Control). P-Value < 0.001 (generalized linear model adapted for over-dispersed data with Benjamini and Hochberg correction) relative to at least one treatment group, compared to control. **B**, Heat map showing differential expression of representative genes (P-Value < 0.05) between AH1-specific TILs from saline- and L19-mIL12-tretaed Tumors. **C**, Expression of all mRNA sequences identified in AH1-specific, IL12-exposed TILs relative to AH1-specific TILs from saline-treated tumors. Significant = P-Value < 0.05, exclusion criteria: Read count < 20 reads for all samples. n = 3 mice per experimental group, data are from one therapy experiment.*

4.2.3 AH1-specific $CD8^+$ TILs are activated by immunocytokine treatment

Overall, AH1-specific TILs from the two groups shared more similarities between each other than with control AH1-negative $CD8^+$ T cells from secondary lymphoid organs. Nevertheless, 2699 differentially-expressed genes were identified (P-Value < 0.05) between treatment-groups (**Figure 10C**). Interestingly, tumor-specific T cells from IL12 tumors expressed higher level of activation markers (e.g., IL2rα and CD30), higher levels of inhibitory receptors, of effector molecules like granzyme-A and perforin and also higher levels of gene associated with increased metabolism and proliferation, like the high-affinity glucose transporter GLUT3, the enzyme thioredoxin reductase 1 and the proliferation marker Ki67 (**Figure 10B**). Consistent with an impact of the immunocytokine on the phenotypic and activation status of these cells,

IL12-exposed tumor-specific TILs significantly overexpressed both subunits of the IL12-receptor and the proprotein convertase furin, a gene induced by IL12, which enhances secretion of IFNγ by T cells [194] . Taken together these results suggest that antigen recognition in the tumor drives $CD8^+$ T cells toward a T_{RM} phenotype and that IL12 may enhance the cytotoxic and proliferative potential of these T_{RM}.

4.3 Concluding remarks

Irrespective of the treatment given to mice, the immune response in CT26 tumors is characterized by an oligoclonal expansion of few $CD8^+$ T cells clones, mostly specific for the AH1 rejection antigen. Single mice of all groups were capable of generating different TCRs able to recognize the AH1 peptide presented on MHC class I. The generated TCRs, including the few dominant clones infiltrating the tumor, were highly individual. We found some treatment-induced preferential usage of TCRB and -J segments, but whether the corresponding TCRs correlate with improved functional avidities toward tumor antigens remain to be investigated. mRNA analysis revealed that AH1-specific TILs had a T_{RM} phenotype and exposure to L19-mIL12 resulted in a significant upregulation of a multitude of genes related to activation, increased metabolism and proliferation. T_{RM} are commonly referred to as $CD69^+$, $CD103^+$ and/or $CD49a^+$. AH1-specific T_{RM} did not express CD103 whereas CD49a was upregulated only in IL12-exposed cells. Interestingly, CD49a was previously described as a marker of functional tumor-resident T cells and its expression correlated with prolonged survival in peptide-vaccinated melanoma patients [195]. The fact that our IL12-based therapeutic selectively accumulates at site of disease, together with the clonality of TCR sequences observed in the tumor, supports the hypothesis of a local activation and expansion of tissue-resident AH1-specific T cells in the tumor and highlights the central role of T_{RM} in cancer immunotherapy. Nevertheless, replenishment of $CD8^+$ T cells from secondary lymphoid organs may also play a role, since we saw an increase of AH1-specific T cells in secondary lymphoid organs upon treatment with both F8-mTNF and L19-mIL12 [175, 193]. Our study also highlights possible limitations associated with the evaluation of $CD8^+$ T cell "fitness" based exclusively on expression of exhaustion markers. PD-1 and other exhaustion markers were found to be overexpressed in AH1-specific TILs from different treatment groups, but targeted cytokine delivery could nonetheless induce complete and durable tumor regression [175, 193]. T_{RM} cells seem to play a central role in anti-tumor immunity and a detailed characterization of this cell population may influence the design of future anticancer therapeutic strategies.

5 Antibody-mediated delivery of LIGHT to the tumor boosts Natural Killer cells and delays tumor progression

This chapter corresponds to the submitted manuscript: "Antibody-mediated delivery of LIGHT to the tumor boosts Natural Killer cells and delays tumor progression", by Marco Stringhini, Jacqueline Mock, Vanessa Fontana, Patrizia Murer and Dario Neri.

5.1 Introduction

Immunotherapy of cancer is gaining momentum based on the realization that a subset of patients may enjoy durable responses upon treatment with immunotherapeutic agents [196]. Immune checkpoint inhibitors (e.g., antibodies directed against PD-1, PD-L1 and CTLA-4) have shown activity against different types of cancer and are widely used in the clinical practice [32, 197, 198]. Cytokines represent a complementary class of therapeutic proteins which modulate the activity of the immune system and engineered cytokine products are increasingly being used (alone or in combination) for oncological applications [180, 199, 200]. Cytokines are typically active in patients at very low doses (often at less than 1 milligram) and have a narrow therapeutic window. Research efforts have been dedicated to the development of more selective types of cytokine-based therapeutics with improved activity and/or safety.

Tumor-targeting antibody-cytokine fusions (also called "immunocytokines") represent a promising class of anticancer agents and some of these products have moved to advanced clinical trials [201]. A preferential accumulation of the cytokine payload in the neoplastic mass may help boosting the activity of tumor-resident T cells and Natural Killer (NK) cells locally [202], resulting in lower systemic toxicity [171, 175]. In a number of comparative preclinical studies, tumor-homing immunocytokines were substantially more active than fusions based on antibodies of irrelevant specificity, even though this difference may be less drastic for long-lived IgG-based products [203-208].

LIGHT (which stands for homologous to **L**ymphotoxin, exhibits **I**nducible expression and competes with HSV **G**lycoprotein D for binding to **H**erpesvirus entry mediator, a receptor expressed on **T** lymphocytes) is a member of the tumor necrosis factor (TNF) superfamily expressed on a number of immune cells, including immature dendritic cells and activated T lymphocytes [209]. The membrane-anchored form of LIGHT can be cleaved by proteases between

residues L81 and I82, resulting in a functional soluble form [154]. This cytokine binds to two receptors: HVEM (expressed on T cells, NK cells and dendritic cells) and LTβR (expressed mainly on non-lymphoid cells) [210]. Upon homotrimerization and interaction with HVEM, LIGHT activates the NF-κB pathway leading to activation and stimulation of target lymphocytes, whereas signaling through LTβR leads to expression of chemokines and adhesion molecules involved in lymphoid organs organization and maintenance [150, 151, 209]. Transgenic expression of LIGHT on tumor cells has been shown to mediate a potent anti-tumor effect in mice [154, 155]. In two independent studies, LIGHT expression resulted in a massive increase of CD8+ T cells infiltration, which played a central role in the tumor rejection process, as demonstrated by depletion experiments [154, 155].

A fusion of murine LIGHT with the F8 antibody (specific to the alternatively-spliced EDA domain of fibronectin, a conserved tumor-associated antigen) has previously been described, using the antibody in scFv format and relying on the ability of LIGHT to form stable non-covalent homotrimers [211]. The resulting fusion protein was homogeneous in biochemical characterization assays and maintained binding ability *in vitro*. However, in contrast to the results obtained with fusions of the F8 antibody with both murine and human TNF (which showed selective uptake at the tumor site with excellent biodistribution results), the fusion of scFv(F8) and murine LIGHT exhibited a poor uptake at the tumor site and a rapid clearance from the body [211]. It has previously been reported that members of the TNF superfamily may gain stability when expressed as a single polypeptide, with linkers connecting the three monomeric subunits [212, 213].

Here, we describe the cloning, expression and characterization of five novel fusion proteins, featuring murine LIGHT expressed as a single polypeptide (comprising the three monomeric subunits) as cytokine payload and the F8 antibody in different formats as tumor-targeting agent. Out of the five fusion proteins that were produced and purified, only the use of the F8 antibody in single-chain diabody format resulted in a product with adequate biochemical and immunological properties. The fusion protein preferentially accumulated in tumor lesions and mediated a potent anticancer activity, which was mainly depended on Natural Killer cells and which was not potentiated by PD-1 blockade.

5.2 Results

5.2.1 Expression and characterization of F8-LIGHT fusion proteins

LIGHT is a homotrimeric protein, that can activate HVEM and LTβ receptors [13,17] (**Figure 11A**). We cloned, expressed and characterized five different versions of the F8 antibody, fused to murine homotrimeric LIGHT expressed as a single polypeptide. Specifically, we fused LIGHT at the C-terminus of the heavy or of the light chain of the F8 antibody in human IgG1 format, at the C-terminus of the F8 antibody in human scFv-Fc format and at the C-terminus of the F8 antibody in human single-chain diabody and diabody format. (**Figure 11B**). All products could be purified to homogeneity by protein A chromatography, as shown by SDS-PAGE analysis. However, a comparative evaluation of size-exclusion chromatography profiles revealed that only the single-chain diabody-based product (termed F8-LIGHT), ran as a single peak in gel filtration (**Figure 11B**), showed a single band in SDS-PAGE and a single peak in mass spectrometry, after PNGase F treatment (**Figure 11C**). F8-LIGHT was able to bind its cognate target antigen with high affinity *in vitro*, as shown by ELISA (**Figure 11E**) and was able to induce death of HT-29 cells in the presence of interferon gamma (**Figure 11F**). When the cytotoxicity experiment on HT-29 cells was repeated with commercially available recombinant murine LIGHT as control, F8-LIGHT showed a higher activity, possibly as a result of the increased stability of the LIGHT moiety expressed as a covalently-linked homotrimer [212, 213] (**Supplementary Figure 1**). Dissolved in saline, the product was stable for months both at 4°C and at -80°C, even after repeated cycles of freeze-and-thaw (**Supplementary Figure 2**).

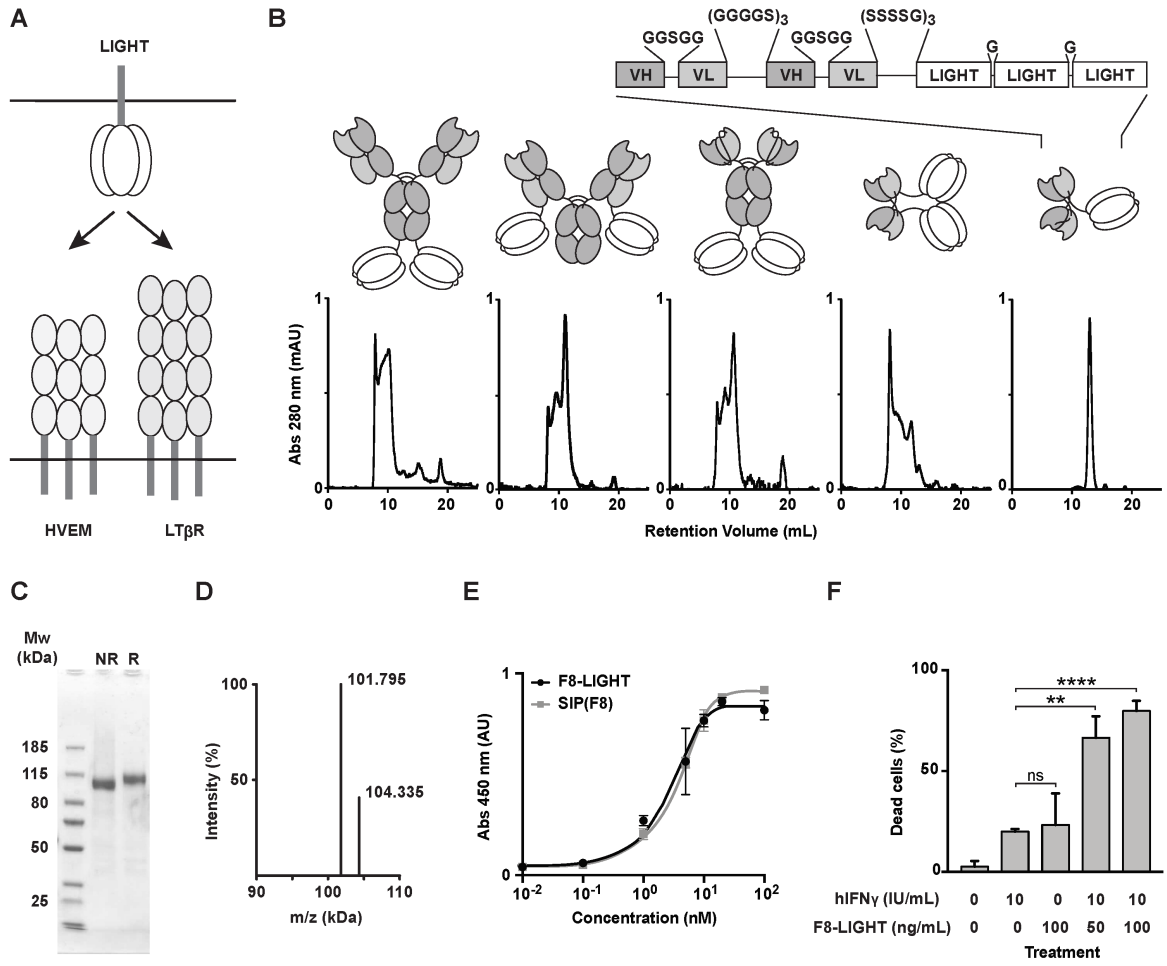

*Figure 11: **In vitro characterization of fusion proteins**. **A**, schematic representation of membrane-anchored LIGHT and cognate receptors HVEM and LTβR. **B**, schematic representation of five LIGHT-based fusion proteins, with respective size exclusion chromatography profiles. The homotrimeric form of LIGHT expressed as a single polypeptide chain was fused to the C-terminus of (from left to right): the heavy chain of F8 in IgG format, the light chain of F8 in IgG format, the F8 in scFv-Fc format, the F8 in diabody format and the the F8 in single-chain diabody format (F8-LIGHT). Detailed linear structure of F8-LIGHT is highlighted. **C-D**, biochemical characterization of F8-LIGHT including SDS-PAGE of F8-LIGHT under non-reducing (NR) and reducing (R) conditions (**C**) and mass spectrometry profile of PNGase F-treated F8-LIGHT (calculated mass = 101791 Da) (**D**). **E**, binding of titrated concentrations of F8-LIGHT and positive control SIP(F8) to immobilized target antigen EDA, measured by ELISA. **F**, activity of F8-LIGHT, measured by a cytotoxicity assay on HT-29 cells in the presence of human Interferon gamma (hIFNγ). Reported concentrations are based on the molecular weight of the LIGHT part of the molecule alone. 7-AAD positive dead cells were detected by Flow Cytometry. Column represent means ± SEM, n = 3 per experimental group, ns = non significant, * = $p < 0.05$, ** = $p < 0.01$, *** $p = < 0.001$, **** = $p < 0.0001$ (unpaired t-test).*

5.2.2 F8-LIGHT selectively accumulate at tumor site in vivo

In order to test the *in vivo* targeting ability of our product, we performed a quantitative biodistribution study by intravenous injection of ^{125}I-labeled F8-LIGHT. We used LIGHT linked to the KSF antibody (specific to hen egg lysozyme) as negative control of identical format (**Figure 12**). After 24h, about 4.5% of the injected dose of F8-LIGHT per gram of tissue was found in the tumor, with a tumor-to-blood ratio of 4.9. Similar to what previously reported for other antibody-cytokine fusion proteins, the transfection protocol used for transient gene

expression procedures had an impact on biodistribution results [214, 215] (**Supplementary Figure 3**).

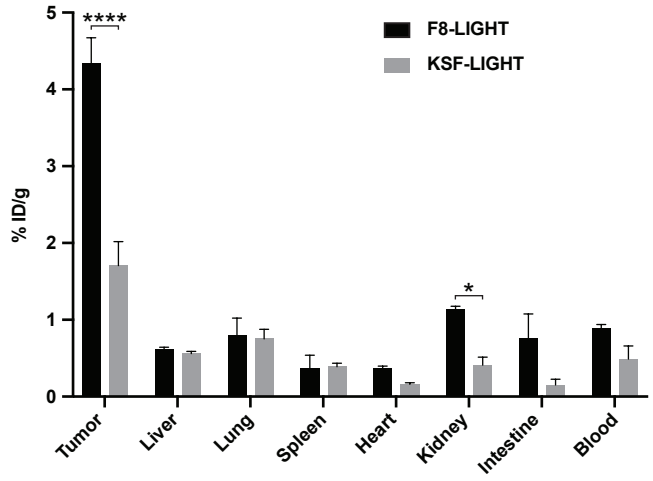

*Figure 12: **Tumor targeting of F8-LIGHT in vivo**. Biodistribution experiment in 129/Sv mice bearing F9 tumor. Radioiodinated F8-LIGHT and KSF-LIGHT (used as negative control) were injected in the lateral tail vein. Accumulation of the fusion proteins in tumor and healthy organs after 24 hours was calculated as percentage of injected dose per gram of tissue (% ID/g). Column represent means ± SEM, n = 4 per experimental group, * = p < 0.05, ** = p < 0.01, *** p = < 0.001, **** = p < 0.0001 (unpaired t-test).*

5.2.3 F8-LIGHT delays progression of established murine tumors

To evaluate the anti-tumor activity of F8-LIGHT, we performed a first therapy experiment in BALB/c mice bearing subcutaneous CT26 murine colon carcinoma, since forced expression of LIGHT in this model had previously shown the ability to induce complete tumor regression [155]. Treatment was initiated when tumors had reached a volume of about 100 mm^3 and consisted in intravenous injection of 100 µg F8-LIGHT every other day, for a total of three injections. Treatment with F8-LIGHT induced tumor growth retardation, whereas the KSF-LIGHT fusion protein used as negative control gave profiles similar to the ones obtained in the saline treatment group. As no toxicity had been observed (**Figure 13A**), the dose was increased to 300 µg/injection, which was still well tolerated but did not significantly improve anti-cancer activity (**Figure 13B**). In order to exclude a direct effect of the antibody portion of F8-LIGHT, we produced and characterized the F8 antibody in single-chain diabody format (**Supplementary Figure 4**) and include it as a control in a new therapy experiment. We also included a group to investigate the effect of F8-LIGHT combined with PD-1 blockade. F8 treatment did not show any detectable anti-tumor effect, whereas combination of F8-LIGHT and anti-PD-1 antibody performed better than F8-LIGHT monotherapy. PD-1 treatment alone had an effect comparable

to that of F8-LIGHT monotherapy till experimental day 14, when 3 out of five mice had to be euthanized because of tumor ulceration (**Figure 13C**). CT26 is an immunologically "hot" murine tumor that exhibits a rich infiltrate of lymphocytes [216, 217]. Flow cytometry experiments on saline treated tumors showed that the proportion of T lymphocytes in CT26 tumors was higher than in another commonly studied BALB/c tumor, the WEHI-164 sarcoma model (**Supplementary Figure 5A**). Also, the percentage of CD8+ T cells specific to the AH1 rejection antigen was significantly higher in CT26 compared to WEHI-164 and, interestingly, to C51 colon carcinoma, where the proportion of CD8+ T cells in the tumor was comparable to CT26 (**Supplementary Figure 5B**). In order to study anticancer activity in a second immunocompetent mouse model, we treated WEHI-164 sarcomas, including a combination treatment with PD-1 blockade. Also in this case, F8-LIGHT monotherapy significantly inhibited tumor-growth compared to saline. Combination treatment with an anti-PD-1 antibody led to tumor regression in all mice. Two out of five animals enjoyed a complete and durable remission, but a similar activity was also observed in the PD-1 blockade monotherapy group, with three out of five animals experiencing complete tumor regression (**Figure 13D**).

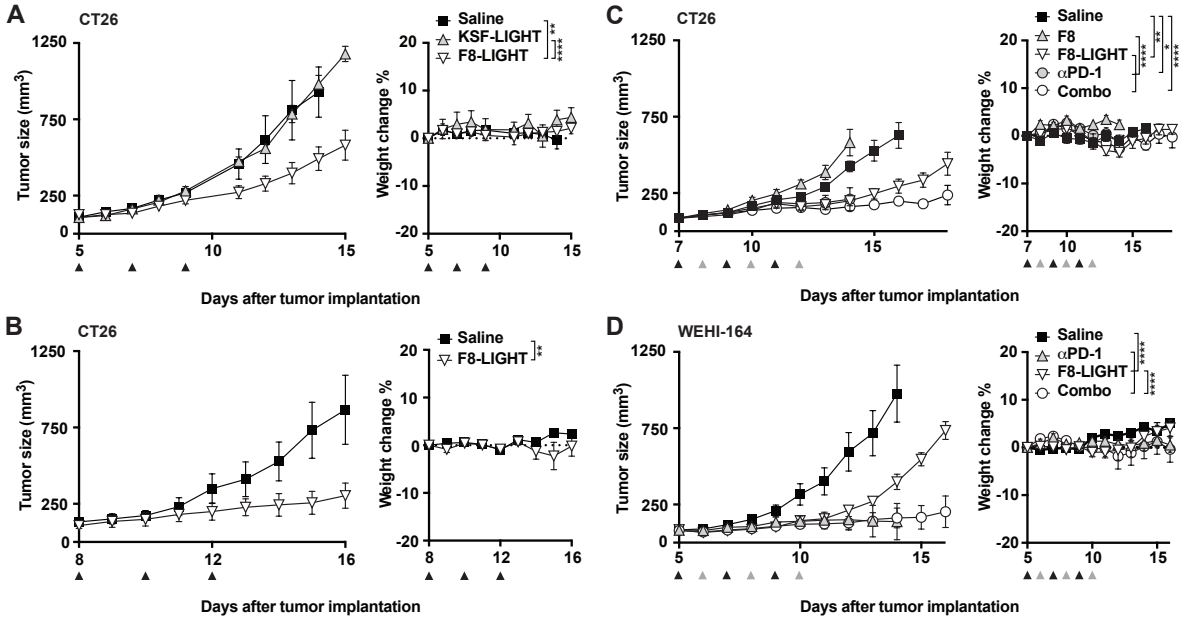

*Figure 13: **Therapy experiments**. **A**, Therapy experiment in BALB/c mice bearing established CT26 tumor. 100 μg of F8-LIGHT or KSF-LIGHT were administered intravenously every other day, as indicated by the black arrows. **B**, as in **A**, but mice received 300 μg of F8-LIGHT. **C**, Therapy experiment in BALB/c mice bearing established CT26 tumor. 300 μg of F8-LIGHT or 150 μg of F8 (black arrows), 200 μg of αPD-1 (grey arrows) or a combination of F8-LIGHT and αPD-1 were administered as depicted in the figure. **D**, Therapy experiment in BALB/c mice bearing established WEHI-164 tumor. 300 μg of F8-LIGHT (black arrows), 200 μg of αPD-1 (grey arrows) or a combination of the two were administered as depicted in the figure. Data represent means ± SEM, n = 5 mice per experimental group. * = p < 0.05, ** = p < 0.01, *** p = < 0.001, **** = p < 0.0001 (regular two-way ANOVA test with Bonferroni post-test correction).*

5.2.4 F8-LIGHT treatment increase Natural Killer cells but not CD8+ T cells infiltration in the tumor

Since previous studies had reported the ability of LIGHT to attract CD8+ T cells into the neoplastic mass, we treated WEHI-164 bearing mice with F8-LIGHT or saline and analyzed tumors and tumor-draining lymph nodes (harvested 48 hours after the last injection) by flow cytometry. In contrast to reports obtained by the transgenic expression of LIGHT by tumor cells, we did not observe any increase of CD8+ T cells in tumors from the F8-LIGHT treatment group compared to saline (**Figure 14A**). Instead, we found a significant increase of tumor-infiltrating cells positive for the Natural Killer cells marker NK1.1 (**Figure 14B**). Within the NK1.1 positive population, we could distinguish three different subpopulations: a CD3-negative (conventional NK cells), a CD3-positive (NKT cells) and a CD3-intermediate, MHC class II-positive population, which was the most abundant one (**Figure 14A**). Inspection of the phenotype composition of the CD8+ T cells revealed an increase in the proportion of CD62L+CD44low naïve CD8+ T cells infiltrating LIGHT-treated tumors (**Figure 14C**). The same feature was observed for the AH1-specific CD8+ T cell population in the tumor, whereas in the draining lymph node the situation was reversed, with an increased proportion of CD62L-CD44+ effector AH1-specific T cells after F8-LIGHT treatment (**Figure 14C**). No significant difference among the different therapy groups could be found in terms of abundance of CD3+, CD4+, MHC class II+ and AH1-specific CD8+ cells. No difference in CD8-to-CD4 ratios was observed in tumors or lymph nodes (**Figure 14A, D-E**). We repeated the analysis in mice bearing CT26. In this model, the population of CD8+ T cells infiltrating the tumor mass was significantly lower in F8-LIGHT-treated mice compared to the control group, supporting the hypothesis that anti-tumor effect of F8-LIGHT is not primarily mediated by these cells (**Supplementary Figure 6**).

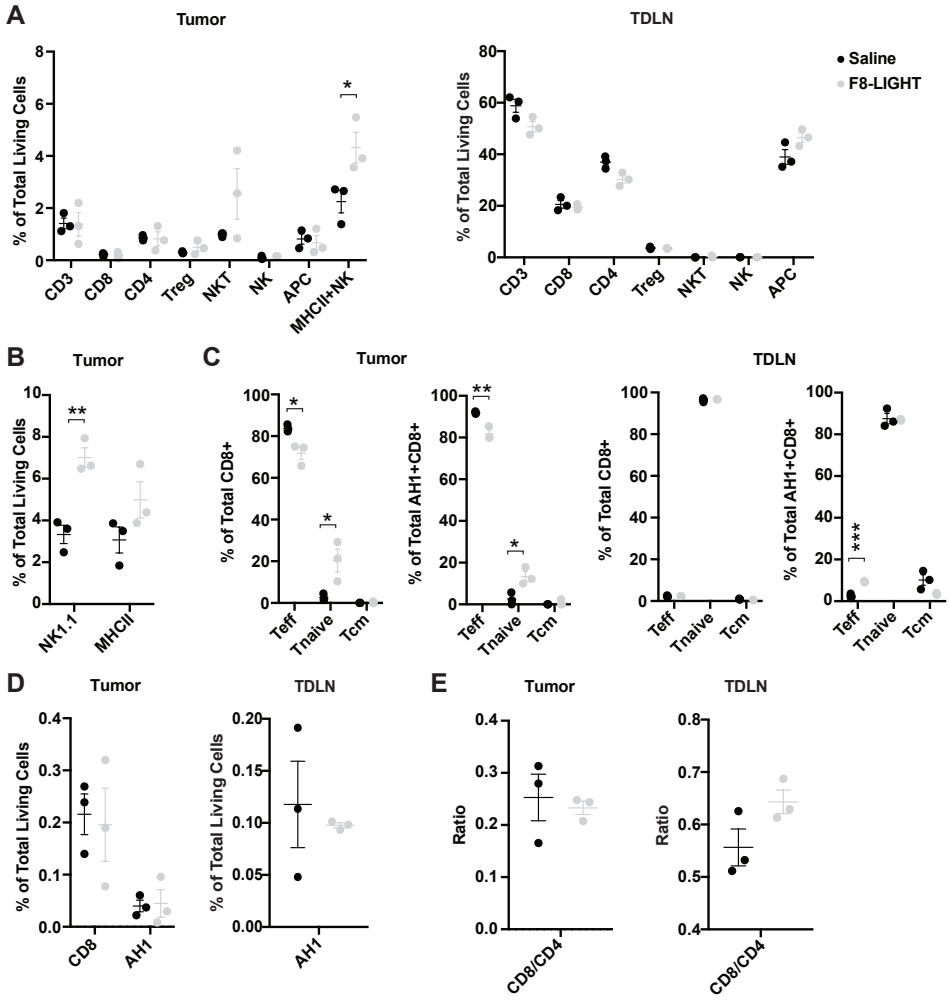

*Figure 14: **Analysis of immune infiltrate**. Analysis of tumors and tumor-draining lymph nodes (TDLN) of BALB/c mice bearing WEHI-164 tumors, 48 hours after the third administration of F8-LIGHT or saline. **A**, lymphocytes infiltration in tumors and composition of TDLN. CD3 = CD3+ lymphocytes, CD8 = CD8+ T cells, CD4 = CD4+ T cells, T_{reg} = CD4+ regulatory T cells, NKT = Natural Killer T cells, NK = Natural Killer cells, APC = Antigen Presenting cells and MHCII+NK = MHC class II+ NK cells. **B**, total NK1.1-positive and MHC class II-positive lymphocytes infiltrating tumors. **C**, phenotype of CD8+ T cells and of AH1-specific CD8+ T cells in tumors and TDLN, based on expression of the markers CD44 and CD62L. T_{eff} = effector T cells, T_{naive} = naïve T cells, T_{cm} = central memory T cells. **D**, AH1-specific CD8+ T cells in tumors and TDLN. **E**, CD8+ T cells:CD4+ T cells ratio in tumor and TDLN. Data represent individual mice, with means ± SEM, n = 3 mice per experimental group. * = $p < 0.05$, ** = $p < 0.01$, *** $p = < 0.001$ (unpaired t-test).*

F8-LIGHT treatment mediated a tumor growth retardation in both WEHI-164 and CT26 models. In WEHI-164-derived samples, however, the proportion of total living cells within the neoplastic mass (determined by 7-AAD staining on total events at time of analysis) was significantly higher in the F8-LIGHT group compared to saline, while leukocyte levels were similar (**Figure 15A-B**). When trying to identify the nature of living cells within the F8-LIGHT-treated neoplastic mass, we observed fewer tumor cells compared to the saline group, accompanied by the emergence of an abundant population of FSC-low and SSC-low particles (which we called SLE, for "small living events") (**Figure 15C**). These SLEs stained negative for 7-AAD, CD3, CD4, CD8, NK1.1 and MHC class II (**Supplementary Figure 8**).

In a separate experiment, staining of lymph nodes cells with the TER-119 antibody suggested that the SLE population may correspond to erythrocytes, in view of size and granularity distribution. The reason why we detected this population in all F8-LIGHT samples and in none of the saline samples, despite the fact that all samples were processed in the exact same way, remains unknown.

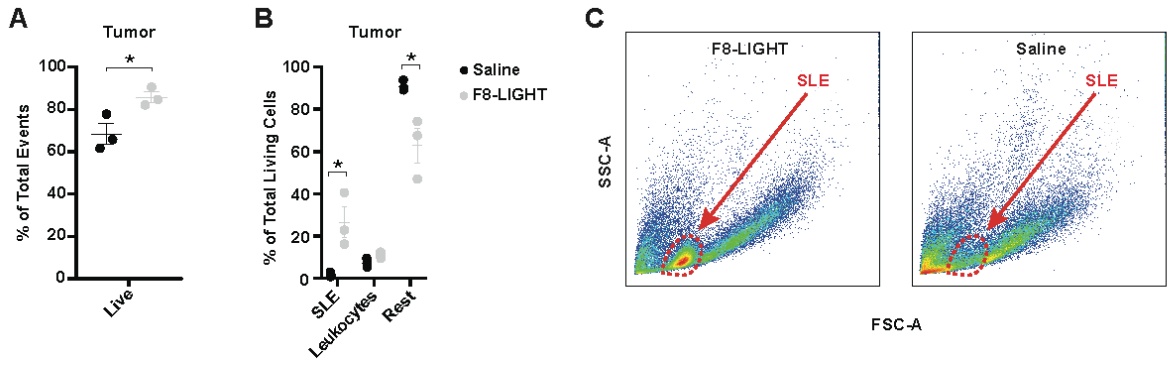

*Figure 15: **Analysis of tumor composition**. WEHI-164 tumors analysis 48 hours after the third administration of F8-LIGHT or saline **A**, fraction of living cells among total events recorded. **B**, composition of living cells in the tumor. "Leukocytes" represent the sum of all T cells, NK cells, Antigen Presenting cells and Granulocytes, "Rest" represent the remaining living cells, after subtracting SLE and Leukocytes from the total number of living cells. SLE = "Small Living Events" **C**, representative analysis of tumor cells suspensions from single mice treated with F8-LIGHT or saline. SSC-A = side scatter area, FSC-A = forward scatter area. Data represent individual mice, with means ± SEM, n = 3 mice per experimental group. * = $p < 0.05$ (unpaired t-test).*

5.3 Discussion

We have generated a novel fusion protein (termed F8-LIGHT), which was able to selectively deliver murine LIGHT to solid tumors, thanks to the binding properties of the F8 antibody, specific to the EDA domain of fibronectin. This immunocytokine product was well-behaved in biochemical assays and fully active *in vitro*, unlike other formats featuring murine LIGHT as module, described in this article or in previous studies [163, 218]. F8-LIGHT induced a specific tumor-growth retardation, that was not observed for a similar fusion protein used as negative control of irrelevant specificity in the mouse (KSF-LIGHT). In spite of its potent anti-cancer activity, F8-LIGHT could not cure CT26 nor WEHI-164 tumors in mice, when used as a single agent.

The strongest evidence linking LIGHT to an anti-cancer activity had emerged from the use of tumor cells, which had been engineered to express large quantities of LIGHT and which were completely rejected by immunocompetent mice in a process that relied on CD8+ T lymphocytes [154, 155, 219]. Delivery of LIGHT to the tumor using the F8 antibody did not boost CD8+ T

lymphocytes and did not mediate tumor rejection. This effect may be explained by differences in the experimental settings. The use of tumor-homing LIGHT fusion proteins may not reach *in vivo* concentrations of cytokine at the site of disease comparable to those achievable by genetic overexpression of LIGHT in tumor cells. Moreover, F8-LIGHT anchored the cytokine payload on the tumor extracellular matrix, which contained the EDA domain of fibronectin, while transgenic tumor cells may display LIGHT on their surface [154, 155, 189]. The antibody-based delivery of cytokines to components of the modified extracellular matrix (e.g., splice variants of fibronectin or of tenascin-C) has been shown to be potently active for other immunomodulatory agents, including interleukin-2, interleukin-12 and tumor necrosis factor [174, 175, 205], but may not be the best strategy to deliver LIGHT.

An EGFR-targeted version of a mutant human LIGHT (EGFR-LIGHT) has recently been described [218]. The fusion protein cross-reacted with murine HVEM and LTβ receptors, as shown by FACS analysis, and exhibited a potent antitumor activity in mice bearing small malignant lesions, but had limited effect in mice bearing more advanced tumors. Unlike what we observed for F8-LIGHT, EGFR-LIGHT treatment induced a strong infiltration of CD8+ T cells in the tumor mass. In a tumor model with a low natural level of immune infiltration, which did not respond to treatment with anti-PD-L1 or EGFR-LIGHT, combination with the two agents led to complete tumor eradication [218].
This study represents an example of a LIGHT-mutant delivered to a cellular-associated antigen (EGFR). It would be of interest to test if an equivalent of our F8 -LIGHT, which features murine wild-type LIGHT and an antibody specific for a tumor-cell surface antigen instead of F8, behave similarly.

Although many studies have focused on the effect of LIGHT on CD8+ lymphocytes [152, 154], Fan Z. et al. demonstrated the essential contribution of NK cells at an early phase of the LIGHT-induced anti-tumor response [219]. They showed that LIGHT was capable of activating and inducing proliferation of NK cells and that the interferon gamma produced by these NK cells contributed to the subsequent activation of CD8+ cells. Treatment of tumor-bearing mice with F8-LIGHT led to an expansion of intratumoral NK cells, but not of CD8+ T cells.

LIGHT is a member of the TNF superfamily. Our group and other researchers have previously studied the possibility to use tumor-homing antibodies for the selective delivery of TNF and related homotrimeric proteins [174, 208, 211, 212, 220]. TNF fusions exhibit an extremely selective

tumor-targeting performance, possibly due to the vasoactive properties of their cytokine payload, while other superfamily members are difficult to deliver [211]. Besides falling in the second category in term of tumor targeting ability, murine LIGHT has also been reported to be difficult to express as a recombinant [163, 164, 218]. In our hands, LIGHT showed a selective accumulation into solid tumors only after extensive engineering of the protein format and of gene expression methods (**Figure 11 and 12**, **Supplementary Figure 3**). Similar features have recently been reported for other cytokine payloads, including interleukin-12 and interleukin-15 [214, 221, 222].

Experimental tumors and neoplastic masses in patients can be defined as "hot" and as "cold", based on the relative density of lymphocyte infiltration. The CT26 model, used in this study and in many other investigations, is considered a "hot" tumor, which readily responds to immunotherapy [216, 217]. By contrast, WEHI-164 fibrosarcoma (also used in our study) exhibits a lower level of lymphocyte infiltration (**Supplementary Figure 5**). Both models grow in BALB/c mice and in both models the antigenic peptide AH1 (derived from the gp70 envelope protein of the murine leukemia virus) can play a role for the tumor-rejection process [176]. Aberrantly-expressed antigens (including retroviral gene products) can act as dominant tumor-rejection antigens in some settings [184]. Unlike what we had previously observed for other antibody-cytokine products [174, 175, 177], treatment with F8-LIGHT did not substantially alter the tumor density of AH1-specific CD8+ T cells (**Figure 14**).

A fully human analogue of F8-LIGHT may represent a useful tool for the *in vivo* boosting of NK cell activity, but this agent may be suboptimal for a selective activation of tumor-specific CD8+ T cells. The EDA domain of fibronectin represents an ideal target for preclinical studies and for clinical translational activities, as the antigen is highly conserved from mouse to man. EDA is expressed in the majority of solid and hematological malignancies [223, 224], while being virtually undetectable in normal adult tissues [135].

6 Cancer therapy in mice using a pure population of CD8+ T cell specific to the AH1 tumor rejection antigen

This chapter corresponds to the submitted manuscript: "Cancer therapy in mice using a pure population of CD8+ T cell specific to the AH1 tumor rejection antigen", by Marco Stringhini, Ilaria Spadafora, Marco Catalano, Jacqueline Mock, Philipp Probst, Roman Spörri and Dario Neri.

6.1 Introduction

The recent success of immunotherapy in the oncology field has highlighted the important role the immune system plays in controlling tumor growth. On one hand, therapeutic proteins like recombinant IL2 or immune checkpoint inhibitors may activate tumor-specific CD8+ cytotoxic T lymphocytes, thus facilitating the killing of malignant cells *in vivo*. On the other hand, T cells themselves can be considered as therapeutics in their own right. Different approaches have been investigated, which make use of patient-derived autologous T cells to treat a variety of malignancies[225]. Collectively named adoptive cell therapies (ACTs), these approaches can be divided in two main groups, depending on whether the autologous T cells are genetically manipulated before infusion. Chimeric-antigen receptor T cells (CAR-T cells) and T cell receptor-transgenic cells (TCR-transgenic cells) are two examples of genetically engineered T cells[226]. In both cases, T cells are forced to express a synthetic receptor, specific for a tumor-associated antigen (TAA). CAR-T cells recognize surface antigens thank to their antibody-like receptors, whereas TCR-transgenic cells are equipped with a native T cell receptor and recognize peptides presented by HLA molecules[226]. The extreme paucity of truly tumor-specific surface antigens has so far limited the use of CAR-T cell therapy to certain haematological malignancies, where the toxicity related to the elimination of TAA-positive healthy cells by CAR-T cells (e.g., elimination of CD19-positive B cells) is manageable[227].

Mutated or aberrantly-expressed peptides may represent a broader source of tumor-specific antigen, suitable for targeting with TCR-transgenic cells, but such targets are challenging to identify in practice[228]. The practical implementation of TCR-transgenic cell therapies would be further complicated by the need to identify and clone cognate TCRs specific to the patient's HLA/peptide complex, which would serve as a basis for highly personalized transduction procedures. As an alternative, the use of naturally-occurring T cells isolated from the tumor of

the patient (tumor-infiltrating lymphocytes, or TILs) has been proposed and clinically investigated[225]. ACT with TILs starts with the resection of the tumor of the patient, from which TILs are cultured, enriched for T cells recognizing the tumor or predicted tumor-specific antigenic peptides, and expanded to high numbers[82]. The expanded T cells are then re-infused in the patient in combination with high dose IL2, following preparative non-myeloablative lymphodepletion[82]. ACT with TILs has been used to treat metastatic melanoma and other solid malignancies[85, 93, 95, 96], with objective responses rates in melanoma around 40-50% and complete responses around 10-20%[86]. Toxicity of this type of treatment is mainly related to the patient preconditioning and the administration of high dose IL2, which are however essential for therapeutic activity[229].

It would be desirable to study T cell-based therapies in syngeneic murine models, as systematic investigations may lead to the identification of optimal dosing/scheduling strategies or combination opportunities. Mouse models may also be ideally suited to investigate whether a single antigen specificity may be sufficient for the eradication of tumors *in vivo*, or whether a polyclonal set of polyspecific cells would be required. Until now, these efforts have been limited to experiments with CAR-T cells, TCR-transgenic cells, or tumor-specific T cells isolated from transgenic mice, mostly due to intrinsic difficulties related to the expansion of murine TILs[230-232]. These approaches, however, may fail to adequately mimic the clinical settings, where T cells need to be extensively cultured *in vitro* before being infused back in the patient.

AH1 is an antigenic peptide presented on H-2L^d, which was first identified as the immunodominant antigen of the murine colon carcinoma cell line CT26[176]. It derives from the endogenous murine leukemia virus envelope glycoprotein 70 (gp70) and it is highly expressed in a multitude of murine tumor cell lines of different histological origin, while being virtually undetectable in murine healthy organs[174, 176]. We previously showed that therapy experiment with two different immunocytokines, able to induce complete tumor rejections in BALB/c mice, resulted in an expansion of AH1-reactive CD8+ lymphocytes, which protected the host from subsequent challenges with diverse AH1-expressing tumors[174, 233]. Moreover, AH1 showed a therapeutic effect when used as a cancer peptide vaccine[177]. Most BALB/c-derived tumors present AH1 on H-2L^d, but one cell line (F1F) has previously been characterized as being essentially AH1-negative, thus serving as negative control for therapy experiments[174].

In this article, we report the use of AH1-specific CD8+ T cells for adoptive cell therapy. We developed and optimized a protocol for the isolation and expansion of AH1-specific T cells from tumors and from secondary lymphoid organs (which may represent an alternative source of tumor-specific T cells, when the tumor is not accessible)[234]. We were able to reach up to 470-fold expansion, with purity consistently close to 100% as judged by FACS with AH1-loaded tetramers. Upon recognition of the antigen, the expanded T cells produced IFNγ and TNFα and specifically killed antigen-positive cells *in vitro* with high efficacy, sparing antigen-negative tumor cells. Administration of AH1-specific CD8+ T cells to mice bearing two different syngeneic tumor models resulted in significant tumor growth retardation, however, cures could not be achieved. Our approach, employing a rare population of naturally occurring tumor-specific T cells isolated from donor mice for ACT in syngeneic tumor models, may serve as a basis for future studies on ACT in a model, which closely replicates the procedures used in the clinic.

6.2 Results

6.2.1 AH1-specific CD8+ T cells do not expand in standard culture conditions

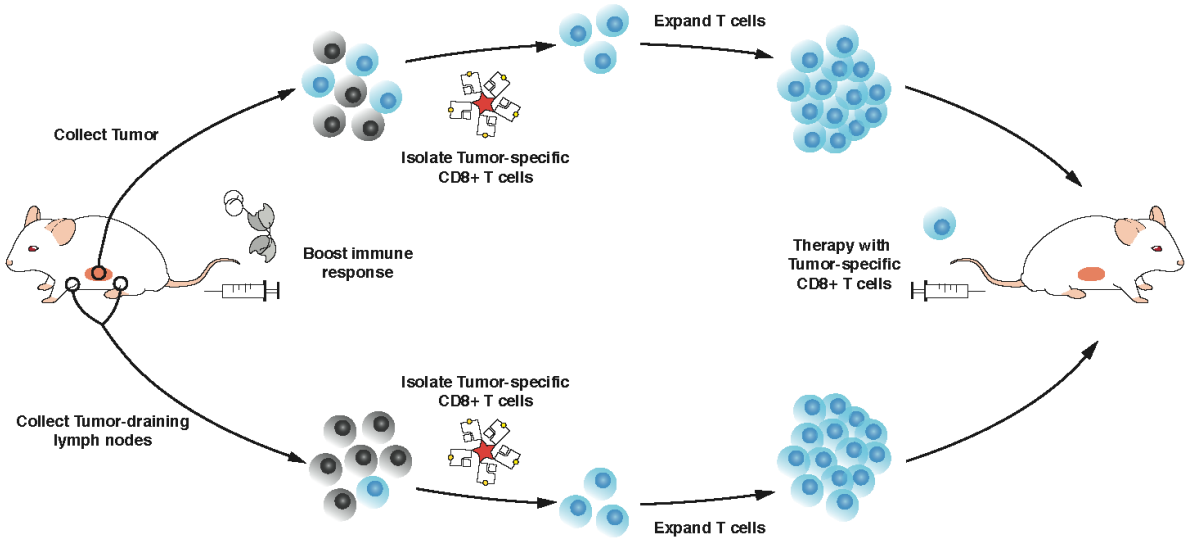

*Figure 16: **Workflow**. Strategy to isolate and expand AH1-specific TILs or T cells from secondary lymphoid organs for ACT.*

In order to be able to perform ACT with a pure population of AH1-specific CD8+ T cells, these cells had to be isolated and expanded *in vitro* (**Figure 16**). We used peptide-loaded MHC class I reversible multimers to isolate AH1-specific CD8+ T cells from TDLNs and tumors of CT26-bearing BALB/c mice. As control, we isolated AH1-multimer-negative CD8+ T cells from

TDLNs (T naïve). We used magnetic beads coated with antibodies against CD3 and CD28 to activate the T cells and grew them in complete medium supplemented with IL2. After three days in culture, T naïve had formed big clumps around beads and were increased in size and number (**Figure 17A**). Some small clumps of cells and beads were also present in wells containing AH1-specific T cells, but these cells were smaller and did not seem to have increased in number. Microscopic analysis was repeated at day seven. T naïve had returned to normal size, but maintained an elongated shape typical of proliferating cells and further increased in number. AH1-specific cells did not seem to have expanded (**Figure 17A**). Cells were collected, counted and analysed by flow cytometry. Viability was low in all samples (**Figure 17B**), but while total number of T naïve was comparable or higher than at culture initiation, AH1-specific T cells from both TDLNs and tumors had significantly decreased (**Figure 17C**). Interestingly, the percentage of AH1-tetramer-positive T cells was also decreased with respect to baseline in AH1-specific T cells samples derived from TDLNs, but not from tumors. This effect was more marked in less diluted samples, where T cells and beads were in closer contact and thus more likely to interact. Collectively, our findings evidenced a clear need for better experimental procedures, which would allow the selective expansion of antigen-specific CD8+ T cells.

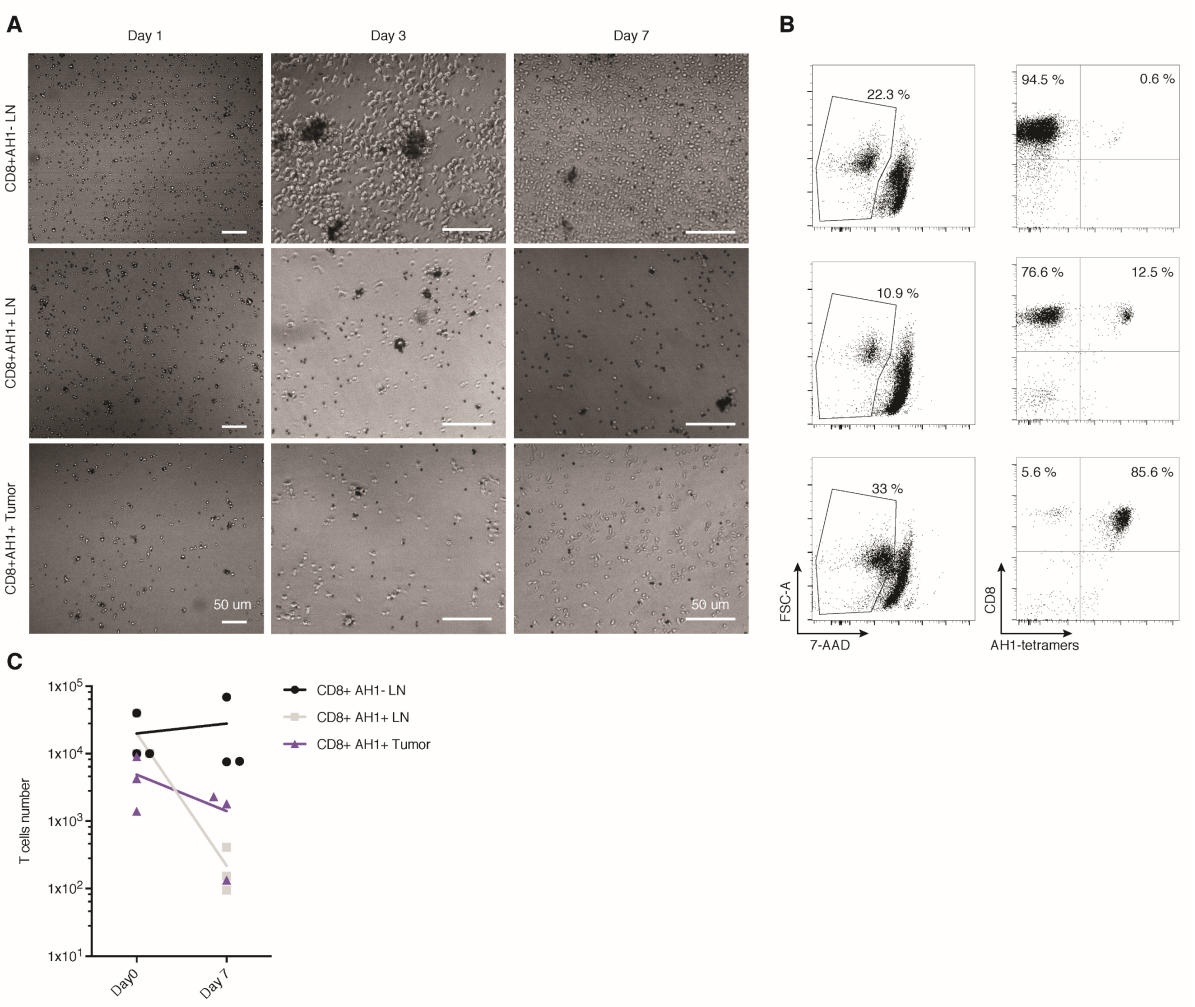

*Figure 17: **T cell culture with anti-CD3, anti-CD28 and IL2**. AH1-specific T cells from tumors (CD8+AH1+ tumor) or TDLNs (CD8+AH1+ LN) were isolated by FACS and grown with activating magnetic beads and IL2 for 7 days. Tetramer-negative T cells isolated similarly from TDLNs (T naïve LN) were used as control. **A**, Representative picture of T cells were taken at day 1 (5x magnification), 3 and 7 (10x magnification). **B**, Representative flow cytometry analysis, performed at day 7. **C**, T cells count at baseline (day 0) and after 7 days in culture. T cells were obtained from 3 different mice. Data are representative for 2 independent experiments.*

6.2.2 AH1-specific CD8+ T cells can be expanded by repetitive stimulation with AH1 peptide-pulsed mature Dendritic Cells

In vitro expansion leads to a gradual maturation of T cells toward a terminally differentiated phenotype. Naïve-like, or minimally expanded T cells have been shown to engraft more efficiently *in vivo*, leading to an increased anti-tumor effect[99]. Many studies have reported that culturing naïve T cells in IL15 and IL7 results in less exhausted or more naïve-like T cells, with respect to expansion in IL2[99]. With preliminary experiments, in which we cultured CD90.2+ BALB/c splenocytes with activating beads and cytokines, we could observe that CD8+ T cell yields and the proportion of CD8+ T cells expressing CD62L increased upon use of IL7 and

IL15, rather than IL2 (**Supplementary Figure 15**). Also, culture in IL2-containing medium required re-activation every 5-6 days, whereas culture in IL15 and IL7 did not. Teague *et al.* had previously shown that tumor-specific tolerant T cells, which failed to proliferate *in vitro*, could be rescued by incubation in medium containing high-dose IL15 (or, less efficiently, IL2)[235]. After isolation of AH1-specific T cells from secondary lymphoid organs and tumor, we incubated cell samples in complete medium supplemented with high-dose IL15 and let them rest for five days. At day five, we stimulated the T cells using peptide-pulsed, mature BMDCs expressing various co-stimulatory molecules (**Supplementary Figure 16**) and we repeated the stimulation after 10 days. After the second stimulation, we started adding IL7 in the medium. Following a slow but constant expansion for the first two weeks, T cells started to expand exponentially about three to four days after the second stimulation. Exponential growth usually lasted 4-5 days, after which proliferation rate slowed down. **Figure 18A** graphically depicts the protocol used to expand AH1-specific T cells. Using this protocol, we were able to reliably expand T cells up to 470-fold in three weeks (**Figure 18B**). Remarkably, almost 100% of the CD8+ T cells were able to bind AH1-loaded MHC I tetramers after the expansion (**Figure 18C**).

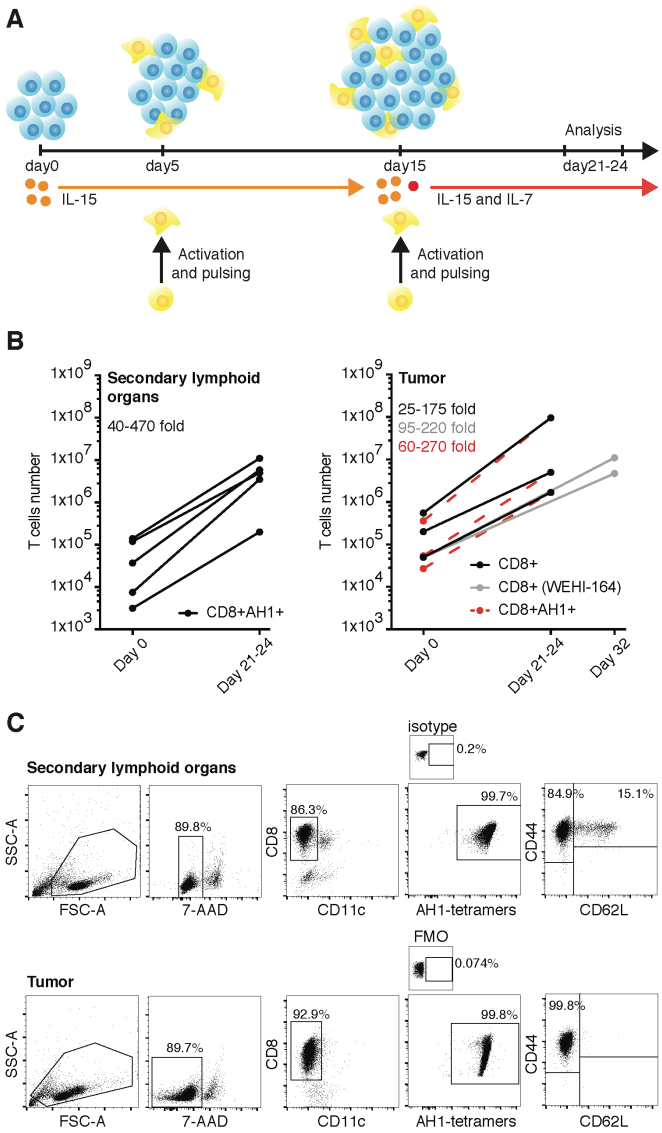

*Figure 18: **Optimized protocol for the expansion of AH1-specific T cells**. **A**, Schematic representation of the protocol used to expand AH1-specific T cells. **B**, T cell count at baseline (day 0) and after 3-4 weeks of in vitro expansion. Each line represents one independent experiment, AH1+CD8+ T cells were isolated by FACS from secondary lymphoid organs (left) and CD8+ TILs from CT26 or WEHI tumors (right). Red scattered lines represent counts of AH1-positive cells in CD8+ TILs samples. **C**, Representative flow cytometry analysis of T cells after expansion. PE-conjugated tetramers loaded with an irrelevant peptide (p29) or Fluorescence Minus One (FMO) controls were used to set the AH1-tetramers gate.*

Activation of unselected CD8+ TILs with peptide-pulsed DCs, but not with DCs and anti-CD3, led to a preferential expansion of AH1-specific T cells (**Supplementary Figure 17**). This effect was not only observed with CD8+ TILs from CT26 tumors, where AH1-specific cells represented about 50-60% of the total T cells, but also with CD8+ TILs from WEHI-164 tumors, where the initial percentage of AH1-specific cells was consistently lower than 10%. CD8+ TILs isolated from WEHI-164 tumors required a third stimulation before starting to expand exponentially (**Figure 18B**). Expanded T cells had an effector phenotype (CD62L-/CD44high) and expressed the IL2Rα subunit CD25. Diverse markers of exhaustion were found

to be heterogeneously expressed among expanded T cells (**Figure 18C and Supplementary Figure 17**).

6.2.3 *In vitro* expanded AH1-specific CD8+ T cells are functional and selectively recognize tumor cells expressing gp70

In order to check if expanded T cells were functional, we tested their biocidal capacity in an *in vitro* cytotoxicity assay. We incubated expanded T cells with different tumor cell lines, which were shown to express the gp70 protein (from where the AH1 peptide is derived) or with F1F tumor cells, which do not express gp70[174, 188]. Already at a 1:1 ratio, AH1-specific T cells were able to selectively eliminate gp70-expressing tumor cells, with variable efficiency (**Figure 19A and B**). CT26, WEHI-164 and C51 were the most sensitive cell lines and were almost completely eliminated by T cells after 24 hours. To test the ability of expanded T cells to secrete effector cytokines, we isolated AH1-specific CD8+ or bulk CD8+ T cells from secondary lymphoid organs, we expanded them using suitable protocols and we incubated them with CT26 cells, F1F cells or activating anti-CD3/anti-CD28 beads. Flow cytometry analysis showed that bulk CD8+ T cells (containing negligible levels of AH1-specific T cells, **Supplementary Figure 18**) were able to produce IFNγ and TNFα upon incubation with beads, but not with tumor cells. AH1-specific T cells, instead, produced IFNγ and TNFα both upon stimulation with beads and CT26, but not with F1F tumor cells (**Figure 19C**).

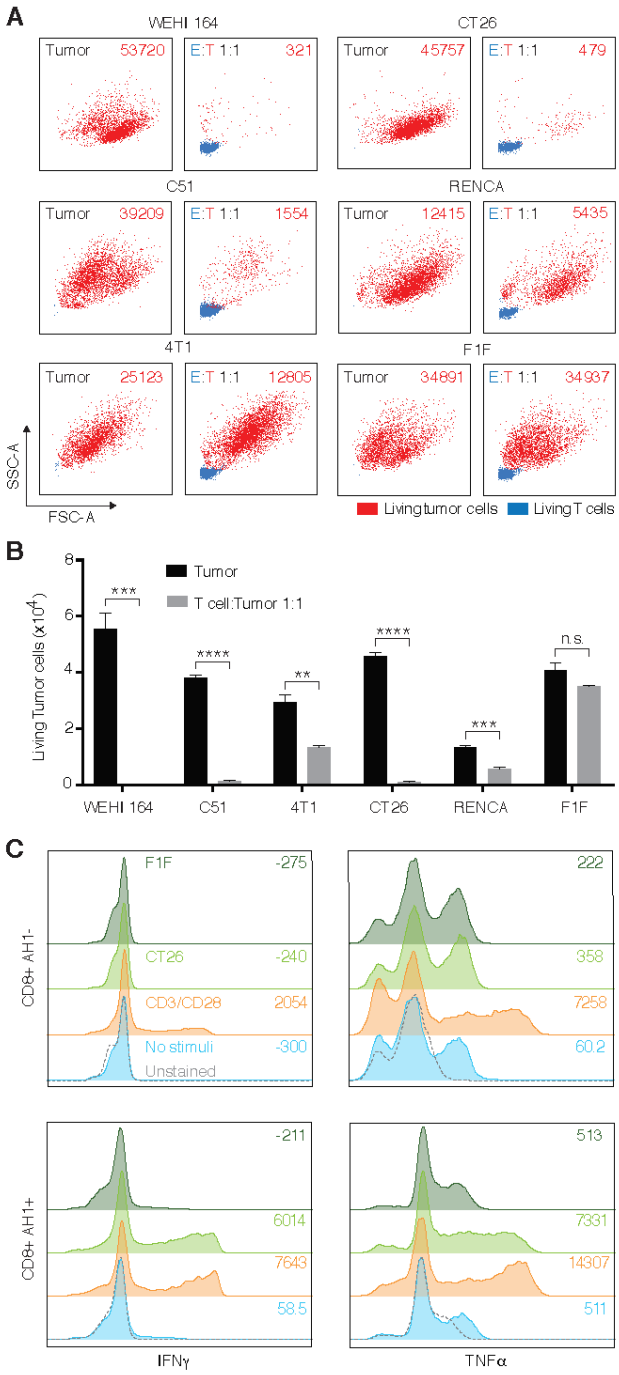

Figure 19: ***In vitro activity of AH1-specific T cells****. **A**, Different tumor cell lines were incubated for 24 hours, either alone (left boxes) or with AH1-specific T cells at a 1:1 ratio (right boxes) and analysed by flow cytometry. Representative graphs showing living tumor cells (red) and living CD8+ T cells (blue). Numbers on the top right corner of the boxes represent count of living tumor cells.* ***B****, Total count of living tumor cells with or without addition of T cells. Column represent means + SEM, n = 3 per experimental group, ns = non-significant, * = p < 0.05, ** = p < 0.01, *** p = < 0.001, **** = p < 0.0001 (unpaired t-test).* ***C****, Flow cytometry analysis of expanded CD8+AH1- or CD8+AH1+ T cells stimulated with antiCD3/antiCD28-coated magnetic beads, F1F or CT26 tumor cells (all at 1:1 ratio). Numbers on the right sides of the boxes represent mean fluorescence intensities. Data representative for at least five independent experiments.*

6.2.4 *In vivo* administration of AH1-specific T cells delays tumor progression in two murine models of cancer

Using our protocol based on pulsed Dendritic Cells and a cocktail of IL7 plus IL15, we were able to successfully expand functional AH1-specific CD8+ T cells. In order to investigate their therapeutic potential *in vivo*, we performed a first therapy experiment in BALB/c mice bearing subcutaneous CT26 tumors. We administered increasing doses of AH1-specific T cells by intravenous injections. As negative control, two additional groups of mice were injected with saline, resp. bulk CD8+ T cells containing negligible levels of AH1-specific T cells (**Supplementary Figure 18**). Administration of AH1-specific T cells at all tested doses lead to a significant tumor growth retardation compared to both the saline and the bulk CD8+ group (**Figure 20A**). Therapy with $1x10^6$ T cells performed substantially better than therapy with $1x10^4$ T cells, but not than therapy with $1x10^5$ T cells. By contrast, therapy with $3.5x10^5$ bulk CD8+ T cells did not show any anti-tumor effect compared to saline. All treatments were well tolerated, with no mice experiencing weight loss. In order to boost the activity of AH1-specific T cells and to assess whether their origin could influence therapeutic potential, we performed a second experiment in the same model, where we combined AH1-specific CD8+ T cells from secondary lymphoid organs or tumors with human IL2. More precisely, we used a targeted version of IL2 genetically fused to the antibody F8, specific for the tumor-associated antigen Extra Domain A of fibronectin[171]. We used this version of IL2 with the goal of maximizing tumor-over-healthy organs exposure. AH1-specific T cells mediated tumor growth retardation regardless of their tissue of origin and the effect was in line with what observed in the first therapy experiment (**Figure 20B**). Administration of the T cells together with F8-IL2 lead to a significantly improved anti-tumor effect, which was however mainly mediated by F8-IL2. We could not observe any significant difference between combination treatments and treatment with F8-IL2 alone. In a third therapy experiment, we investigated the effect of AH1-specific T cells in a second model, the WEHI-164 fibrosarcoma. With the goal of investigating if an increase in the number of injected T cells would improve anti-tumor activity, we devoted considerable efforts to obtaining higher yields of AH1-specific T cells. We were able to administer up to $30x10^6$ T cells to three mice, but surprisingly we did not observe any further therapeutic improvement compared to previous experiments (**Figure 20C**). We hypothesize that absence of therapy improvement upon administration of a high number of T cells may be due to an insufficient survival of those cells *in vivo*. In fact, AH1-specific cells had been extensively expanded *in vitro*, possibly impairing their subsequent proliferative fitness.

Moreover, availability of supportive cytokines, growth factors and nutrients for the newly infused T cells may be limited due to competition with lymphocytes already present in the tumor and tumor cells themselves, allowing only a limited amount of administered T cells to survive. It has already been demonstrated that lymphodepletion prior to ACT substantially improve engraftment of infused T cells and, consequently, their efficacy[236, 237]. As an attempt to find an alternative strategy to improve anti-tumor effect without employing lymphodepletion, we performed an additional therapy in CT26, using a modified administration schedule. Instead of administering T cells as a single bolus injection, we injected low doses of T cells for four consecutive days, alone or in combination with F8-IL2. Unfortunately, we did not observe any significative improvement compared to the previous therapies (**Figure 20D**).

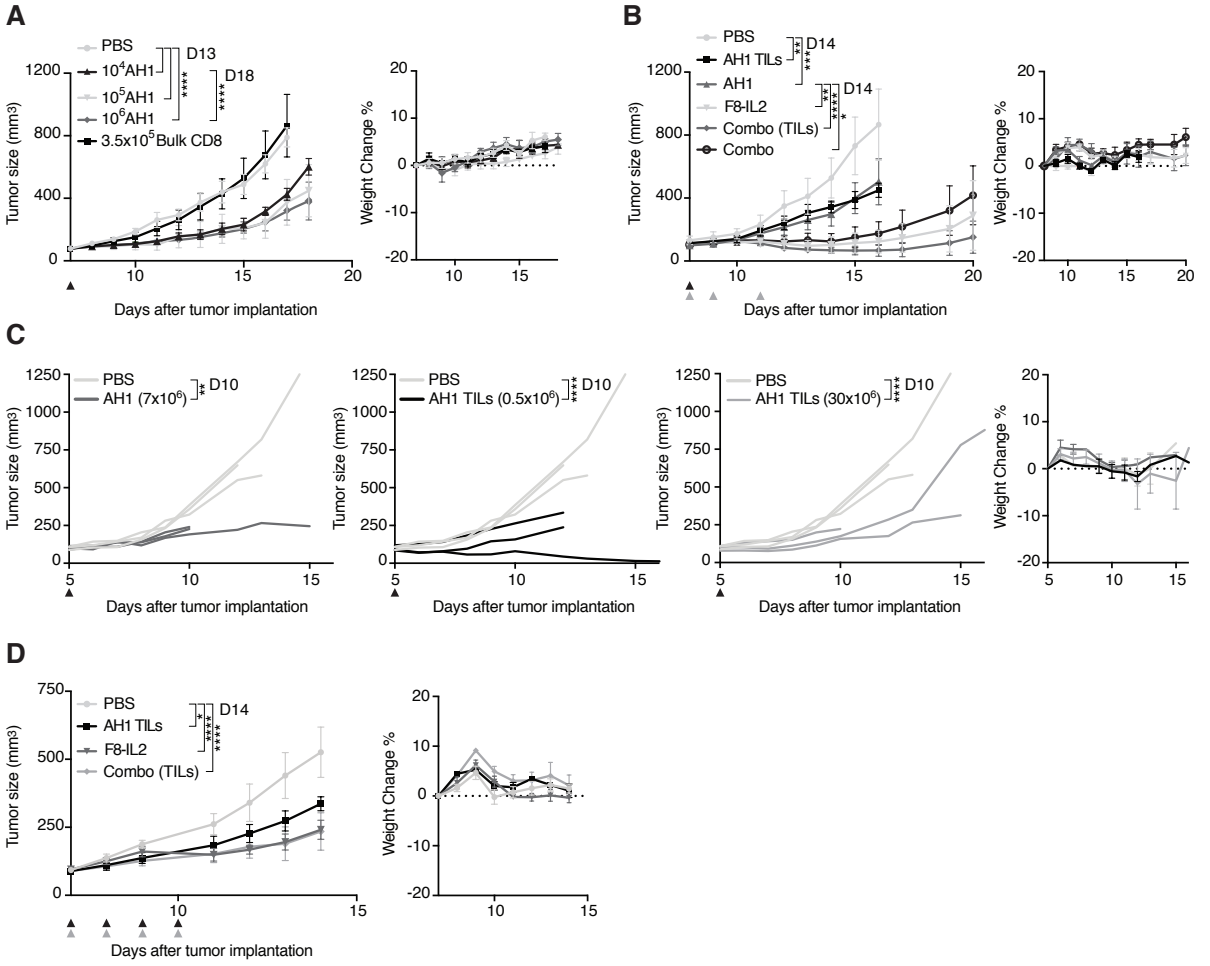

Figure 20: ***Tumor therapy with AH1-specific T cells****. **A**, Tumor growth over time with respective weight change, in BALB/c bearing CT26 tumors and treated with one intravenous injection (i.v.) of AH1-specific T cells or CD8+AH1- T cells (bulk CD8) expanded from secondary lymphoid organs. Data represent means ± SEM, n=5 per experimental group.* ***B****, Same as in A, but mice received either saline (PBS), 5x10^5 AH1-specific T cells expanded either from secondary lymphoid organs (AH1) or from tumors (AH1 TILs), 3x45ug F8-IL2, or combinations of T cells and F8-IL2, as indicated by arrows. Data represent means ± SEM, n=5 per experimental group.* ***C****, Therapy experiment in BALB/c bearing WEHI-164 tumors and receiving either saline, or the indicated doses of AH1-specific T cells from TDLNs (AH1) or tumors (AH1 TILs). Data represents single mice, n=3 per experimental group. Some mice had to be euthanized before the end of the therapy because of tumor ulceration, in accordance to the license 04/2018* ***D****, Therapy in CT26-bearing BALB/c and receiving 4x i.v. injections of either saline, 5x10^5 AH1-specific*

*TILs, 20ug F8-IL2 or 5x10^5 AH1-specific TILs pre-mixed with 20ug F8-IL2 before administration. Data represent means ± SEM, n=5 per experimental group. Statistical analyses were performed on the day indicated in the legends, ns = non-significant, * = p < 0.05, ** = p < 0.01, *** p = < 0.001, **** = p < 0.0001 (2-way ANOVA with Bonferroni correction).*

6.2.5 Administered T cells fail to persist in tumor or secondary lymphoid organs

Numerous studies have reported the ability of *in vitro* expanded T cells to accumulate in the tumor mass[238, 239]. Mechanistically, T cells ability to migrate into the tumor after intravenous administration depends on expression of various adhesion molecules and chemokine receptors. CXCR3 is expressed on activated TILs found in various cancer types and it is thought to play an important role in T cell migration to inflamed tissues[240]. Flow cytometry analysis revealed that expanded AH1-specific CD8+ T cells homogeneously expressed CXCR3, but lacked expression of the secondary lymphoid-homing chemokine receptor CCR7 (**Figure 21A**). We performed an *in vivo* biodistribution study by injecting CFSE-labeled AH1-specific T cells into BALB/c bearing subcutaneous CT26 tumors, in order to evaluate whether T cells were able to engraft and persist *in vivo*. Analysis of single cell suspensions from tumors, TDLNs and spleens 72h after administration of 3x10^6 T cells revealed the presence of extremely few CFSE-positive CD8+ T cells in tumors and spleens only, with CFSE-positive T cells reaching less than 0.1% of the total CD8+ T cells in those tissues (**Figure 21B**). With so few adoptively transferred T cells present in the tumor (i.e., the site in which they would be expected to exert their activity) and in secondary lymphoid organs (where they could potentially proliferate and replenish the TIL-pool) it may be difficult to achieve a sufficiently potent and sustained anti-tumor effect. In support of this hypothesis, *in vitro* cytotoxicity experiments with T cells-to-tumor cells ratios lower than 1:2 (which may better mimic the *in vivo* situation), revealed that effector-to-target ratios as low as 1:10 not only did not have any effect on tumor cells growth, but negatively affected T cells viability (**Figure 21C**).

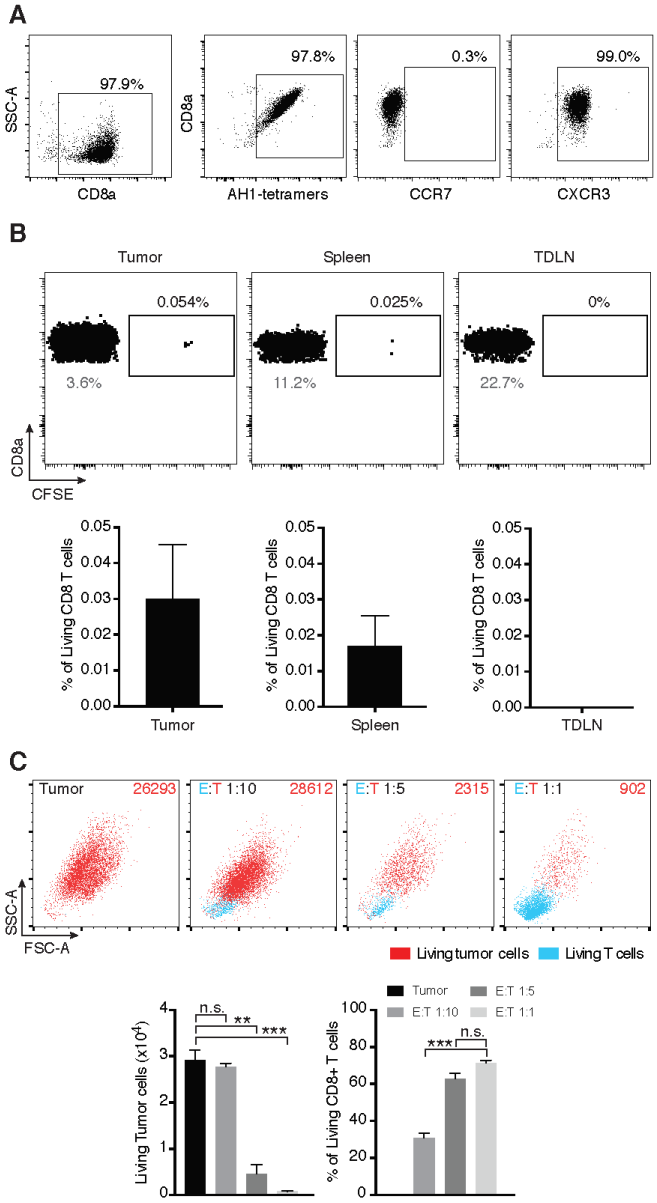

Figure 21: ***In vivo biodistribution and in vitro survival of AH1-specific T cells****. **A**, Expression of chemokine receptors CCR7 and CXCR3 on expanded AH1-specific TILs, analyzed by flow cytometry. **B**, 3x10^6 CFSE-labelled AH1+ TILs were i.v. injected in BALB/c bearing established CT26 tumors. Mice were sacrificed after 72 hours and presence of CFSE+ CD8+ T cells was analyzed in tumors, TDLNs and spleens. Representative dot plots showing fractions of CFSE+ cells over total CD8+ cells in each tissue, with respective bar-plots, representing means ± SEM (n = 3 mice). Numbers in grey represent the percentage of CD8+ cells over total living cells for each tissue.* ***C****, Representative flow cytometry analysis from a cell-cytotoxicity assay featuring CT26 tumor cells and AH1-specific TILs at indicated effector-to-target ratios, with respective bar plots. Bar plots represent total number of living tumor cells (left) and percentage of living CD8+ T cells on total CD8+ T cells (right), for each experimental group (means ± SEM, n = 3 per experimental group). ns = non-significant, * = p < 0.05, ** = p < 0.01, *** p = < 0.001, **** = p < 0.0001 (unpaired t-test).*

6.2.6 Expansion of TILs in the presence of Notch-ligand or inhibitors of GSK-3b and p38, do not results in T cells with favourable phenotype

Culture protocols employing GSK-3b inhibitor TWS119 or, more recently, p38 inhibitor Doramapimod have been effectively employed to expand naïve tumor-specific T cells, while

limiting their maturation[241, 242]. The so-obtained T cells maintained naïve- or stem cell-like characteristics and were shown to perform better in ACT experiments. Another study reported that Notch-signalling during culture of activated T cells could increase the proportion of CD62L+ naïve or central memory T cells[243]. In order to test if those agents could also reprogram antigen-experienced T cells to become more naïve-like and thus more fit for survival *in vivo*, we cultured TILs in the presence of each of these three agents. T cells cultured in the presence of Doramapimod and recombinant Notch-ligand efficiently expanded, but phenotype analysis based on expression of CD44 and CD62L revealed that none of the additive was able to reliably expand T cells with a central memory or naïve-like phenotype (**Figure 22**). Prolonged exposure to TWS119 was toxic for T cells.

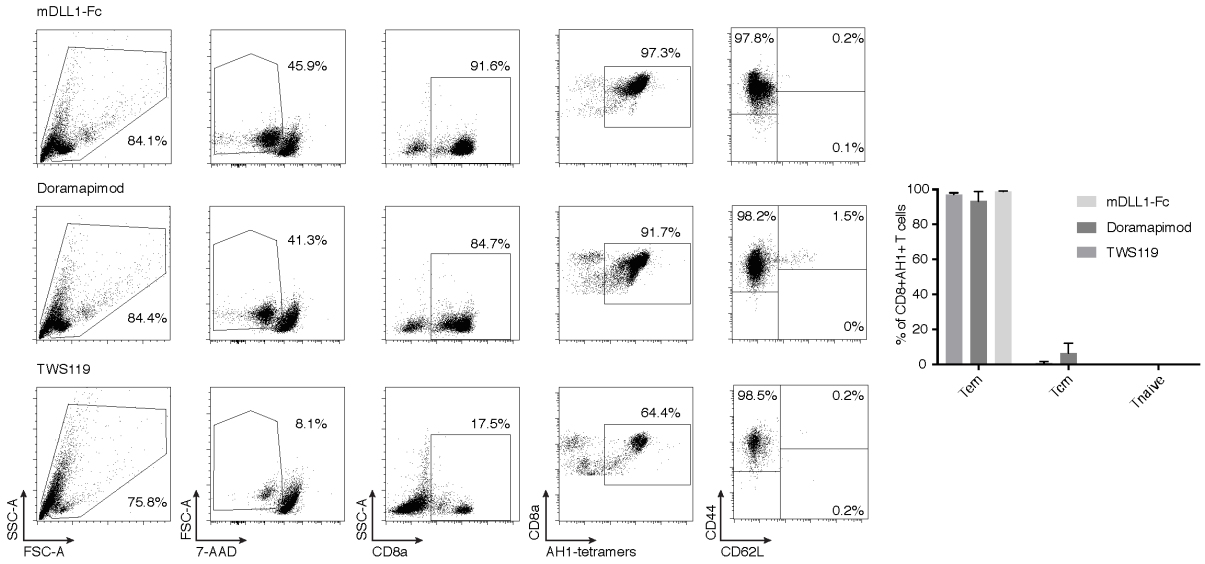

*Figure 22: **TILs expansion in the presence of additives**. Representative phenotypic analysis of TILs expanded in the presence of recombinant Notch-Ligand (mDLL1-Fc), p38 inhibitor Doramapimod, or GSK-3b inhibitor TWS119, with respective bar plots (columns represent means ± SEM, n = 3 per experimental group). Tcm = central memory T cells (CD44high/CD62+), Tem = effector memory T cells (CD44high/CD62-) Tnaive = naïve T cells (CD44low/CD62+).*

6.3 Discussion

In the present study, we were able to develop a protocol for the reliable expansion of AH1-specific T cells isolated from natural infiltrates of tumors and secondary lymphoid organs. The expanded T cells maintained their specificity, recognized and killed antigen-positive tumor cells with high efficiency *in vitro* and delayed tumor progression when used as ACT in two syngeneic murine models of cancer. When used alone, AH1-specific T cells failed to induce regression of established tumors in immunocompetent mice. Combination with F8-IL2, a tumor-targeted version of human IL2, did result in substantially improved therapeutic effect, which was however not superior to F8-IL2 monotherapy, suggesting that IL2 preferentially acted on the pre-existing immune infiltrate, rather than on injected T cells.

Since the number of infused T cells positively correlates with therapeutic activity in patients, it may be argued that curative results were not obtained because an insufficient number of AH1-specific T cells was used. We investigated doses ranging from $1x10^4$ to $30x10^6$ AH1-specific T cells. We cannot exclude that a higher number of T cells may be sufficient to obtain complete rejections. Similar experiments in a different model showed how established tumors could be completely eradicated by increasing the doses of administered tumor-specific T cells [230, 244]. Such studies, however, were performed using T cells from transgenic mice, which gives the authors access to very high numbers of naïve tumor-specific T cells, an ideal but unrealistic scenario. It is common knowledge, that expanding murine TILs (and, as we showed, antigen-experienced, tumor-specific T cells from lymphoid organs) is not trivial and the yields of these *bona fide* impaired T cells one can obtain may be limited. Although expanding human TILs may be easier than expanding murine TILs, in both species, naturally-occurring tumor-specific T cells are rare. Extensive *in vitro* expansion with current protocols, needed to obtain high cell numbers, inevitably drives the T cells to a gradual loss of survival and proliferation potential[245]. Thus, also the number of human TILs one can obtain for therapy may be limited. This, together with the fact that we did not observe any improvement by injecting up to $30x10^6$, compared to $0.5x10^6$ AH1-specific T cells, may suggest that focusing on alternative strategies, rather than on trying to further increase the dose of T cells, may be needed in order to achieve better tumor control. For example, many preclinical studies have shown that minimally-cultured, phenotypically younger T cells perform better in ACT, achieving higher anti-tumor effect at lower doses[99].

Considerable efforts in the field of ACT are being devoted to the development of new methods to control the phenotype of T cell products. Different strategies have been proposed to expand T cell with naïve- or T memory stem cell-like characteristics, including the use of anti-oxidants[246], the inhibition of Akt or p38 kinases[66, 242], or the enhancement of Wnt- or Notch-signalling[241, 243]. These experiments have so far been performed using naïve T cells (or *in vitro* activated T naïve, in one case) and may not be as effective on TILs. In our hands, expansion of TILs in the presence of GSK-3b or p38 inhibitors, as well as recombinant Notch-ligand, did not induce expression of CD62L, a marker of naïve and central-memory T cells. The AH1 model and our culture method, could serve as a basis for the systematic investigation of new conditions for the reprogramming of antigen-experienced T cells to a younger phenotype.

AH1 has a number of characteristics, which make it a very attractive target for cancer therapy. It is highly expressed in the tumor but not in healthy organs, it is expressed in multiple tumors of different histological origin and it is derived from a viral protein, which increases its chances to be immunogenic, as T cells are unlikely to have undergone negative selection against it in the thymus[247]. The presence of endogenous retroviral elements has been confirmed also in the human genome and aberrantly expressed retroviral protein may represent a good source of tumor-specific antigen, analogously to AH1[248]. Aberrantly expressed antigen as a whole have been shown to account for about 90% of the total tumor antigens in both mice and humans and aberrantly-expressed antigenic peptides other than AH1, have been identified in murine CT26 tumors[184, 249]. Some of these antigens may contribute to the rejection process. In fact, we could identify T cells specific for some of the identified CT26 antigens in tumors and TDLNs of tumor-bearing mice, which received L19-IL12 (**Supplementary Figure 19**). Our protocol could be potentially used to expand and study those T cells, analogously to what has been done with AH1-specific T cells.

Protocols for the preparation of T cell therapeutics for ACT should aim at generating the highest number of phenotypically fit tumor specific T cells. TILs have been originally chosen as a source of T cells for ACT, with the rational that a higher concentration of tumor-specific T cells may be found at the site of disease. It has been shown, however, that the fraction of T cells infiltrating human tumors and able to recognize malignant cells is variable and generally low[97]. Tumor-specific T cells are enriched during the expansion protocol, but their content in the infusion bag is still variable[96]. Since survival factors, nutrients and activating molecules are limited *in vivo*, the more tumor-specific T cells are infused, the higher is their chance to engraft

and exert their therapeutic potential. It may thus be desirable to perform ACT with pure populations of tumor-specific T cells. With our protocol, we were able to generate high numbers of pure AH1-specific T cells. Such protocol, together with methods to predict antigenic peptides, may be implemented for the expansion of tumor-specific T cells in the clinic.

7 Conclusions and Outlook

Cancer is a global health problem in modern society. Longer life expectancy and aging of the population in the developed- and developing countries, increase in environmental pollution, and exposure to UV radiation are all related to increased cancer incidence. The development of new therapies against cancer has thus become a major focus of the pharmaceutical research industry and immunotherapy represents the most promising strategy in this regard. Although the anti-tumor immune response is extremely complex and involves a multitude of different cells and interactions, successful immunotherapeutic approaches seem to converge to a common final aim: generating functional CD8+ T cells able to destroy the tumor. Immunocytokines and ACTs are two promising types of immunotherapy. All the immunocytokines currently investigated in clinical trials have demonstrated potent anti-tumor activity in preclinical models, which was mainly dependent on CD8+ T cells and most ACTs are based on CD8+ T cells.

The work presented in this thesis aimed at exploring novel ways to exploit the potential of CD8+ T cells in an indirect way, using an immunocytokine featuring LIGHT, which has demonstrated to be able to recruit and activate CD8+ T cells in the tumor, and in a direct way, employing a pure population of tumor-specific CD8+ T cells as a therapy.

In the first part of the thesis, we studied the clonality, the phenotype, and the activation status of CD8+ T cells in response to treatment with the two immunocytokines F8-TNF and L19-IL12 in the CT26 syngeneic tumor model. We observed that upon administration of these agents, capable of inducing complete and durable tumor regression, the immune response proceeded through an oligoclonal expansion of tissue-resident CD8+ T cells infiltrating the tumor and that the majority of these cells recognized the rejection antigen AH1. We found a diverse repertoire of AH1-specific TCR and we could identify 27 unique complete TCR sequences. In relation to the thesis, this work indicates how immunocytokines can activate CD8+ T cells into the tumor and further highlights the role of the rejection antigen AH1, which we used as target for ACT.

The second part of the thesis focused on the development of F8-LIGHT. An immunocytokines featuring LIGHT attached to the F8 antibody in the single-chain variable fragment (scFv) format had been already produced in our laboratory, but was unable to accumulate at the site of disease *in vivo*[211]. We cloned and expressed the immunocytokines in five additional formats,

out of which only one could be produced in the desired quality. F8-LIGHT retained its functionality, accumulated at the tumor site *in vivo,* and substantially delayed tumor progression. We could show that F8-LIGHT was able to boost NK cells in a tumor model, however, analysis of the immune infiltrate indicated a decrease in CD8+ T cells upon administration of LIGHT compared to saline, contrarily to what expected. An agent able to boost NK cells in the tumor may be useful for example in tumors with low MHC expression, but it is far less attractive than an agent able to recruit and activate CD8+ T cells. Moreover, both IL2 and IL12 can stimulate NK cells and immunocytokines products based on these two cytokines are already being investigated in the clinic. It would be interesting to test if the desired effect on CD8+ T cells can be obtained by delivering LIGHT to the surface of tumor cells instead of to the tumor ECM, as shown elsewhere[162]. In order to move to the clinic, the murine LIGHT would need to be replaced by the human version, which may be easier to produce[162]. Additionally, the LIGHT-trapping receptor DcR3, overexpressed in various human tumors but absent in mice, may further complicate the direct translation of LIGHT-based therapies. In this regard, LIGHT mutants with a decreased affinity toward DcR3 have already been described[250] and may represent suitable payloads for a fully human immunocytokines product.

In the last part of this thesis, the antitumor activity of AH1-specific CD8+ T cells was investigated. To the best of our knowledge, this study represents the first attempt in treating tumor-bearing immunocompetent mice, with a pure population of tumor-specific T cells obtained simulating clinical procedures and not from transgenic mice. Rare AH1-specific T cells from tumors and secondary lymphoid organs could be reproducibly expanded to high numbers, demonstrated high and specific cytotoxic activity against tumor cells *in vitro*, and induced modest tumor-growth retardation in two murine tumor models when administered alone. However, *ex vivo* expanded AH1-specific CD8+ T cells showed extremely poor engraftment potential, and fail to mediate tumor regression. These results may not seem surprising when compared to similar studies in mice, where transgenic T cells are usually administered in an irradiated (or immunocompromised) host together with high dose IL2 and vaccination. Moreover, also in the clinic ACT is given after preconditioning and with supportive IL2. Nevertheless, our study suggests that extensive *ex vivo* expansion with current protocols may lead to T cell products with suboptimal therapeutic potential and that more effective protocols may be needed to routinely expand rare neoantigen-specific T cells for the therapy of epithelial cancers other than melanoma. In our model, AH1-specific T cells could be selectively expanded from bulk CD8+ TILs, without the need for sorting, but employing

antigen-pulsed DCs for activation. The implementation of current clinical procedures with our protocol may thus allow to avoid a sorting step, which further increases the amount of stress to which TILs are exposed.

In conclusion, despite the substantial advances in melanoma, certain hematological malignancies, and rare subsets of other solid tumors, immunotherapy is still not effective in the majority of solid epithelial cancers (accounting for about 80% of cancer deaths in the United States)[251]. An immunotherapeutic agent able to recruit CD8+ T cells in the tumor bed would be particularly useful as a combination therapy, especially in tumors with an immune desert or -excluded phenotype. Targeted delivery of LIGHT by means of an immunocytokine may represent a suitable strategy, although more preclinical work is needed.
For tumors with an inflamed phenotype, instead, ACT with TILs have shown promising results. However, successful therapy has so far been limited to a few anecdotal cases and more work needs to be done to implement this strategy. Our methodology may help to investigate novel ways to do so in the future.

8 Appendix 1: Immunotherapy of CT26 murine tumors is characterized by an oligoclonal response of tissue-resident memory T cells against the AH1 rejection antigen

8.1 Materials and methods

8.1.1 Animals and tumor models

CT26 colon carcinoma cells (ATCC) were handled according to supplier's protocol. Authentication including check of post-freeze viability, growth properties and morphology, test for mycoplasma contamination, isoenzyme assay and sterility test were performed by the cell bank before shipment. Eight-week-old female BALB/c mice were obtained from Charles River (Germany). All animal experiments were performed under a project license granted by the Veterinäramt des Kantons Zürich, Switzerland (04/2018).

8.1.2 Immunocytokine treatment

Exponentially growing CT26 tumor cells were harvested, repeatedly washed and resuspended in saline prior to injection. $3x10^6$ cells per animal were implanted subcutaneously in the right flank. Tumor volume was calculated as follows: ((length [mm] x (width [mm])^2)/2. When tumors were clearly palpable, mice were randomly divided into the different treatment groups. F8-mTNF and L19-mIL12 were injected intravenously in the lateral tail vein. Mice received two injections of either 2 µg F8-mTNF or 12 µg of L19-mIL12 every 48 h. Saline treated mice were used as control.

8.1.3 Sample preparation for flow cytometry

Spleens, tumor-draining lymph nodes and tumors were excised 48 h after the second F8-mTNF or L19-mIL12 injection and cells suspensions were obtained as already described [193]. Single cell suspensions were used for sorting, either directly, or following pre-treatment with MojoSort Mouse CD8 T Cell Isolation Kit (BioLegend) or CD8 (TIL) microbeads (Miltenyi Biotec) according to manufacturers' protocol.

8.1.4 Cell sorting

Surface staining was performed with PE-coupled AH1 tetramers (generated in-house as already described [193]) and fluorochrome-conjugated antibodies against CD8 (53-6.7, BioLegend). Cells were stained in PBS containing 0.5% bovine serum albumin and 2 mM EDTA for 30 min at 4 ºC. 7-AAD was used for staining dead cells. Cells were sorted on a FACSAria II (BD).

8.1.5 Bulk TCR Sequencing

100'000 CD8+ T cells from spleen and tumor cell suspensions of individual mice were sorted into 96-well plates. Genomic DNA was extracted using the QIAamp® DNA Micro kit (Qiagen) according to the manufacturer's protocol. DNA quality and concentration were assessed using a NanoDrop 2000c spectrophotometer (Thermo Scientific). DNA was shipped to Adaptive Biotechnologies (Seattle, WA, USA) for TCRB library preparation and high-throughput sequencing using the immunoSEQ Service for mouse TCRB.

8.1.6 Single-cell TCR Sequencing

Pooled cell suspensions of tumors and spleens from mice of each group were used to sort single $AH1^{+}CD8^{+}$ T cells into 96-well plates containing 2 µL 5x iScript reaction mix (iScript Advanced cDNA Synthesis kit, BioRad), 6 µL mQ and 1 µL 1% Triton-X. After sorting, 1 µL of iScript reverse transcriptase was added to each well and RT-PCR was conducted according to the supplier's protocol. Nested PCR for amplification of TCRα and TCRβ was performed as described by Dash et al. with slight modifications [252]. In brief, cDNA synthesis was performed from single cells using the iScript cDNA Synthesis Kit (Bio-Rad) according to the manufacturer's instructions in the presence of 0.1% Triton X-100 (Sigma-Aldrich). Following RT, two rounds of multiplex nested PCRs were performed with the GoTaq G2 Green Master Mix (Promega) to amplify the CDR3α and CDR3β transcripts from each cell. The PCR products were analyzed on a 1% agarose gel and samples containing both CDR3 subunits were sequenced using TRAC or TRBC reverse primers for α and β PCR products, respectively. Sequences were matched with the IMGT database (www.imgt.org).

8.1.7 Total mRNA sequencing

Cells from tumors and secondary lymphoid organs of mice treated with L19-mIL12 or saline were isolated and $CD8^+$ T cells were pre-enrichment with respective kits, before sorting directly in Buffer RLT (Qiagen). RNA was extracted and purified using RNeasy® Micro kit (Qiagen), following manufacturer's protocol. RNA Quality was determined using a TapeStation high sensitivity RNA (Agilent). Transcriptome analysis were performed by the FGCZ (University of Zurich, Zurich, Switzerland). Briefly, cDNA synthesis was performed using the SmartSeq2 method [253] and sequencing libraries were prepared by adding specific adapters [151] using the NexteraXT kit (Illumina). Magnetic beads (SeraMag, GE Healthcare) were used to recover library fragments in a size of 300-800bp. After normalization samples were sequenced on Illumina's NovaSeq6000 targeting ~20M reads per sample (Novaseq S1 Reagent Kit, 100 cycles, Illunima).

8.1.8 Data analysis

The Gini coefficient and the Simpson's index are two values that have been proposed to describe the diversity of TCR sequencing data. We have previously described to calculation of the Gini coefficient [254] for CD8+ T cell sequencing data. The generation of the Simpson's index has been described elsewhere [255].

Data were analyzed using Prism 7.0 (GraphPad Software, Inc.). Statistical significances were determined with a regular two-way ANOVA test with the Bonferroni post-test. Data represent means ± SEM. $P < 0.05$ was considered statistically significant. * = $p < 0.05$, ** = $p < 0.01$, *** $p = < 0.001$, **** = $p < 0.0001$.

Analysis of total mRNA sequencing data was performed by the FGCZ. Briefly, raw reads were cleaned by removing adapter sequences, trimming low quality ends, and filtering reads with phred quality <20 using Trimmomatic (Version 0.36) [256]. Sequence pseudo alignment of the resulting reads to the murine reference genome (build GRCm38.p6, gene annotation from GENCODE Release M23) and quantification of gene level expression was carried out using Kallisto (Version 0.44) [257]. The read alignment was done with STAR (v2.7.3) [258]. STAR alignment options were "--outFilterType BySJout –outFilterMatchNmin 30 --outFilterMismatchNmax 10 --outFilterMismatchNoverLmax 0.05 --alignSJDBoverhangMin 1 --alignSJoverhangMin 8 --alignIntronMax 100000 --outFilterMultimapNmax 50". To detect differentially expressed genes a count based negative binomial model implemented in the software package EdgeR (R version: 3.6.1, EdgeR version: 3.28.0) was applied [259]. The

differential expression was assessed using a generalized linear model adapted for over-dispersed data. Genes showing altered expression with adjusted (Benjamini and Hochberg method) p-value < 0.05 were considered differentially expressed.

8.2 Supplementary information

8.2.1 Supplementary Tables

Table 1: TCRB nucleotide sequences shared between TILs from mice of same treatment group

Group	Rearrangement from start of CDR3 to J-Gene (nt)	Present In
saline	TGTGCCAGCAGTTTAACTGGGAGTGCAGAAACGCTGTAT	3
	TGTGCCAGCAGACAGGGCCGCAACGAAAGATTATTT	2
	TGTGCCAGCAGTGAAGGGGATTCTGGAAATACGCTCTAT	2
	TGTGCCAGCAGTATAGCAGTTTCCAACGAAAGATTATTT	2
	TGTGCTAGCAGTTTACAGGGGACCAACGAAAGATTATTT	2
	TGTGCCAGCGGTTCTGGGACAGGGAACCAGGCTCCGCTT	2
	TGTGCCAGCGGTGAACTGGGGGGCTCCTATGAACAGTAC	2
	TGTGCTAGCAGTTTTGGGGATGAACAGTAC	2
	GTGCTAGCAGTTTAGGGGACACCCAGTAC	2
	TGTGCCAGCAGCCCCCGGGACAGAAACACAGAAGTCTTC	2
	TGTGCTAGCAGTTTACGGACAGGGGGCTATGCTGAGCAGTTC	2
	TGTGCCAGCAGTTCTCGGACTGGGGGCTATGCTGAGCAGTTC	2
	TGTGCCAGCAGTATAAAGACAGGGGGCTATGCTGAGCAGTTC	2
	TGTGCCGGCAGTTCTCGGACTGGGGGCTATGCTGAGCAGTTC	2
	TGTGCCAGCAGTATAAAGACAGGGGGCTATGCTGAGCAGTTC	2
	TGTGCCGGCAGTTTAACTGGGAGTGCAGAAACGCTGTAT	2
	TGTGCCAGCGGTGATGCAGGGTATGAACAGTAC	2
L19-mIL12	TGTGGTGCTAGGACAGCAAACTCCGACTACACC	2
	TGTGCCAGCAGCGACAATTCTGGAAATACGCTCTAT	2
	TGTGCAAGCAGCTCCGGGACAAACACAGAAGTCTTC	2
	GTGCTAGCAGTTGGGGAGACACCCAGTAC	2
	TGTGCCAGCAGCCAGGGACTGGGGGTCTCCTATGAACAGTAC	2
	TGTGCCAGCAGGGGGGATGAACAGTAC	2
	TGTGCCAGCAGTTTAACTGGGAGTGCAGAAACGCTGTAT	2
F8-mTNF	TGTGCCAGCAGTTCTCGGACTGGGGGCTATGCTGAGCAGTTC	3
	TGTGCCAGCAGTTTAACTGGGAGTGCAGAAACGCTGTAT	3
	TGTGCTAGCAGTTTAAAGACAGGGGGCTATGCTGAGCAGTTC	2
	TGTGCCGGCAGTTTAACTGGGAGTGCAGAAACGCTGTAT	2

Table 2: Top five tumor-infiltrating T cell clones in each treated animal

Mouse	CDR3β	Frequency (%)	TRBJ	TRBV
L19-mIL12 1	**CASGDAWGSAETLYF**	20.48%	J02-03	V13-02
	CASWGGENTGQLYF	9.44%	J02-02	V04-01
	CASSPGAGYEQYF	8.18%	J02-07	V19-01
	CASSPPGVEQYF	4.77%	J02-07	V05-01
	CASGDFRGSDYTF	4.44%	J01-02	V13-02
L19-mIL12 2	CAWSLGGTGGNNQAPLF	11.14%	J01-05	V31-01
	CASSISRGANSDYTF	8.51%	J01-02	V19-01
	CAWTTGQAPLF	7.31%	J01-05	V31-01
	CASGPTGGTNTGQLYF	5.35%	J02-07	V13-02
	CASSIEGGIEQYF	5.34%	J02-02	V19-01
L19-mIL12 3	**CASSDNSGNTLYF**	47.06%	J01-03	V02-01
	CAWSLGDNQAPLF	21.15%	J01-05	V31-01
	CASSLWGNSDYTF	6.50%	J01-02	V24-01
	CASSIGRAPNERLFF	3.99%	J01-04	V19-01
	CASSQGDGGNSDYTF	3.69%	J01-02	V02-01
F8-mTNF 1	CASSRDRNTGQLYF	21.97%	J02-02	V17-01
	CASGEYGYEQYF	17.00%	J02-07	V13-02
	CASGDGLGVNQDTQYF	6.06%	J02-05	V13-02
	CASSRDWGYEQYF	5.88%	J02-07	V14-01
	CASSSVLGNQDTQYF	3.07%	J02-05	V03-01
F8-mTNF 2	CASGDALGSYEQYF	12.59%	J02-07	V13-02
	CASSEGQYEQYF	11.47%	J02-07	V13-01
	CAWSLEGGNANSDYTF	9.84%	J01-02	V31-01
	CASSDGWGYEQYF	7.52%	J02-07	V13-03
	CASRTGTGGYEQYF	6.52%	J02-07	V19-01
F8-mTNF 3	CASSFGDEQYF	16.35%	J02-07	V04-01
	CASRGDEQYF	15.44%	J02-07	V13-03
	CASSQEGLGGNNYAEQFF	7.76%	J02-01	V05-01
	CASSLRLGGYAEQFF	7.49%	J02-01	V19-01
	CASGDTYEQYF	6.27%	J02-07	V13-02

Red**:** AH1-specific CD8+ T cells identified by single cell sequencing (**Bold**), or by [188] (Regular)

Table 3: Top five tumor-infiltrating T cell clones in each untreated animal

Mouse	CDR3β	Frequency (%)	TRBJ	TRBV
saline 1	**CASSSRTGGYAEQFF**	10.77%	J02-01	V19-01
	CASSPRWGGEFEQYF	8.11%	J02-07	V05-01
	CASSDWGGAYEQYF	7.27%	J02-07	V16-01
	CASSERVAQDTQYF	6.83%	J02-05	V13-01
	CTCSAPGHSNERLFF	5.72%	J01-04	V01-01
saline 2	CASSPQGAREQYF	15.82%	J02-07	V02-01
	CASGSGTGNQAPLF	14.20%	J01-05	V13-02
	CASSEGQYEQYF	10.72%	J02-07	V13-01
	CASSQPGQSNERLFF	6.71%	J01-04	V02-01
	CAWSAGGLYEQYF	4.36%	J02-07	V31-01
saline 3	CASSRPGHEQYF	13.86%	J02-07	V13-01
	CASSIKTGGYAEQFF	10.16%	J02-01	V19-01
	CASSLRLGGYAEQFF	4.87%	J02-01	V19-01
	CASSQDLGLGPSQNTLYF	4.12%	J02-04	V05-01
	CAWSPTGTNNNQAPLF	3.90%	J01-05	V31-01

Red**:** AH1-specific CD8+ T cells identified by single cell sequencing (**Bold**), or by [188] (Regular)

Table 4: Matching CDR3β and CDR3α sequences of AH1-specific T cells

CDR3β	TRBJ	TRBV	CDR3α	TRAJ	TRAV	Treatment
CASGDLGYEQYF	J2-7	V13	CIVTEGGGSGNKLIF	J32	V2	saline
CAWSLAGASAETLYF	J2-3	V31	CAVSMPSGSWQLIF	J22	V7	saline
CASSDFYEQYF	J2-7	V13	CILQGGSAKLIF	J57	V21	saline
CAWSLAGASAETLYF	J2-3	V31	CIVTEGGGSGNKLIF	J32	V2	saline
CASSYRNYAEQFF	J2-1	V4	CALSPPPNTDKVVF	J34	V6	saline
CAWSGQGVSYNSPLYF	J1-6	V31	CAVTSSSGSWQLIF	J22	V7	L19-mIL12
CASSQGDGGNSDYTF	J1-2	V2	CAVRGNYKPTF	J6	V7	L19-mIL12
CASSQGDGGNSDYTF	J1-2	V2	CALSSSGSWQLIF	J22	V6	L19-mIL12
CASSDNSGNTLYF	J1-3	V2	CIVTASSGSFNKLTF	J4	V2	L19-mIL12
CASSFYNTEVFF	J1-1	V19	CATDANQGGSAKLIF	J57	V8	L19-mIL12
CASSSRTGGYAEQFF	J2-1	V4	CAVSKNSGTYQRF	J13	V3	L19-mIL12
CASGDAWGSAETLYF	J2-3	V13	CIVTASSGSFNKLTF	J4	V2	L19-mIL12
CASAGGYEQYF	J2-7	V13	CILDTGYQNFYF	J49	V21	L19-mIL12
CAWSLTGGADNQAPLF	J1-5	V31	CATAPSSGSWQLIF	J22	V8	L19-mIL12
CASGAGANYAEQFF	J2-1	V13	CATEGTGSKLSF	J58	V8	F8-mTNF
CASGEFGNSDYTF	J1-2	V13	CILVGGSAKLIF	J57	V21/12	F8-mTNF
CASGGSQNTLYF	J2-4	V13	CASFSAGNKLTF	J17	V6-6	F8-mTNF
CASGGTLNTLYF	J2-4	V13	CALWELSNTGYQNFYF	J49	V15	F8-mTNF
CASSDGGSYEQYF	J2-7	V13	CILRDSNYQLIW	J33	V21/12	F8-mTNF
CASSDRGRDQDTQYF	J2-5	V19	CAVSEPSGSWQLIF	J22	V3	F8-mTNF
CASSGQGSSGNTLYF	J1-3	V29	CAFSTGGYKVVF	J12	V16/11	F8-mTNF
CASSIRLGGYAEQFF	J2-1	V4	CAVSESGTYQRF	J13	V3	F8-mTNF
CASSLPGQEVFF	J1-1	V5	CVLGEEGRALIF	J15	V6-2	F8-mTNF
CASSQDTGGYEQYF	J2-7	V2	CALRAYQGGSAKLIF	J57	V6-6	F8-mTNF
CASSRQNSDYTF	J1-2	V4	CIRAGTGGYKVVF	J12	V2	F8-mTNF
CASSWTGGAYEQYF	J2-7	V3	CILRGLNSGGSNAKLTF	J42	V21/12	F8-mTNF
CAWSLAGVSYNSPLYF	J1-6	V31	CAVSKPSGSWQLIF	J22	V7	F8-mTNF

A total of 27 unique TCR were identified among 80 sequenced samples (containing both CDR3 subunits) from 308 cells.

Table 5: Summary of $CD8^+$ cells TCR sequencing

	Templates		Rearrangements				
Sample	**Total**	**Productive**	**Total**	**Productive**	**Unique CDR3 (Aa)**	**Productive clonality**	**Max productive frequency**
saline tumor 1	2216	1801	265	173	153	0.2796	0.108
saline tumor 2	19771	16828	1476	1004	875	0.4555	0.158
saline tumor 3	33794	25690	3588	2531	2292	0.3981	0.139
L19-mIL12 tumor 1	14897	11178	1825	1253	1145	0.4195	0.203
L19-mIL12 tumor 2	9053	6966	531	341	280	0.3647	0.111
L19-mIL12 tumor 3	19455	15177	725	480	428	0.6447	0.470
F8-mTNF tumor 1	1278	1106	342	252	241	0.3129	0.220
F8-mTNF tumor 2	2344	1596	221	142	115	0.2881	0.122
F8-mTNF tumor 3	16539	10789	1380	927	792	0.4302	0.163
saline spleen 1	489	359	352	250	240	0.017	0.011
saline spleen 2	26196	19660	18774	13899	13002	0.0175	0.008
saline spleen 3	28185	20638	19767	14173	13164	0.0143	0.004
L19-mIL12 spleen 1	10630	7657	7364	5163	4908	0.013	0.001
L19-mIL12 spleen 2	3007	2170	2065	1476	1429	0.0167	0.007
L19-mIL12 spleen 3	1529	1128	1000	718	698	0.0258	0.028
F8-mTNF spleen 1	395	295	238	168	161	0.055	0.071
F8-mTNF spleen 2	1585	1151	1070	762	746	0.0179	0.005
F8-mTNF spleen 3	8287	6154	5859	4312	4148	0.0115	0.005
Sum	199650	150343	66842	48024	44817		

Table 6: Combined TCR rearrangements

Sample	**Unique CDR3 (nt)**	**Unique CDR3 (Aa)**
saline tumors	3690	3269
saline spleens	28142	25338
saline total	31452	27917
L19-mIL12 tumors	2067	1835
L19-mIL12 spleens	7340	6933
L19-mIL12 total	9298	8575
F8-mTNF tumors	1315	1138
F8-mTNF spleens	5233	5019
F8-mTNF total	6491	6061
Tumors total	7029	6086
Spleens total	40388	35481
Total	46793	40175

9 Appendix 2: Antibody-mediated delivery of LIGHT to the tumor boosts Natural Killer cells and delays tumor progression

9.1 Materials and Methods

9.1.1 Cell lines and animal models

CT26 colon carcinoma (ATCC CRL-2638), WEHI-164 fibrosarcoma (ATCC CRL-1751), F9 teratocarcinoma (ATCC CRL-1720) and HT-29 (ATCC HTB-38) human adenocarcinoma cells were obtained from ATCC, CHO-S cells from Invitrogen. Cells were handled according to supplier's protocol and maintained as cryopreserved aliquots in liquid nitrogen. Authentication including check of post-freeze viability, growth properties and morphology, test for mycoplasma contamination, isoenzyme assay and sterility test were performed by the cell bank before shipment. Tumor cell lines were kept in culture no longer than 3 weeks, CHO-S cells no longer than 4 weeks. Eight-weeks-old female BALB/c or 129/Sv mice were obtained from Janvier (France). All animal experiments were performed under a project license granted by the Veterinäramt des Kantons Zürich, Switzerland (04/2018).

9.1.2 Cloning, expression and biochemical characterization of fusion proteins

The DNA sequence encoding murine LIGHT extracellular domain (amino acids 87-239) in a single-chain format (in which three LIGHT subunits were genetically linked together by a Glycine codon) including a N-terminal $(SSSSG)_3$-linker, was purchased from Eurofins genomics. The LIGHT gene was fused by PCR assembly to the C-terminal end of various formats of the F8 antibody via its 15 amino acids linker. The resulting genes were cloned into the mammalian vectors pcDNA3.1+ (for F8 in scFv-Fc and diabody formats) or pMM137 (for F8 in IgG format) by restriction enzymes digestion and ligation, followed by amplification in TG1 electrocompetent *E. coli* bacteria. pMM137 was kindly provided by Philochem AG and has been described elsewhere [260]. Fusion proteins were produced in CHO-S by transient gene expression as already described [261, 262]. Both "low density" (LD) [261] and "high density" [217 262] protocols were used. Proteins were purified to homogeneity by protein A affinity chromatography and characterized by size exclusion chromatography on a Äkta Pure FPLC system (GE Healthcare) with a Superdex S200 10/300 increase column (GE Healthcare) and by SDS-PAGE.

9.1.3 Mass spectrometry analysis of F8-LIGHT

The fusion protein was treated with glycerol free PNGase F (NEB, P0705S) in non-denaturing reaction conditions, as indicated by the manufacturer, to remove N-linked glycans. The resulting protein was analyzed by Liquid chromatography-Mass spectrometry on a Waters Xevo G2-X2 Qtof instrument coupled to a Waters Acquity UPLC H-class system, using a 2.1 x 50 mm Acquity BEH300 C4 1.7 µm column (Waters).

9.1.4 Functional in vitro characterization of F8-LIGHT

Binding of the F8 moiety to its cognate antigen was tested by ELISA. Briefly, wells of a F96 Maxisorp nunc-immuno plate (Thermofisher) were coated with EDA and blocked with 2% milk powder in PBS. F8-LIGHT and positive control F8 in small immune protein format (SIPF8) were added at different concentrations in wells, followed by incubation with polyclonal antibodies against human kappa light chains (Dako, A0192) and by HRP-conjugated protein A (GE Healthcare, NA9120V). Colorimetric reaction was started by adding BM Blue POD substrate (Roche, 11442066001) and quenched with 1M H_2SO_4. Absorbance at 450 nm was measured with a Spectra Max Paradigm multimode plate reader (Molecular Devices). *In vitro* activity of the LIGHT moiety was tested with a cytotoxicity assay on HT-29 cells, which have been shown to be sensitive to LIGHT in the presence of human interferon gamma (hIFNγ) [263]. Briefly, F8-LIGHT and recombinant hIFNγ (Biolegend, 570202) at given concentrations were added to wells containing 40000 HT-29 cells in McCoy's 5A (Modified) Medium (Thermofisher, 16600082) supplemented with 10% fetal bovine serum (Thermofisher, 10270106) and 1x Antibiotic-Antimycotic (Thermofisher, 15240062). After incubation for 72 hours at 37°C, 5% CO_2, cells were detached using Trypsin-EDTA solution (Thermofisher, 25200056), re-suspended in PBS containing 0.5% BSA and 2mM EDTA and stained with 7-AAD (Biolegend, 420404) for 5' at 4°C. Percentage of living cells was determined by Flow cytometry analysis using a CytoFLEX S (Beckman Coulter). Data were analyzed with FlowJo software (FlowJo, LLC, version 10).

9.1.5 Quantitative biodistribution

In vivo targeting ability of F8-LIGHT was determined by quantitative biodistribution as already described [189]. Briefly, $1x10^7$ F9 cells were subcutaneously injected in the right flank of 129/Sv mice. Tumor size was determined daily using the formula: ½ x (major diameter) x (minor diameter)^2. When tumors reached a volume of 100-300 mm^3, fusion proteins were labeled with

Iodine-125, using Chloramine T. Radiolabeled protein was purified by size exclusion chromatography (PD-10 column, GE Healthcare, 17-0851-01) and injected in the lateral tail vein of tumor-bearing mice. Animals were sacrificed after 24 hours. Organs and tumors were harvested, weighted and radioactivity was determined using a Packard Cobra II Gamma Counter (GMI).

9.1.6 Tumor therapy experiments

Anti-tumor activity of F8-LIGHT was tested in two syngeneic murine models of cancer. CT26 and WEHI-164 tumors were implanted in the right flank of BALB/c mice by subcutaneous injection of $3x10^6$ resp. $2.5x10^6$ cells. Treatments were started when tumors reached a volume of about 100 mm3. The indicated dose of immunocytokines or the corresponding volume of saline, were administered by intravenous injection in the lateral tail vein, every other day for a total of three injections. The immune-checkpoint inhibitor anti-PD-1 (BioXCell, clone 29F.1A12) was administered in the same way, at alternate days. Mice were inspected daily. Body weight was monitored, tumor was measured with a caliper and tumor size was determined using the formula: ½ x (major diameter) x (minor diameter)2. Mice with ulcerated hemorrhagic tumor, or with tumor bigger than 1500 mm3 where euthanized.

9.1.7 Antibody and reagents for Flow Cytometry

Fluorophore-conjugated antibodies against CD3 (clone 17A2), CD4 (clone GK1.5), CD8 (clone 53-6.7), NK1.1 (clone PK136), I-A/I-E (clone M5/114.15.2), CD62L (clone MEL-14), CD44 (clone IM7), and FoxP3 (clone MF-14), as well as 7-AAD and Zombie Red viability dies were all purchased from BioLegend. AH1-loaded, PE-conjugated H-$2L^d$ tetramers were obtained as already described [177].

9.1.8 Analysis of immune infiltrates

Immune infiltrates were analyzed in tumors and tumor-draining lymph nodes of mice bearing WEHI-164 sarcoma, 48 hours after the last injection of either saline or F8-LIGHT. Mice were euthanized and tumors, right axillary and right inguinal lymph nodes were harvested. Tumors were cut into small fragments and incubated in an orbital shaker at 37°C for 30' in RPMI 1640 Medium (Thermofisher, 21875034) containing 1x Antibiotic-Antimycotic (Thermofisher, 15240062), 1 mg/mL Collagenase II (Thermofisher, 17101015) and 0.1 mg/mL DNAse I (Roche, 10104159001). Tumor cells suspensions were passed through a 70μm cell strainer

(Corning) and treated with Red Blood Cells Lysis buffer (Biolegend, 420301) following supplier's recommendations. Lymph nodes were harvested and smashed on a 70μm cell strainer (Corning) using the back of a syringe plunger. The resulting tumor and lymph nodes single cell suspensions were washed in PBS, before incubation with staining reagents. Where appropriate, cells were stained with Zombie Red dye (diluted 1:500 in PBS) for 15' at room temperature, followed by staining with antibodies and tetramers in FACS buffer (0.5% BSA, 2mM EDTA in PBS) for 30' at 4°C. Cells, which were not stained with Zombie Red, were stained with 7-AAD (diluted 1:100 in FACS buffer) for 5' at 4°C. Intracellular staining with antibodies against FoxP3 was performed using eBioscience™ Foxp3 / Transcription Factor Staining Buffer Set (Thermofisher), following supplier's protocol. Samples were analysed with CytoFLEX S (Beckman Coulter) and data were processed using FlowJo software (FlowJo, LLC, version 10). A detailed description of the gating strategies can be found in Additional files (**Supplementary Figures 7-9**). Total of living cells in the tumor was calculated by subtracting dead cells and debris from the total number of recorded events.

9.1.9 Data analysis

Data were analyzed using Prism 7.0 (GraphPad Software, Inc.). Statistical significances of tumor therapy and flow cytometry data were determined with a regular two-way ANOVA test with Bonferroni post-test correction and with an unpaired, two-tailed t-test, respectively. Data represent means ± SEM. $P < 0.05$ was considered statistically significant.

9.2 Supplementary information

9.2.1 F8-LIGHT amino acids sequence (Mw: 101790.95)

EVQLLESGGGLVQPGGSLRLSCAASGFTFSLFTMSWVRQAPGKGLEWVSAISGSGGSTYYAD
SVKGRFTISRDNSKNTLYLQMNSLRAEDTAVYYCAKSTHLYLFDYWGQGTLVTVSSGGSGG
EIVLTQSPGTLSLSPGERATLSCRASQSVSMPFLAWYQQKPGQAPRLLIYGASSRATGIPDRFS
GSGSGTDFTLTISRLEPEDFAVYYCQQMRGRPPTFGQGTKVEIKGGGGSGGGGSGGGGSEVQ
LLESGGGLVQPGGSLRLSCAASGFTFSLFTMSWVRQAPGKGLEWVSAISGSGGSTYYADSVK
GRFTISRDNSKNTLYLQMNSLRAEDTAVYYCAKSTHLYLFDYWGQGTLVTVSSGGSGGEIVL
TQSPGTLSLSPGERATLSCRASQSVSMPFLAWYQQKPGQAPRLLIYGASSRATGIPDRFSGSGS
GTDFTLTISRLEPEDFAVYYCQQMRGRPPTFGQGTKVEIKSSSSGSSSSGSSSSGSHQANPAAH
LTGANASLIGIGGPLLWETRLGLAFLRGLTYHDGALVTMEPGYYYVYSKVQLSGVGCPQGLA
NGLPITHGLYKRTSRYPKELELLVSRRSPCGRANSSRVWWDSSFLGGVVHLEAGEEVVVRVP

GNRLVRPRDGTRSYFGAFMVGSHQANPAAHLTGANASLIGIGGPLLWETRLGLAFLRGLTYH
DGALVTMEPGYYYVYSKVQLSGVGCPQGLANGLPITHGLYKRTSRYPKELELLVSRRSPCGR
ANSSRVWWDSSFLGGVVHLEAGEEVVVRVPGNRLVRPRDGTRSYFGAFMVGSHQANPAAH
LTGANASLIGIGGPLLWETRLGLAFLRGLTYHDGALVTMEPGYYYVYSKVQLSGVGCPQGLA
NGLPITHGLYKRTSRYPKELELLVSRRSPCGRANSSRVWWDSSFLGGVVHLEAGEEVVVRVP
GNRLVRPRDGTRSYFGAFMV

9.2.2 Supplementary Figures

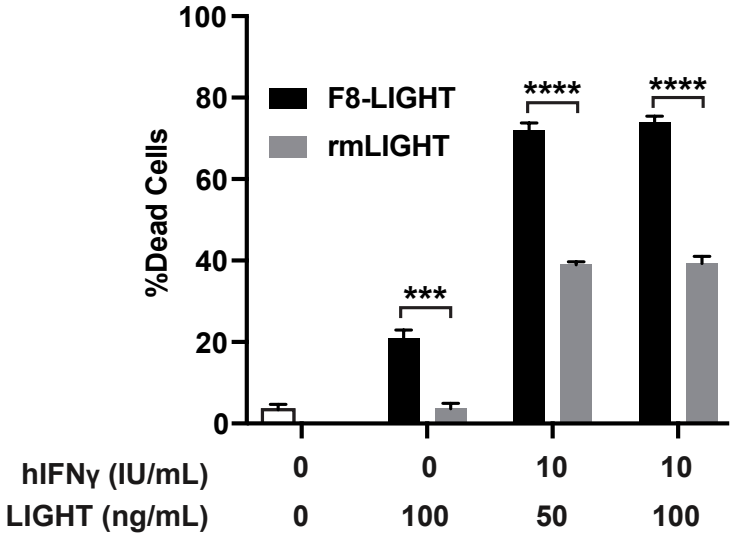

Supplementary Figure 1: ***In vitro activity of F8-LIGHT versus recombinant murine LIGHT****. Activity of F8-LIGHT was compared to activity of recombinant murine LIGHT (rmLIGHT, BioLegend) in a cytotoxicity assay on HT-29 cells. hIFNγ = human Interferon gamma. Concentration are based on the molecular weight of the LIGHT monomer. Columns represent means + SEM, n = 3 per experimental group, *** p = < 0.001, **** = p < 0.0001 (unpaired student t-test).*

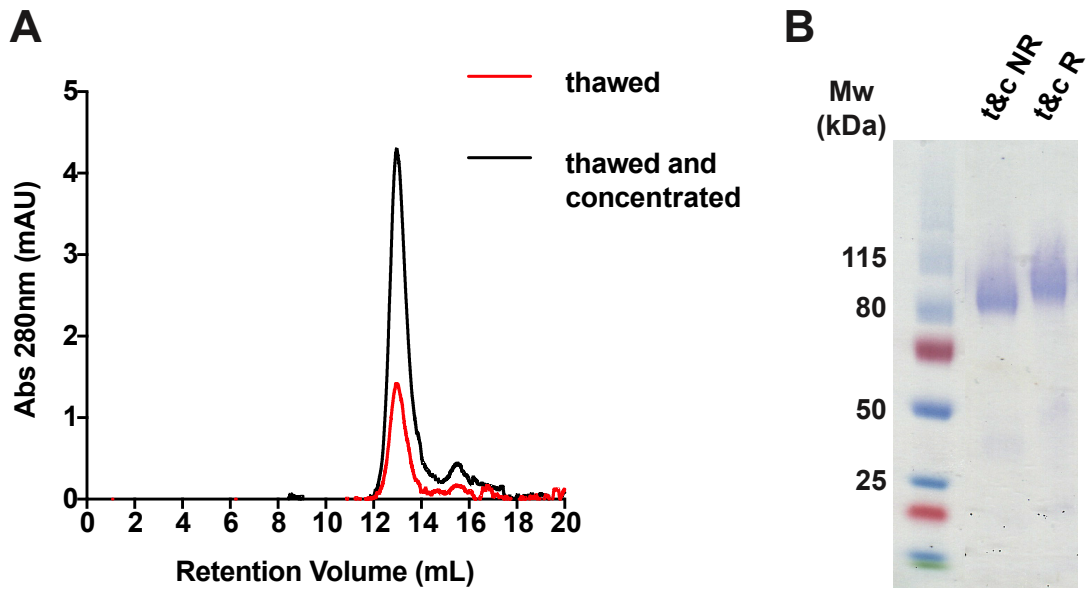

Supplementary Figure 2: ***Stability of F8-LIGHT****. Biochemical characterization of F8-LIGHT, after freeze and thaw and concentration by ultracentrifugation. A, size exclusion chromatography profile. B, SDS-PAGE under non-reducing (NR) and reducing (R) conditions, t&c = thawed and concentrated.*

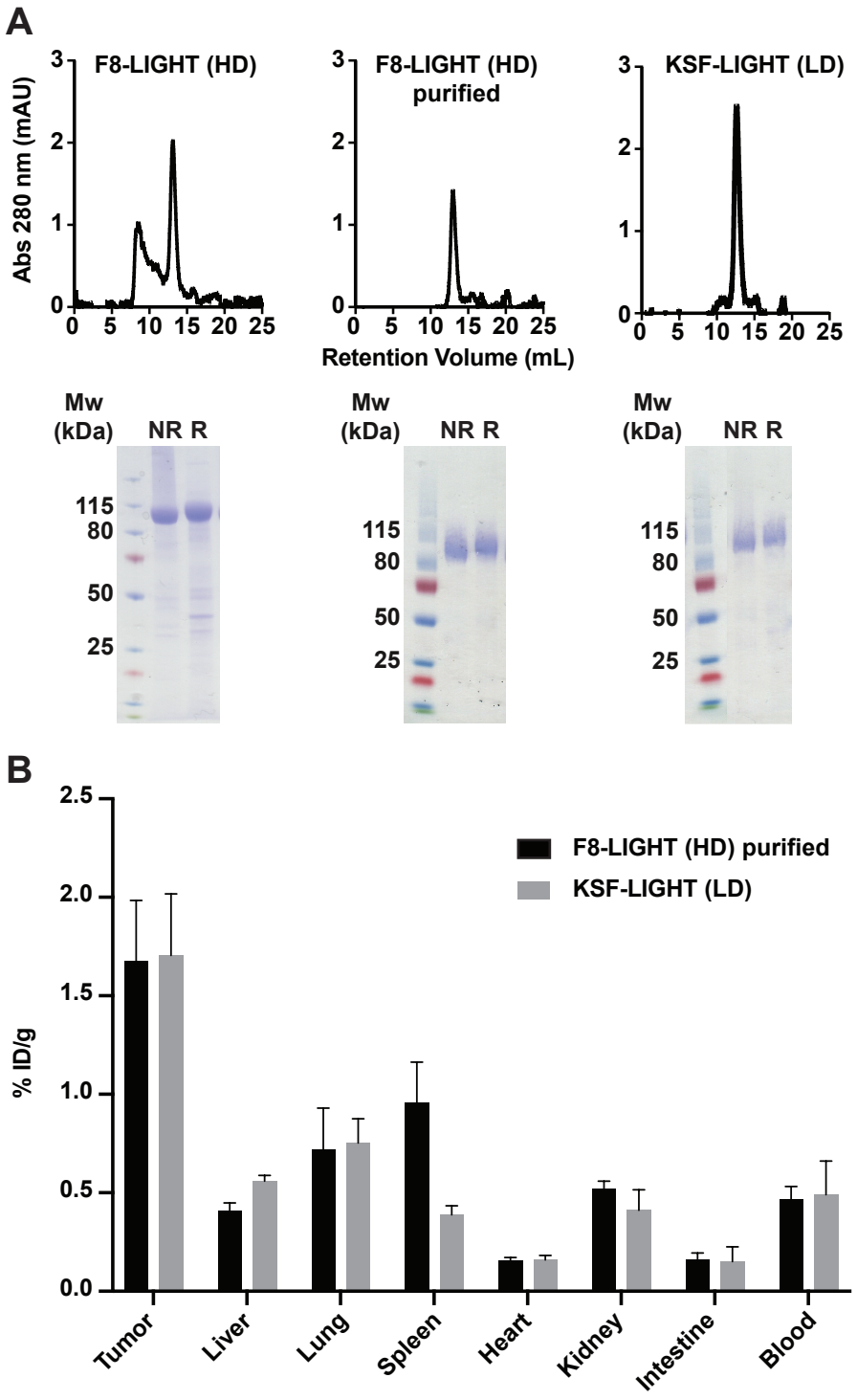

*Supplementary Figure 3: **In vivo targeting of F8-LIGHT produced with the "High density" protocol**. **A**, Biochemical characterization of F8-LIGHT produced with the HD protocol and KSF-LIGHT produced with the LD protocol, including size exclusion chromatography profiles and SDS-PAGE under non-reducing (NR) and reducing (R) conditions of F8-LIGHT before and after purification by gel filtration (KSF-LIGHT, as F8-LIGHT, eluted as a single peak and did not need to be purified, when produced with the LD protocol). **B**, accumulation of radiolabelled preparations of purified F8-LIGHT (HD) and KSF-LIGHT (LD) in tumors and healthy organs of 129/Sv mice bearing F9 tumors, 24 hours after intravenous administration.*

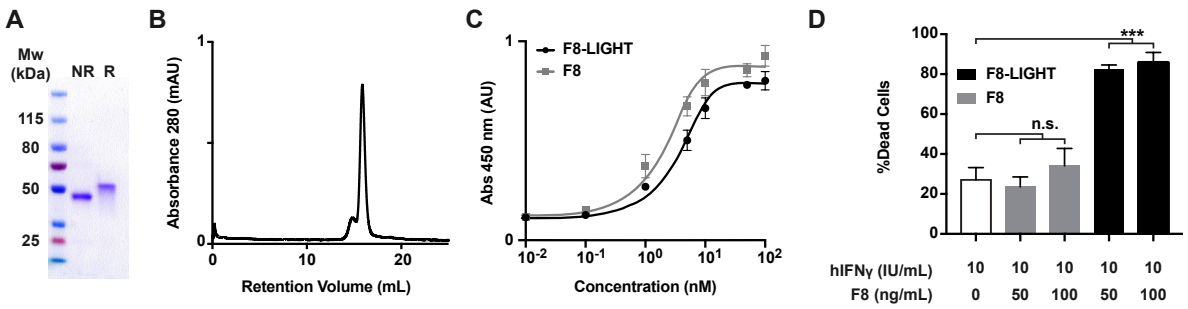

Supplementary Figure 4: ***Characterization of the F8 protein in single-chain diabody format****. Biochemical characterization of F8, including SDS-PAGE under non-reducing (NR) and reducing (R) conditions (**A**) and size exclusion chromatography profile (**B**). **C**, binding of titrated concentrations of F8 and F8-LIGHT to immobilized target antigen EDA, measured by ELISA. **D**, activity of F8-LIGHT compared to F8, measured by a cytotoxicity assay on HT-29 cells in the presence of human Interferon gamma (hIFNγ). Reported concentrations are based on the molecular weight of the F8 part of the molecule alone. 7-AAD positive dead cells were detected by Flow Cytometry. Column represent means ± SEM, n = 3 per experimental group, ns = non significant, * = p < 0.05, ** = p < 0.01, *** p = < 0.001, **** = p < 0.0001 (unpaired t-test).*

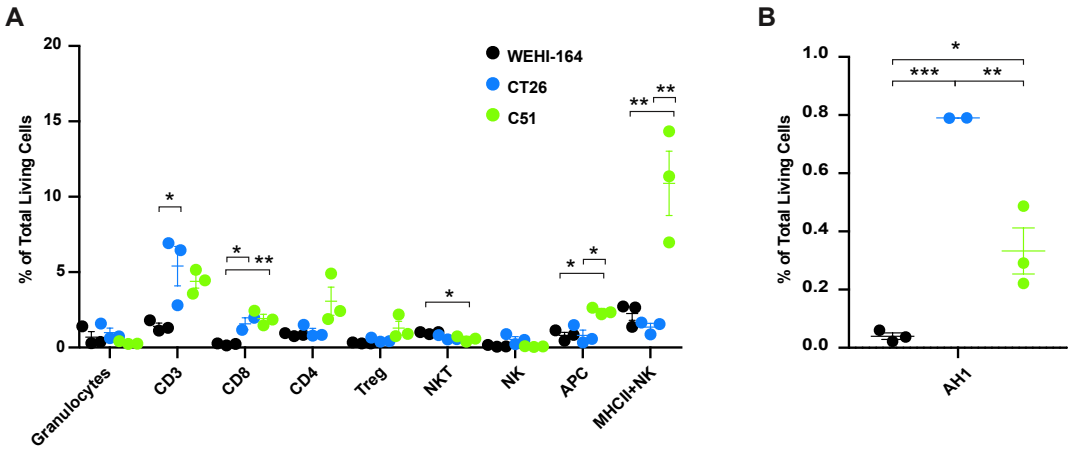

Supplementary Figure 5: ***Analysis of leukocyte infiltrate in different BALB/c syngeneic tumor models****. Flow Cytometry analysis of the immune infiltrate in BALB/c bearing WEHI-164, CT26 or C51 tumors, 48 hours after the third i.v. injection of saline (saline administered every other day starting when the tumor was about 100mm^3). **A**, analysis of different population of leukocytes. **B**, analysis of tumor-infiltrating AH1-specific CD8+ T cells. Data represent means ± SEM, n = 3 mice per experimental group. * = p < 0.05, ** = p < 0.01, *** p = < 0.001 (regular one-way ANOVA test with Bonferroni post-test correction).*

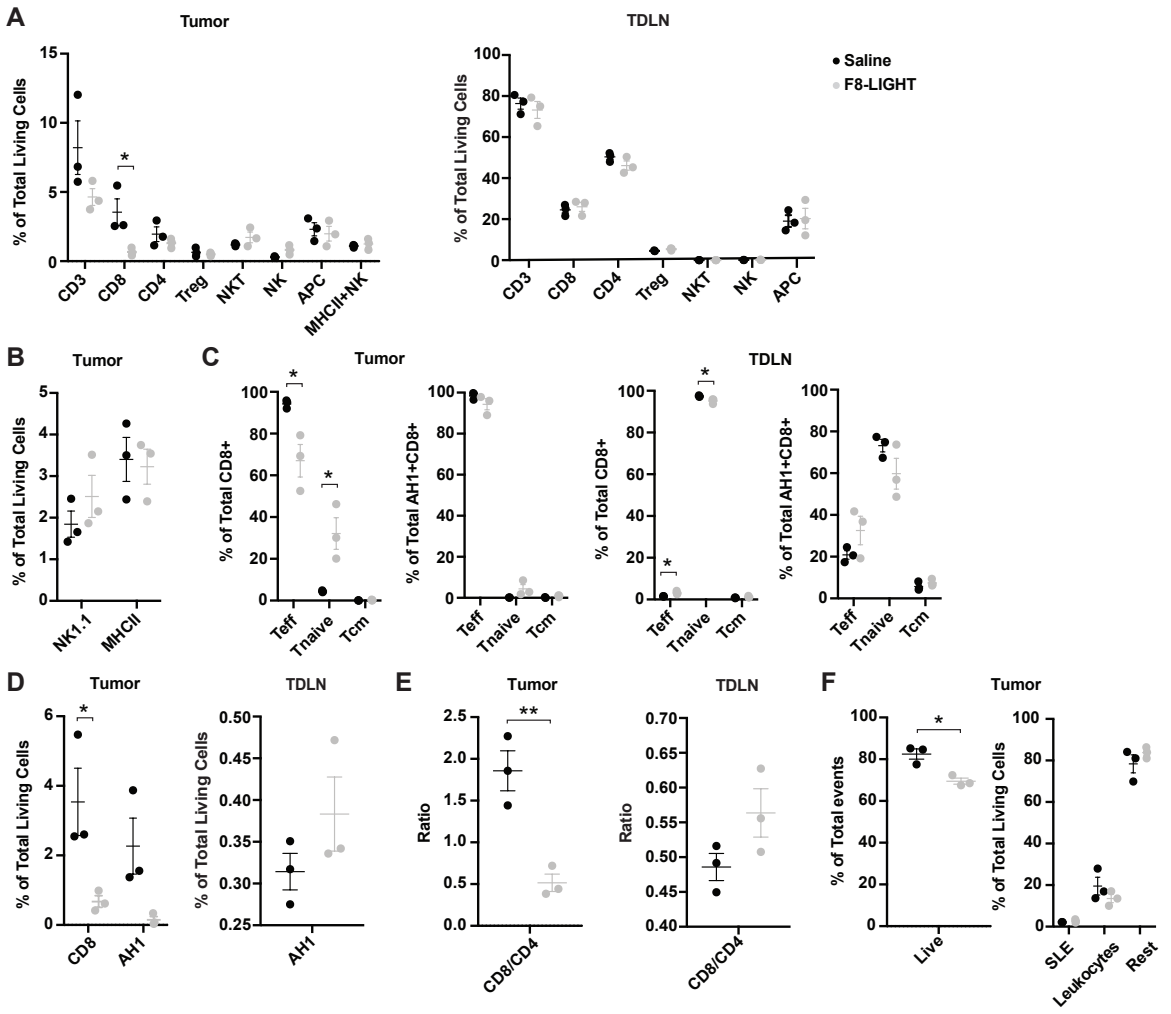

Supplementary Figure 6: ***Analysis of immune infiltrate in CT26****. Analysis of tumors and tumor-draining lymph nodes (TDLN) of BALB/c mice bearing CT26 tumors, 48 hours after the third administration of F8-LIGHT or saline.* ***A****, lymphocytes infiltration in tumors and composition of TDLN. CD3 = CD3+ lymphocytes, CD8 = CD8+ T cells, CD4 = CD4+ T cells, T_{reg} = CD4+ regulatory T cells, NKT = Natural Killer T cells, NK = Natural Killer cells, APC = Antigen Presenting cells and MHCII+NK = MHC class II+ NK cells.* ***B****, total NK1.1-positive and MHC class II-positive lymphocytes infiltrating tumors.* ***C****, phenotype of CD8+ T cells and of AH1-specific $CD8^+$ T cells in tumors and TDLN, based on expression of the markers CD44 and CD62L. T_{eff} = effector T cells, T_{naive} = naïve T cells, T_{cm} = central memory T cells.* ***D****, AH1-specific CD8+ T cells in tumors and TDLN.* ***E****, CD8+ T cells:CD4+ T cells ratio in tumor and TDLN.* ***F****, fraction of living cells among total events recorded and composition of living cells in the tumor. "Leukocytes" represent the sum of all T cells, NK cells, Antigen Presenting cells and Granulocytes, "Rest" represent the remaining living cells, after subtracting SLE and Leukocytes from the total number of living cells. SLE = "Small Living Events", in analogy with data from WEHI-164 tumors. Data represent individual mice, with means ± SEM, n = 3 mice per experimental group. * = $p < 0.05$, ** = $p < 0.01$, *** $p = < 0.001$ (unpaired t-test).*

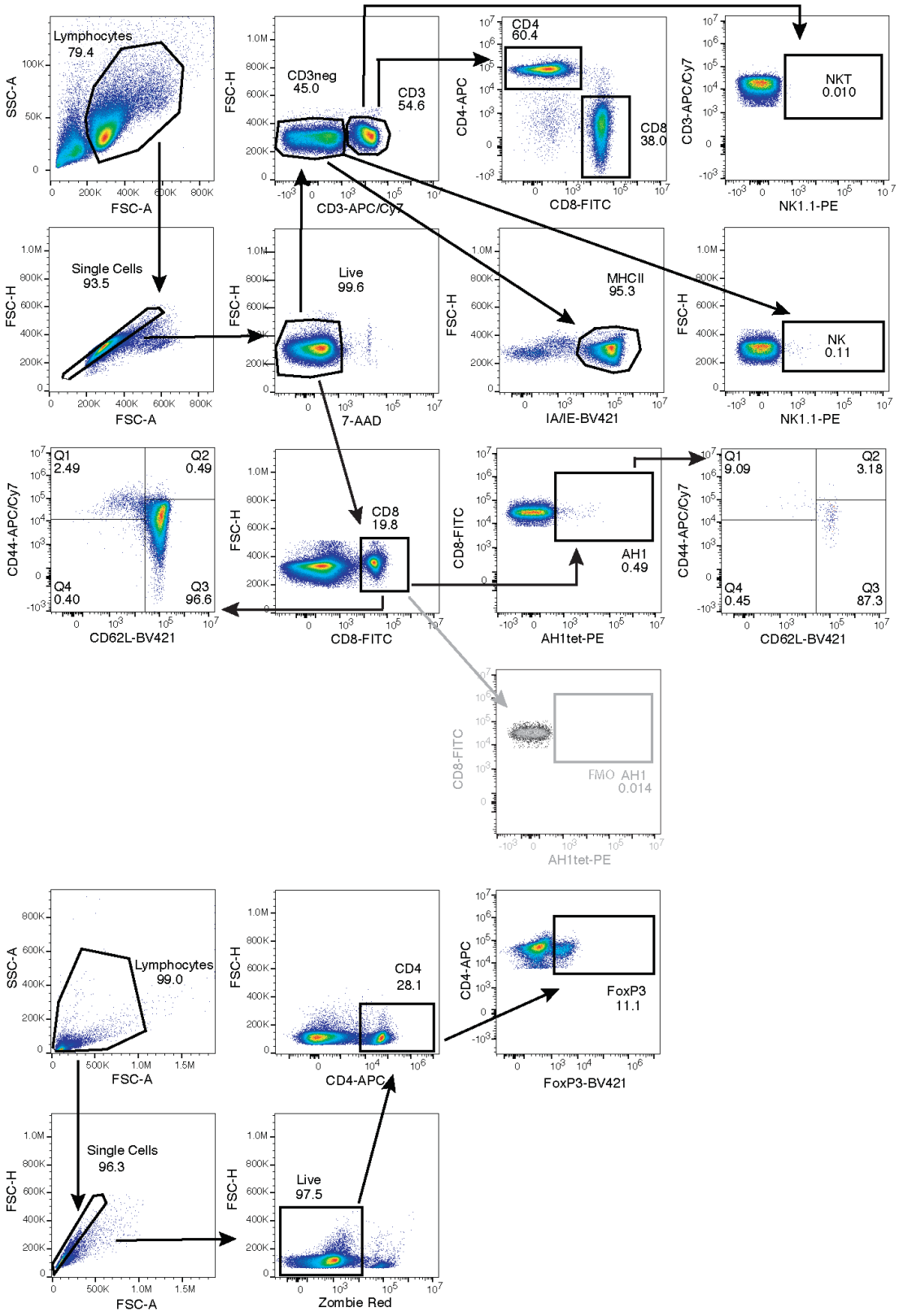

Supplementary Figure 7: ***Gating strategy for analysis of TDLN****. Detailed gating strategy used to analyse TDLN composition, including fluorescence-minus one control (FMO) to set the gate for AH1-specific cells.*

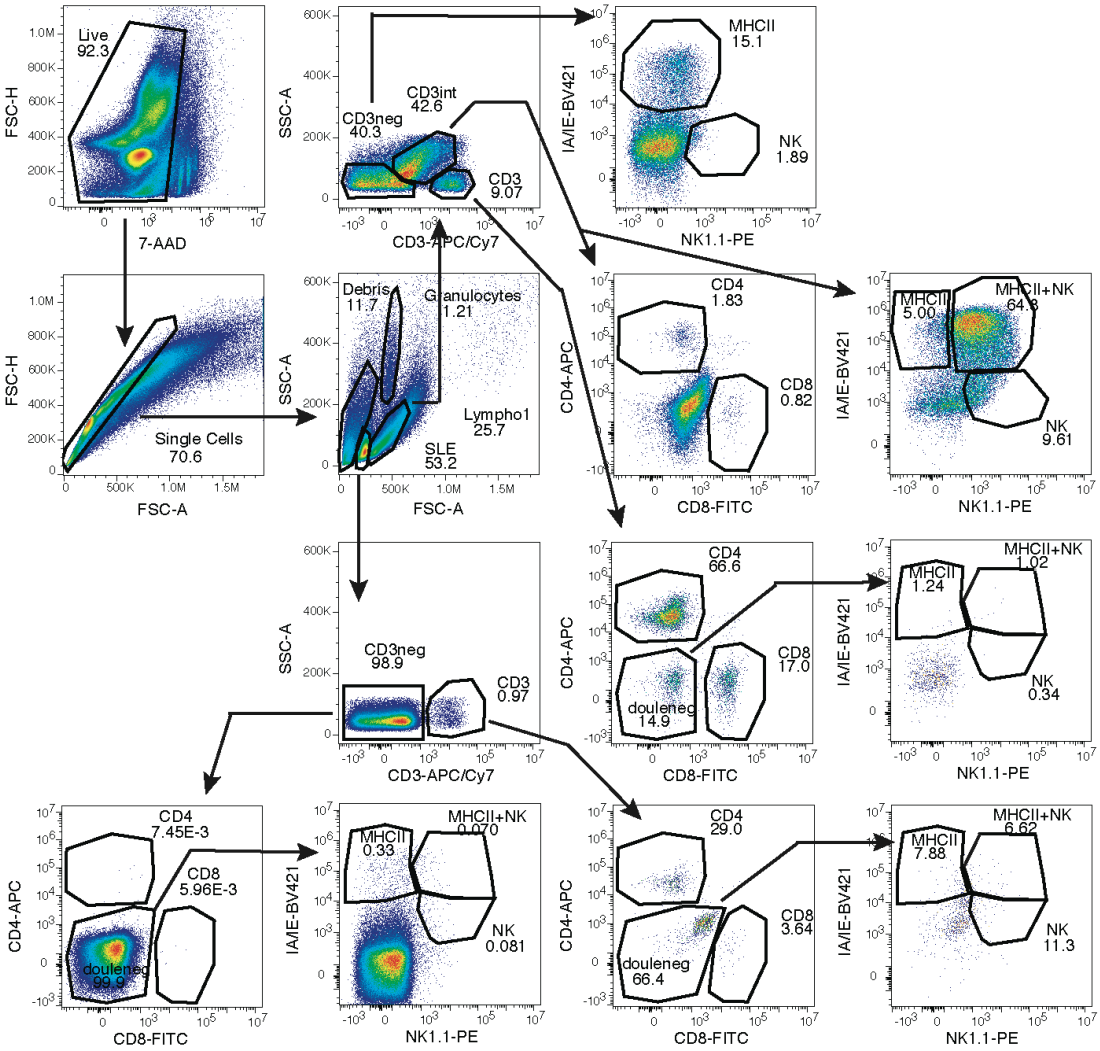

Supplementary Figure 8: ***Gating strategy for analysis of tumor****. Detailed gating strategy used to analyse tumor composition.*

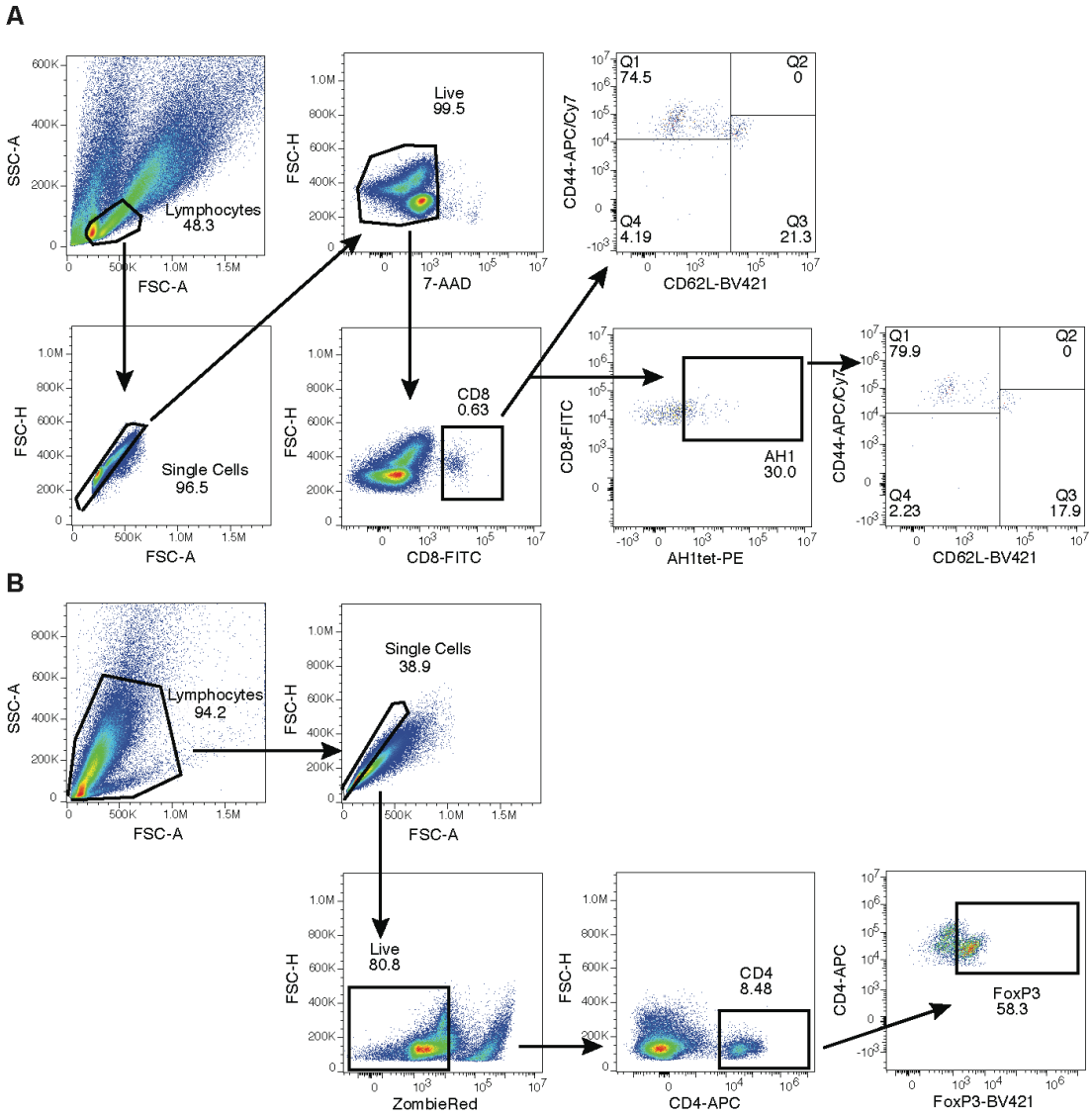

Supplementary Figure 9: ***Gating strategy for tumor infiltrating CD8+ and CD4+ T cells****. Detailed gating strategy used to analyse AH1-specificity and phenotype of tumor-infiltrating CD8+ T cells* ***(A)*** *and CD4+ regulatory T cells (T_{reg})* ***(B)****. Gates for AH1, phenotype and FoxP3 were set using TDLN samples.*

10 Appendix 3: Cancer therapy in mice using a pure population of CD8+ T cell specific to the AH1 tumor rejection antigen

10.1 Materials and methods

10.1.1 Animals and tumor cells lines

All the in vivo experiments were conducted under the project license 04/2018, granted by the Veterinäramt des Kantons Zürich (Zurich, Switzerland). Seven to eight weeks-old female BALB/c mice were purchased from Janvier (France). CT26 colon carcinoma (ATCC CRL-2638), WEHI-164 fibrosarcoma (ATCC CRL-1751) and RENCA renal adenocarcinoma (CRL-2947) were obtained from ATCC, C51 colon carcinoma and F1F fibrosarcoma were kindly provided by M.P. Colombo (Istituto Nazionale Tumori Milan, Italy). 4T1-luc2 mammary carcinoma (Perkin Elmer, former Caliper Life Sciences) were kindly provided by M. Detmar (ETH Zurich, Zurich, Switzerland). Tumor cells were handled and expanded according to supplier's protocol. Aliquots of cells in complete growing medium containing 10% DMSO were cryopreserved and stored in liquid nitrogen. Authentication including check of post-freeze viability, growth properties and morphology, test for mycoplasma contamination, isoenzyme assay and sterility test was performed by the cell bank before shipment. Tumor cells were kept in culture for no longer than two weeks.

10.1.2 Immunocytokine production

The recombinant fusion proteins L19-IL12 and F8-IL2, were expressed in stably-transfected CHO-S cells, as already described[171, 175]. Fusion proteins were purified by Protein A chromatography and stored in Phosphate buffer saline pH 7.4 (PBS) at -80°C. Characterization of the product included SDS-PAGE under reducing and non-reducing conditions, size exclusion chromatography (S200 10/300 increase column, GE Healthcare) and LC-MS after treatment with PNGase F (NEB), following supplier's protocol.

10.1.3 Reversible multimers production

Reversible, AH1-peptide-loaded H-2L^d multimers were obtained as described elsewhere[264], with minor adaptations. Briefly, C-terminal Histidine-tagged murine H-2L^d and human b2-microglobulin were expressed in *E.coli* and assembled into MHC class I monomers in the presence of AH1 peptide following established protocols. AH1 peptide was obtained from

Biomatik. Synthesis of the biotinylated, NTA-containing scaffold (here referred as MVP compound) is described in Supplementary Data. MVP compound was incubated in PBS containing $NiSO_4$ (final concentration 10mM) for 1h at 4°C. 0.25 molar equivalent of PE-conjugated Streptavidin (BioLegend) were added. After 1h incubation at 4°C, followed by 1h at RT, AH1-loaded, Histidine-tagged H-$2L^d$ monomers, purified by size exclusion chromatography, were added (1:1 molar equivalent with respect to MVP compound) and newly formed multimers were stored at 4°C (for at least 48h, before use).

10.1.4 Antibodies and reagents for flow cytometry

Fluorophore-conjugated antibodies against murine CD8a (53-6.7), CD62L (MEL-14), CD44 (IM7), PD-1 (29F.1A12), CTLA-4 (UC10-4B9), Tim-3 (RMT3-23), Lag-3 (C9B7W), CD25 (PC61), CD11c (N418), CD11b (M1/70), XCR1 [16], CD80 (16-10A1), IL12 (C15.6), CD137L (TKS-1), CD215 (6B4C88), CCR7 (4B12), CXCR3 (CXCR3-173), as well as fluorophore-conjugated Streptavidin, TruStain FcX mouse anti-CD16/32 antibody (93) and reagents for life/dead discrimination 7-AAD and ZombieRed were all purchased from BioLegend. Anti-TNFα (TN3-19.12) and anti-IFNγ (XMG1.2) were purchased from eBiosciences. Anti-IL2 (JES6-5H4) and anti-CD212 (114) were purchased from BD Biosciences. Anti-iNOS2 (sc-7271) was purchased from Santa Cruz Biotechnology. PE-conjugated, peptide-loaded MHC class I tetramers were produced in-house as already described[174].

10.1.5 Therapy experiments

Eight- to Nine-weeks-old female BALB/c mice were subcutaneously injected with $3x10^6$ CT26 (or $2.5\ x10^6$ WEHI 164) tumor cells in the right flank. Animals were inspected daily; body weight was monitored and tumor size was determined using the following formula: tumor volume [mm^3] = 0.5 x (major diameter) x (minor diameter)^2. All therapy experiments were initiated when tumors reached a volume of about $100mm^3$. Pre-therapy to boost tumor-specific T cells consisted in a total of three intravenous injections of 15μg L19-IL12 at 48h intervals. Mice were sacrificed 48-72h after the last injection to isolate T cells. Prior to ACT experiments, mice were randomized. ACT was performed with *in vitro* expanded T cells, repeatedly washed and resuspended in PBS before administration, without any preconditioning of the animals. In combination experiments only, mice received F8-IL2, as described in corresponding figures.

10.1.6 T cells isolation

Tumors, spleens and tumor-draining lymph nodes (right inguinal, right axillary) of L19-IL12-treated mice were harvested. Single cells suspensions of each tissue were obtained as already described (https://doi.org/10.1101/2020.05.08.084277). In some cases, splenocytes and lymphocytes from TDLNs were pooled and processed together. Splenocytes were treated with MojoSort Mouse CD8 Isolation kit (BioLegend), following supplier's protocol and enriched CD8+ T cells were incubated for 15' at 4°C with 1.4μM Avidin to quench residual free Biotin in the sample, which could bind to Streptavidin in reversible multimers. Cells suspensions were stained with fluorophore-conjugated anti-CD8a and PE-conjugated reversible multimers for 30' at 4°C; 7-AAD was used following supplier's protocol to exclude dead cells. Multimer-positive CD8+ T cells were sorted on a FACS Aria II. Cells were collected in tubes or wells containing Complete Medium (CM: RPMI-1640 supplemented with 10% FBS, 1xAntiAnti, 50μM BME, 25mM HEPES, 4mM Ultraglutamine) supplemented with 100mM Imidazole.

10.1.7 Preparation of Dendritic Cells

Dendritic cells were derived from bone marrow cells with established protocols. Briefly, bone marrow was harvested from femurs and tibiae of BALB/c mice, treated with red-blood cells lysis buffer (BioLegend) and plated in R10 medium (RPMI-1640 supplemented with 10% heat-inactivated FBS, 1xAntiAnti, 12.5mM HEPES, 4mM Ultraglutamine) supplemented with either 20ng/mL murine GM-CSF (BioLegend) or 200ng/mL murine Flt3L (eBiosciences). Cells grown in GM-CSF were plated in 100mm non-adherent petri dishes at a density of $2.5x10^5$ cells/mL in 10mL, whereas cells grown in Flt3L in wells of 6-well-plates at a density of 1.5-$2x10^6$ cells/mL. After 3 days 5mL R10 supplemented with 20ng/mL murine GM-CSF were added to cultures grown in GM-CSF. Cells grown in GM-CSF were activated overnight at day 6, with 1μg/mL LPS (Sigma), whereas Cells grown in Flt3L were activated overnight at day 9, with 1μg/mL poly I:C (GE Healthcare). Non-adherent cells were harvested, resuspended in R10 containing 10% DMSO and cryopreserved in liquid nitrogen.

10.1.8 T cells culture with IL2 and Dynabeads

Multimer positive CD8+ T cells from tumors and TDLNs, respectively multimer negative CD8+ T cells from TDLN of BALB/c bearing CT26 tumors were isolated as described above. After washing, cells were resuspended in CM containing 60 IU/mL Proleukin (Novartis) and Dynabeads Mouse T-Activator CD3/CD28 (Thermofisher, 1:1 Dynabeads-to-T cells) and

incubated at 37°C, 5% CO_2. Plate was incubated tilt for the first 6 hours. Half of the medium with fresh Proleukin was replaced every three days. Cells were resuspended and distributed in additional wells when confluent. Pictures were taken on a Zeiss AxioVert 200M equipped with a AxioCam MRm, using AxioVision software (version 4.8.2) at day 1, 3 and 7. Flow cytometry analysis was performed at day 7.

10.1.9 Expansion of T cells

Sorted T cells were washed once with CM supplemented with 100mM Imidazole and once with CM, before being plated in pre-warmed CM supplemented with 100ng/mL IL15. Cells were plated in wells of either 96- or 48-well-plates and plates were incubated at 37°C, 5% CO_2 for 5 days (tilt for the first 12 hours). T cells were activated at day 5 by adding peptide-pulsed DCs (1:5 to 1:1 DCs-to-T cells) suspended in CM supplemented with IL15. DCs were thawed the night before activation, let rest in R10 for 12-14 hours and activated with 1µg/mL LPS or poly I:C for 6 hours. During the last hour, DCs were pulsed with 1-5µM AH1 peptide. Before adding them to T cells, DCs were washed in CM. One-half of the medium was replaced every 3-4 days. T cells were re-activated at day 15 and 10ng/mL IL7 were added to culture medium from day 15 onwards. One-half of the medium was replaced every 3-4 days and cells were split in additional wells whenever confluent. T cells were harvested and used for analysis and therapy between day 21-24. In some experiments, T cells were expanded in the presence of either 0.5µM Doramapimod (Cayman Chemical), 7µM TWS119 (Sigma) or 2.5µg/mL mDLL1-Fc (R&D Systems).

10.1.10 Flow cytometry analysis

For flow cytometry analysis, T cells were stained for 30' at 4°C in FACS buffer with fluorophore-conjugated antibodies against CD8a, CD62L, CD44, PD-1, Tim-3, Lag-3, CTLA-4, CD212, CD25, CCR7, CXCR3 and with PE-conjugated, peptide-loaded tetramers. Dead cells were excluded from analysis by 5' staining in 7-AAD at 4°C.

Bone marrow-derived, AH1 peptide-pulsed dendritic cells cultured and matured in different conditions were stained using the same protocol, with antibodies against CD11c, CD11b, XCR1, PD-L1, CD137L, CD80 and CD215, after Fc-Receptor blocking with TruStain FcX mouse anti-CD16/32 (following supplier's protocol). For intracellular staining of DCs, cells were first stained with ZombieRed (1:500 in PBS), for 15' at RT. After surface staining, cells were treated with the Foxp3 / Transcription Factor Staining Buffer Set (eBiosciences), as

described by the supplier and stained with antibodies against IL2, IL12 and NOS2. In some cases, dendritic cells were pulsed with a FITC-lated version of the AH1-peptide (produced in-house as described in Supplementary data). Cells were analyzed on a CytoFlex S (Beckman Coulter) and data processed with FlowJo software (version 10).

10.1.11 Cytokine release assay

T cells were incubated either alone, with Dynabeads Mouse T-Activator CD3/CD28 (Thermofisher) or with tumor cells (CT26 and F1F) at a 1:1 ratio in CM. After 1h incubation at 37°C, Brefeldin A (Biolegend) was added to the samples (final concentration 5µg/mL). After 4-5h in incubator, cells were harvested for staining and flow cytometry analysis. Beads were removed with a magnet before staining. Cells were stained in ZombieRed, followed by staining with anti-CD8a. Cells were fixed and permeabilized using the Foxp3 / Transcription Factor Staining Buffer Set (eBiosciences), following supplier's protocol, and subsequently stained with fluorophore-conjugated antibodies against TNFα, and IFNγ, for 30' at 4°C. Fluorescence Minus One (FMO) controls were used to define negative populations.

10.1.12 Cell cytotoxicity assay

T cells and target tumor cells at different effector-to-target ratios in CM were incubated in a static incubator at 37°C for 24h. Cells were spun down, medium was removed completely and cells were washed once with PBS. Adherent tumor cells were detached using 0.05% Trypsin/EDTA solution (Thermofisher), CM was added to neutralize trypsin. Cells were pelleted, washed in FACS buffer and stained with fluorophore-conjugated anti-CD8a and 7-AAD. Cells were analyzed on a CytoFlex S (Beckman Coulter) and data processed with FlowJo software (version 10). Living, CD8+ T cells were plotted together with living CD8- tumor cells.

10.1.13 *In vivo* biodistribution

In vitro expanded T cells were harvested and stained using the CFSE Cell Division tracker kit from BioLegend, following supplier's protocol. Number of living T cells was determined by Trypan Blue exclusion using a hemocytometer and $3x10^6$ CFSE-labeled T cells were intravenously injected in BALB/c bearing established subcutaneous CT26 tumors. An aliquot of labeled T cells was stained with ZombieRed and anti-CD8a and analyzed by flow cytometry to determine viability and intensity of CFSE signal at baseline. After 72h, mice were euthanized and tumors, TDLNs and spleens were harvested and processed to single cells suspensions.

Samples were stained with ZombieRed and fluorophore-conjugated antibodies against CD8a and analyzed by flow cytometry.

10.1.14 Statistical analysis

Data were analyzed using Prism 7.0 (GraphPad Software, Inc.). Statistical significance in tumor therapies was determined with a regular two-way ANOVA test with Bonferroni post-test correction. All the other statistical analyses were performed using a two-tailed, unpaired student t-test. $P < 0.05$ was considered statistically significant.

10.2 Supplementary information

10.2.1 Synthesis of MVP-compound and FITC-lated AH1-peptide

General Remarks

High-Resolution Mass Spectrometry (HRMS) spectra and analytical Reversed-Phase Ultra Performance Liquid Chromatography (UPLC) were recorded on a Waters Xevo G2-XS QTOF coupled to a Waters Acquity UPLC H-Class System with PDA UV detector, using an ACQUITY UPLC BEH C18 Column, 130 Å, 1.7 µm, 2.1 mm × 50 mm at a flow rate of 0.6 ml/min with linear gradients of solvents A and B (A = Millipore water with 0.1% FA, B = MeCN with 0.1% FA). Preparative reversed-phase high-pressure liquid chromatography (RP-HPLC) were performed on a Waters Alliance HT RP-HPLC with PDA UV detector, using a Synergi 4µm, Polar-RP 80Å 10 × 150 mm C18 column at a flow rate of 4 ml/min with linear gradients of solvents A and B (A = Millipore water with 0.1% TFA, B = MeCN with 0.1% TFA).

All compounds and chemical reagents were obtained from Sigma-Aldrich and TCI Europe and used without further purification. The AH1- and the biotinylated-peptide scaffold were purchased from Biomatik.

10.2.2 Synthesis of MVP-compound

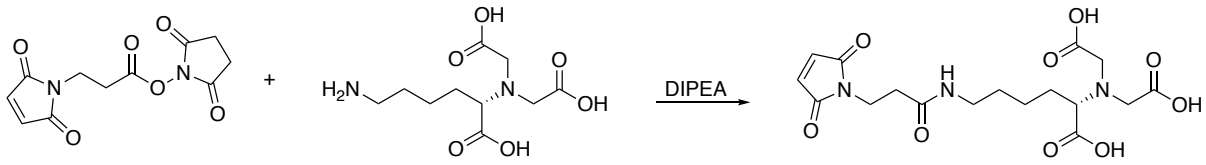

Supplementary Figure 10: Functionalization of NTA-Lysine with 3-(Maleimido)propionic acid N-hydroxysuccinimide ester.

NTA-Lysine (60 mg, 0.229mmol, 1eq) was dissolved in 1 mL of dry-DMSO in presence of DIPEA (d=0.742, 160uL, 4eq). In another vial, 3-(Maleimido)propionic acid N-hydroxysuccinimide ester (54 mg, 0.9 eq) was dissolved in dry-DMSO. The solution was added to the vial and let react at 35°C, until no starting-material was detected on UPLC-MS (ca. 1 hour). The mixture was purified directly on reverse-phase HPLC (Synergi RP Polar, 5% MeCN in 0.1% aq. TFA to 70% over 14 min), to obtain 25 mg of a white pure compound (30% yield). HRMS (ES) calculated for $[M+H]^+$ (m/z): 414.1507, found 414.1581.

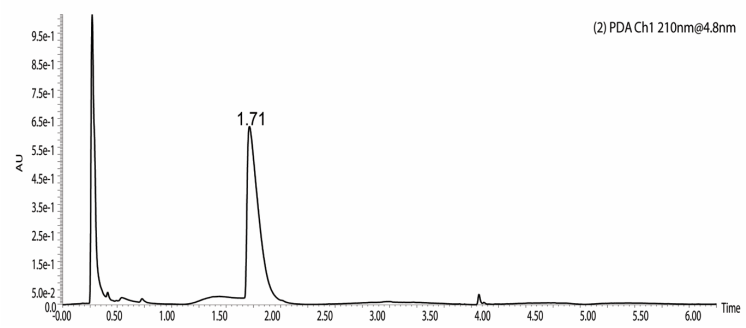

Supplementary Figure 11: UPLC-profile of the purified product.

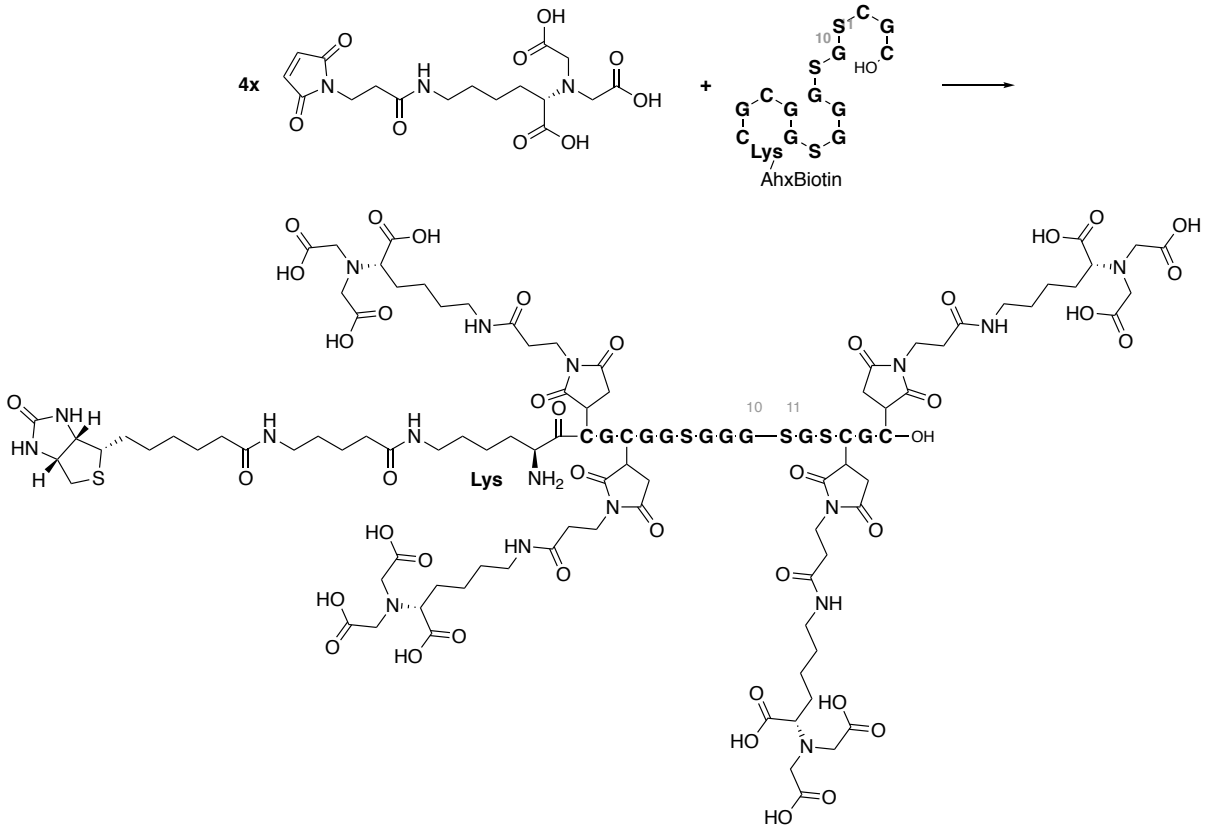

Supplementary Figure 12: Synthesis of MVP compound.

Biotinylated peptide scaffold (10 mg, 1 eq) with the following sequence:
(Biotin-NεLys)-CGCGGSGGGSGSCHC-COOH
was dissolved in DMSO at 0.1M concentration in presence of MVP_1 compound (8 eq, 0.1 M in DMSO). The reaction was kept at 37°C for 5 hours until no starting material was detected by UPLC-MS analysis. The mixture was purified on reverse-phase HPLC (Synergi RP Polar, 5% MeCN in 0.1% aq. TFA to 50% over 14 min), to obtain 5 mg of a white compound (25% yield).
HRMS (ES) calculated for $[M+H]^{2+}$ (m/z): 1635.0817, found 1635.5149.

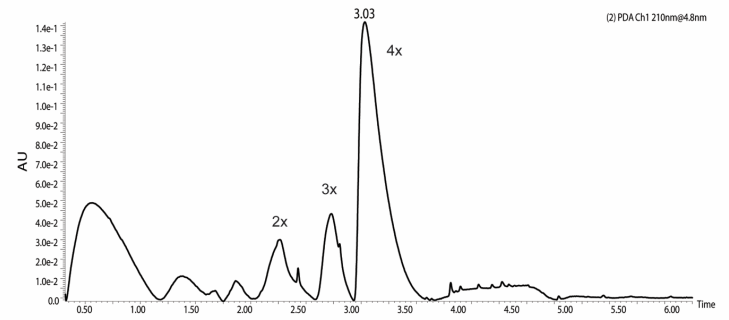

Supplementary Figure 13: UPLC-profile of the purified MVP-compound (low UV-absorption).

10.2.3 Synthesis AH1-FITC

AH1 peptide (10 mg, 1 eq) was dissolved in 100 µL of dry-DMSO in presence of DIPEA (1 eq). Fluorescein isothiocyanate (1 eq, FITC) was added portion-wise at room temperature from a 0.1 M solution in dry-DMSO until neither starting material nor free-FITC were detected by UPLC-MS analysis. The mixture was purified on reverse-phase HPLC (Synergi RP Polar, 5% MeCN in 0.1% aq. TFA to 80% over 14 min), to obtain 6 mg of a yellow powder (45% yield). HRMS (ES) calculated for $[M+H]^{2+}$ (m/z): 1517.5582, found 1517.4576

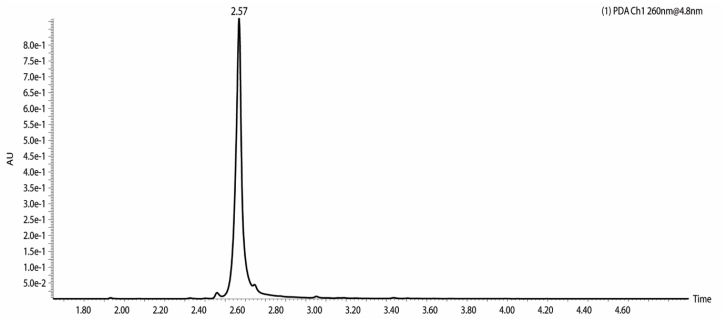

Supplementary Figure 14: UPLC-profile of the purified FITC-lated AH1-peptide.

10.2.4 Supplementary Results

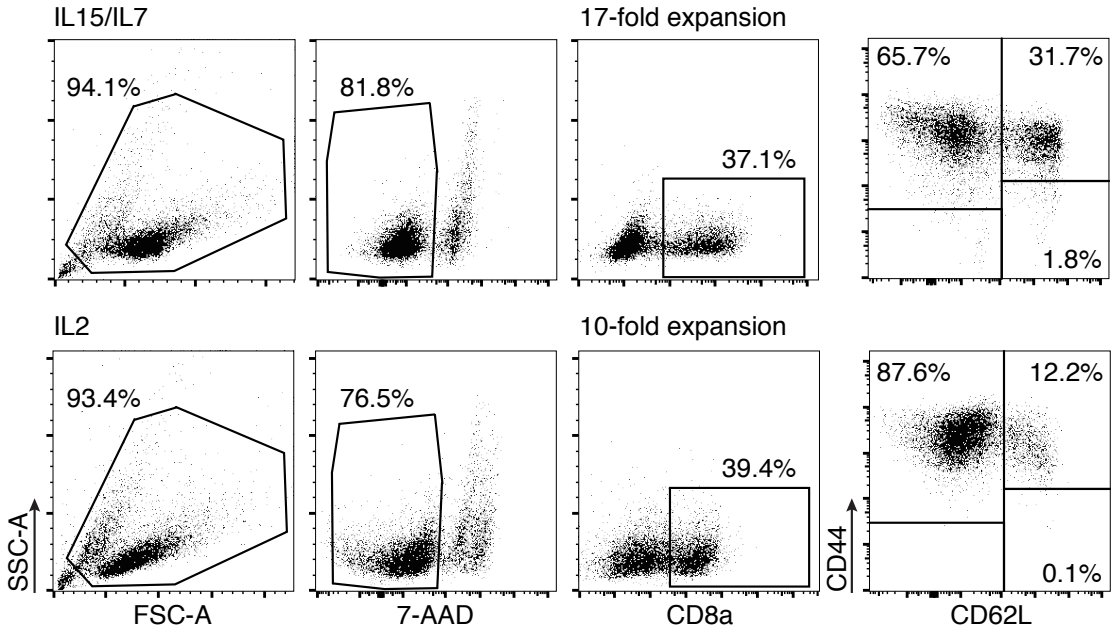

Supplementary Figure 15: ***Culture of CD90.2+ splenocytes in IL2 vs IL15/IL7****. Flow cytometry analysis of CD90.2+ splenocytes, purified using MojoSort Mouse CD90.2 Selection Kit (Biolegend) and cultured in CM containing Dynabeads Mouse T-activator CD3/CD28 (Thermofisher, 1:1 Dynabeads to T cells) and either 60 IU/mL human IL2 (Proleukin, Novartis), or 10ng/mL of both recombinant murine IL15 and IL7 (Biolegend) for 14 days. Half of the medium containing corresponding cytokines was replaced every 3-4 days. For culture in IL2 only, new Dynabeads were added every 5-6 days.*

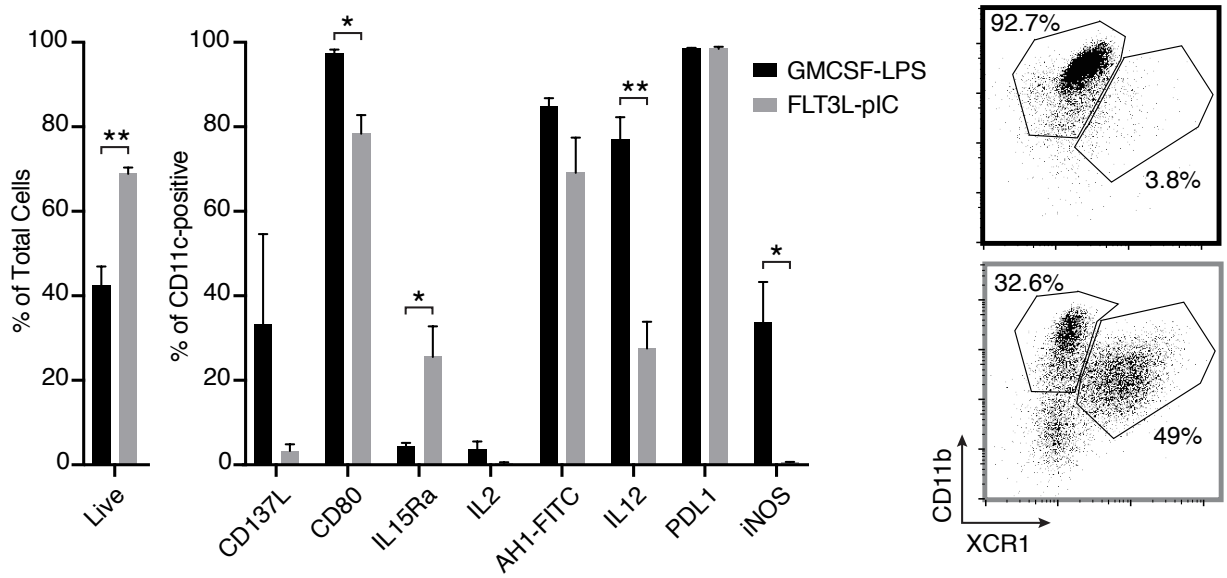

Supplementary Figure 16: ***Characterization of Bone marrow-derived Dendritic Cells (BMDCs)****. BMDCs cultured either in GM-CSF or Flt3L and matured with LPS resp. poly I:C, were pulsed with AH1 peptide (or a FITC-lated version of the AH1-peptide) and expression of various markers was characterized by flow cytometry. Columns represent means ± SEM, n = 3 biological replicates for each experimental condition, * = $p < 0.05$, ** = $p < 0.01$, *** $p = < 0.001$, **** = $p < 0.0001$ (unpaired t-test).*

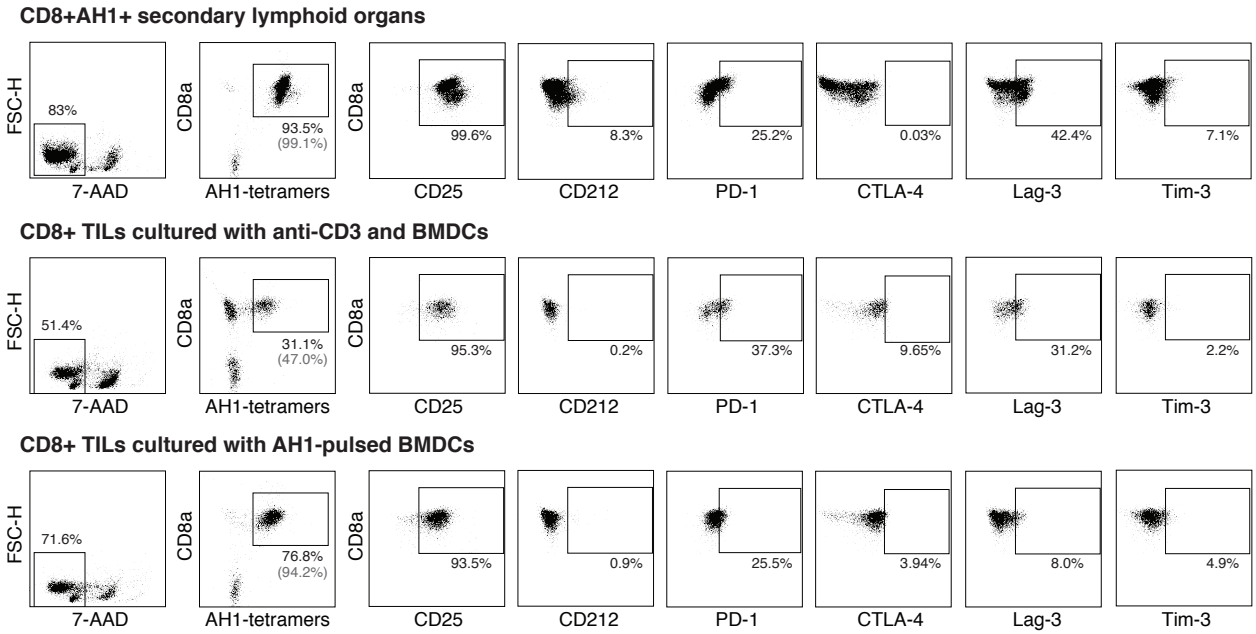

Supplementary Figure 17: ***Characterization of AH1-specific T cells from secondary lymphoid organs, resp. CD8+ TILs****. FACS-purified, AH1-multimers specific CD8+ T cells from secondary lymphoid organs, or bulk CD8+ TILs were expanded using our optimized protocol, or a slightly modified protocol employing non-pulsed BMDCs and anti-CD3 antibody (145-2C11, Biolegend). Sample were analysed by flow cytometry after 3 weeks of in vitro culture. Percentages of living cells, of AH1-tetrmers positive CD8+ T cells over living cells (black) and over living CD8+ T cells (grey, in brackets), as well as percentages of CD8+ T cells, which stained positive for selected activation or exhaustion markers, are shown.*

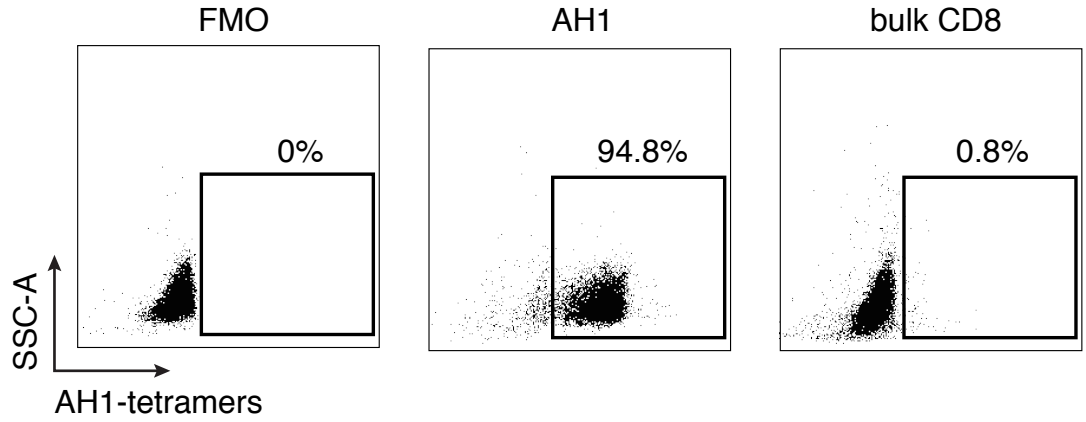

Supplementary Figure 18: ***AH1-tetramers specific CD8+ T cells in "bulk CD8"****. AH1-multimers negative CD8+ T cells from secondary lymphoid organs (bulk CD8) were purified by FACS and cultured with the modified protocol employing non-pulsed BMDCs and anti-CD3 antibody instead of AH1-pulsed BMDCs. After 3 weeks of in vitro culture, T cells were analysed for reactivity against AH1-tetramers. AH1+CD8+ T cells isolated the same way, but expanded with the normal protocol (AH1), were used as positive control.*

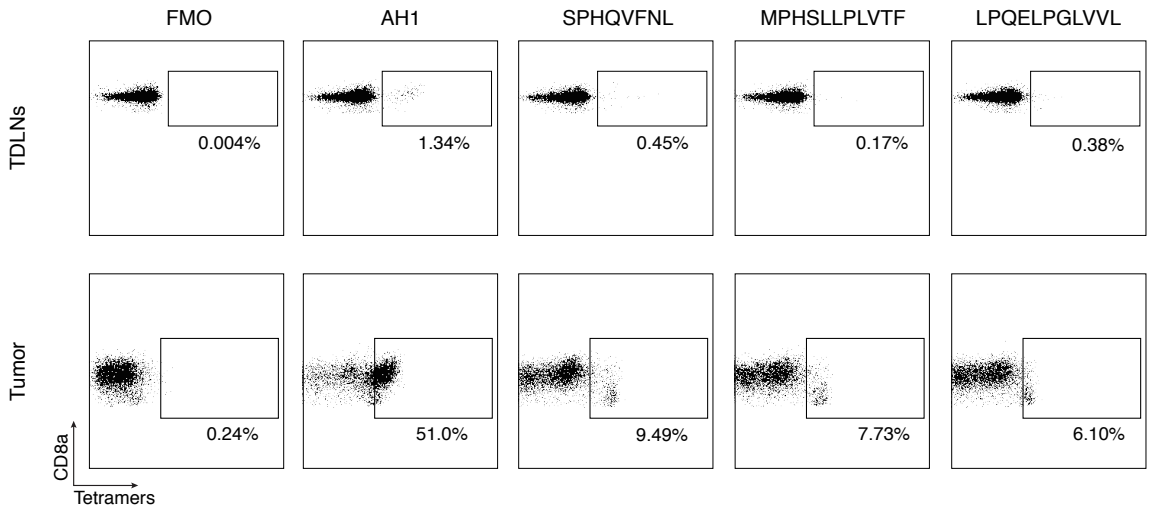

Supplementary Figure 19: ***T cells specific for additional CT26-derived antigenic peptides****. Flow cytometry analysis of CD8+ T cells from tumor and tumor-draining lymph nodes (TDLNs). Cells were stained with H-2L^d-tetramers loaded with the AH1 peptide (AH1) or with other three CT26-derived peptides (amino acids sequence provided) identified in a previous study[184].*

11 Acronyms

ACT	Adoptive Cell Therapy
ADCC	Antibody Dependent Cellular Cytotoxicity
APC	Antigen Presenting Cell
BCG	Bacillus Calmette-Guerin
Bcl2	B-cell lymphoma 2
BiTE	Bispecific T cell Engager
BTLA	B- and T-Lymphocyte Attenuator
CAIX	Carbonic Anhydrase IX
CAR-T	Chimeric Antigen Receptor T cell
CD44v6	CD44 version 6
CEA	Carcino-Embryogenic Antigen
CRS	Cytokine-Release Syndrome
CTA	Cancer Testis Antigen
CTLA-4	Cytotoxic T-Lymphocyte-Associated protein 4
DC	Dendritic Cell
DcR3	Decoy Receptor 3
EDA	Extra Domain A (of Fibronectin)
EDB	Extra Domain B (of Fibronectin)
EGFR	Epidermal Growth-Factor Receptor
EpCAM	Epithelial Cell Adhesion Molecule
GALV	Gibbon Ape Leukemia Virus
GD2	Disialoganglioside 2
GITR	Glucocorticoid-Induced Tumor-necrosis-factor Receptor
GM-CSF	Granulocyte-Macrophage Colony-Stimulating Factor
HER2	Human Epidermal Growth Factor Receptor 2
HLA	Human Leukocyte Antigen
HSV-1	Herpes-Simplex Virus 1
HVEM	Herpes Virus Entry Mediator
ICOS	Inducible T cell Co-Stimulator
IDO	Indoleamine 2,3-dioxygenase
IL2	Interleukin 2
IL10	Interleukin 10

IL12	Interleukin 12
IL15	Interleukin 15
IL21	Interleukin 21
IL23	Interleukin 23
IFN	Interferon
LAG-3	Lymphocyte-Activation Gene 3
LAK	Lymphokine Activated Killer Cell
LTβR	Lymphotoxin beta Receptor
MadCAM-1	Mucosal Addressin Cell Adhesion Molecule 1
MAGE	Melanoma-associated Antigen
MART-1	Melanoma Antigen Recognized by T cell 1
MDSC	Myeloid-Derived Suppressor Cell
MHC	Major Histocompatibility Complex
MIC-A/B	MHC class I chain-related protein A/B
MuLV	Murine Leukemia Virus
NK	Natural Killer cell
NKG2D	Natural Killer Group 2D
NKT	Natural Killer T cell
NY-ESO-1	New York Esophageal Squamous cell carcinoma 1
PAMPs	Pathogen-Associated Molecular Patterns
PBMCs	Peripheral Blood Mononuclear Cells
PD-1	Programmed cell death protein 1
PD-L1	Programmed death-ligand 1
PD-L2	Programmed death-ligand 2
PRR	Pattern Recognition Receptor
REP	Rapid Expansion Protocol
ScFv	Single-chain variable domain
STAT3	Signal Transducer and Activator of Transcription 3
TAA	Tumor-Associated Antigen
TCR	T cell Receptor
TILs	Tumor-Infiltrating Lymphocytes
TIM-3	T-cell immunoglobulin and mucin-domain containing-3
TLR	Toll-like Receptor
TLS	Tertiary Lymphoid Structure

TGFβ	Tumor Growth Factor beta
TNF	Tumor Necrosis Factor
TNFR	Tumor Necrosis Factor Receptor
Tcm	Central memory T cell
Tem	Effector memory T cell
Tn	Naïve T cell
Treg	Regulatory T cell
Trm	Tissue-resident memory T cell
Tscm	Stem cell-like memory T cell
Tte	Terminally-differentiated effector T cell
VEGF-A	Vascular Endothelial Growth Factor A

12 Acknowledgments

The journey to my Ph.D. has finally come to an end. I just finished writing over 35000 words, and yet the few that I still have to write are the most meaningful. I will try to find the right ones.

I would like to start expressing my sincere gratitude to my supervisor Prof. Dr. Dario Neri, for his continuous support, his precious pieces of advice, and his exceptional patience. It has been a privilege to work under his expert guidance. The respect and admiration I have always felt for him, have been motivating me to give my best and not give up in the face of the (many) challenges I have come across during my Ph.D. I will always be grateful for all the numerous lessons he taught me.

I would like to thank also Prof. Dr. Cornelia Halin, who agreed to co-supervise my Ph.D. exam and allowed me to spend my last few months at ETH under her supervision.

A scientific laboratory is a very dynamic environment. People come and go: with some, you share more time, with others less. I feel lucky to say, I have not only met wonderful and brilliant colleagues, but also good friends. I thank all the many Ph.D. students, the few postdocs, and the master students, who have contributed to creating a nice and productive work environment during my stay. Among all, I want to give an extra-special thanks to Dr. Patrizia Murer, Dr. Davor Bajic, Marco Catalano, and Jacqueline Mock: it has been a real pleasure to be surrounded by such caring people.

A special thank also to Dr. Philipp Probst for involving me in his project and for the nice and fruitful collaborations which followed.

I am very grateful to all the people I could collaborate with, not only from the Neri group, but also from Philochem and the Oxenius lab. Thanks to Dr. Philipp Probst, Dr. Emanuele Puca, Dr. Barbara Ziffels, Dr. Patrizia Murer, Jacqueline Mock, Marco Catalano, Riccardo Corbellari, Tiziano Ongaro, Ilaria Spadafora, and to my former master student Vanessa Fontana. Discussing science and performing experiments with them has always been much more enjoyable. Thanks also to Alessandro Pedrioli (Zivi), Dr. Luca Ducoli, Jihye Kim, Dr. Lothar Dieterich, and Dr. Carlotta Tacconi: we have not actively collaborated, but they were always ready to help.

Furthermore, I would like to thank Pia Steinbak and Dr. Jörg Scheuermann for all the support and help with administrative issues.

Life in the lab is a big part of a Ph.D., but at the end of the day one still needs to disconnect and recharge. I have been blessed with many good friends, who took care of that, and I am grateful to them for all the chats, beers, and hangouts. In particular, I need to thank my friend and long-time flatmate Jan Stutz (Jean). I will certainly miss living with him, his kindness, but also our running jokes. A big thank you also to the friends of "A.C. Tua": we were not the best on the field, but we were definitely the better-dressed!

I will always be grateful to my dear Sheila. I casually met her in the least-expected place and time and I was lucky enough to get to know her. She has been a colleague, a friend, a confidant. She has supported me, motivated me, cared about me. She has been an example in many ways, she has been my strength, and also my weakness. I thank her for all the good moments and I will keep her forever in my heart.

Finally, I am immensely grateful to my family. To my father and my mother, for inspiring me to try and become a better person, following their example. To my sisters Lia, Ada, and Isa, and my little brother Luca, because I know I can always count on them in times of need. To my grandparents, for the interest and admiration they have always shown for what I do, and for always remembering me in their prayers. This journey would not have been possible without them.

13 Bibliography

1. Hanahan, D. & Weinberg, R.A. Hallmarks of cancer: the next generation. *Cell* **144**, 646-674 (2011).
2. WHO Global Cancer Observatory (https://gco.iarc.fr/). (2020).
3. Brierley, J., Gospodarowicz, M. & O'Sullivan, B. The principles of cancer staging. *Ecancermedicalscience* **10**, ed61 (2016).
4. Delaney, G., Jacob, S., Featherstone, C. & Barton, M. The role of radiotherapy in cancer treatment: estimating optimal utilization from a review of evidence-based clinical guidelines. *Cancer* **104**, 1129-1137 (2005).
5. Pratt, W.B.E., W.D.; Ruddon, R.W. The Anticancer Drugs. (Oxford University Press, 1994).
6. P., E. Ueber den jetzigen Stand der Karzinomforschung. *Ned Tijdschr Geneeskd*, 273-290 (1909).
7. Lewis, M.R. & Aptekman, P.M. Atrophy of tumors caused by strangulation and accompanied by development of tumor immunity in rats. *Cancer* **5**, 411-413 (1952).
8. Gross, L. Intradermal immunization of C3H mice against a sarcoma that originated in an animal of the same line. *Cancer research* **3**, 326-333 (1943).
9. Foley, E.J. Antigenic properties of methylcholanthrene-induced tumors in mice of the strain of origin. *Cancer research* **13**, 835-837 (1953).
10. Thomas, L. & Lawrence, H. Cellular and humoral aspects of the hypersensitive states. *New York: Hoeber-Harper*, 529-532 (1959).
11. Burnet, F.M. The concept of immunological surveillance. *Prog Exp Tumor Res* **13**, 1-27 (1970).
12. Dunn, G.P., Bruce, A.T., Ikeda, H., Old, L.J. & Schreiber, R.D. Cancer immunoediting: from immunosurveillance to tumor escape. *Nature immunology* **3**, 991-998 (2002).
13. Dunn, G.P., Old, L.J. & Schreiber, R.D. The immunobiology of cancer immunosurveillance and immunoediting. *Immunity* **21**, 137-148 (2004).
14. Mittal, D., Gubin, M.M., Schreiber, R.D. & Smyth, M.J. New insights into cancer immunoediting and its three component phases--elimination, equilibrium and escape. *Current opinion in immunology* **27**, 16-25 (2014).
15. Teng, M.W. et al. Opposing roles for IL-23 and IL-12 in maintaining occult cancer in an equilibrium state. *Cancer research* **72**, 3987-3996 (2012).
16. Cossarizza, A. et al. Guidelines for the use of flow cytometry and cell sorting in immunological studies (second edition). *European journal of immunology* **49**, 1457-1973 (2019).
17. Schreiber, R.D., Old, L.J. & Smyth, M.J. Cancer immunoediting: integrating immunity's roles in cancer suppression and promotion. *Science (New York, N.Y.)* **331**, 1565-1570 (2011).
18. Busch, W. Aus der Sitzung der medicinischen Section vom 13 November 1867. *Berl Klin Wochenschr* **5**, 137 (1868).
19. Fehleisen, F. Ueber die Züchtung der Erysipelkokken auf künstlichem Nährboden und ihre Übertragbarkeit auf den Menschen. *Dtsch Med Wochenschr* **8**, 553-554 (1882).
20. Coley, W.B. The Treatment of Inoperable Sarcoma by Bacterial Toxins (the Mixed Toxins of the Streptococcus erysipelas and the Bacillus prodigiosus). *Proc R Soc Med* **3**, 1-48 (1910).
21. Starnes, C.O. Coley's toxins in perspective. *Nature* **357**, 11-12 (1992).
22. Morton, D.L. et al. BCG immunotherapy of malignant melanoma: summary of a seven-year experience. *Ann Surg* **180**, 635-643 (1974).

23. Kohler, G. & Milstein, C. Continuous cultures of fused cells secreting antibody of predefined specificity. *Nature* **256**, 495-497 (1975).
24. Murphy, K.M. Janeway's Immunobiology. (Taylor & Francis Group, 2011).
25. Baldo, B.A. in Safety of Biologics Therapy: Monoclonal Antibodies, Cytokines, Fusion Proteins, Hormones, Enzymes, Coagulation Proteins, Vaccines, Botulinum Toxins 57-140 (Springer International Publishing, Cham; 2016).
26. Urquhart, L. Top companies and drugs by sales in 2019. *Nat Rev Drug Discov* **19**, 228 (2020).
27. Morgan, D.A., Ruscetti, F.W. & Gallo, R. Selective in vitro growth of T lymphocytes from normal human bone marrows. *Science (New York, N.Y.)* **193**, 1007-1008 (1976).
28. Rosenberg, S.A. IL-2: the first effective immunotherapy for human cancer. *J Immunol* **192**, 5451-5458 (2014).
29. Pardoll, D.M. The blockade of immune checkpoints in cancer immunotherapy. *Nat Rev Cancer* **12**, 252-264 (2012).
30. Brunet, J.F. et al. A new member of the immunoglobulin superfamily--CTLA-4. *Nature* **328**, 267-270 (1987).
31. Krummel, M.F. & Allison, J.P. CD28 and CTLA-4 have opposing effects on the response of T cells to stimulation. *The Journal of experimental medicine* **182**, 459-465 (1995).
32. Hodi, F.S. et al. Improved survival with ipilimumab in patients with metastatic melanoma. *N Engl J Med* **363**, 711-723 (2010).
33. Robert, C. et al. Ipilimumab plus dacarbazine for previously untreated metastatic melanoma. *N Engl J Med* **364**, 2517-2526 (2011).
34. Mellman, I., Coukos, G. & Dranoff, G. Cancer immunotherapy comes of age. *Nature* **480**, 480-489 (2011).
35. Baumeister, S.H., Freeman, G.J., Dranoff, G. & Sharpe, A.H. Coinhibitory Pathways in Immunotherapy for Cancer. *Annu Rev Immunol* **34**, 539-573 (2016).
36. Peggs, K.S., Quezada, S.A. & Allison, J.P. Cancer immunotherapy: co-stimulatory agonists and co-inhibitory antagonists. *Clin Exp Immunol* **157**, 9-19 (2009).
37. Chen, L. & Flies, D.B. Molecular mechanisms of T cell co-stimulation and co-inhibition. *Nat Rev Immunol* **13**, 227-242 (2013).
38. Bai, R., Lv, Z., Xu, D. & Cui, J. Predictive biomarkers for cancer immunotherapy with immune checkpoint inhibitors. *Biomark Res* **8**, 34 (2020).
39. Patel, S.A. & Minn, A.J. Combination Cancer Therapy with Immune Checkpoint Blockade: Mechanisms and Strategies. *Immunity* **48**, 417-433 (2018).
40. Thakur, A., Huang, M. & Lum, L.G. Bispecific antibody based therapeutics: Strengths and challenges. *Blood Rev* **32**, 339-347 (2018).
41. Nisonoff, A. & Rivers, M.M. Recombination of a mixture of univalent antibody fragments of different specificity. *Arch Biochem Biophys* **93**, 460-462 (1961).
42. Suresh, M.R., Cuello, A.C. & Milstein, C. Advantages of bispecific hybridomas in one-step immunocytochemistry and immunoassays. *Proc Natl Acad Sci U S A* **83**, 7989-7993 (1986).
43. Labrijn, A.F., Janmaat, M.L., Reichert, J.M. & Parren, P. Bispecific antibodies: a mechanistic review of the pipeline. *Nat Rev Drug Discov* **18**, 585-608 (2019).
44. FDA Highlights of prescribing information for Blincyto (https://www.accessdata.fda.gov/drugsatfda_docs/label/2018/125557s013lbl.pdf). (2018).
45. Hollingsworth, R.E. & Jansen, K. Turning the corner on therapeutic cancer vaccines. *NPJ Vaccines* **4**, 7 (2019).

46. Sahin, U. et al. Personalized RNA mutanome vaccines mobilize poly-specific therapeutic immunity against cancer. *Nature* **547**, 222-226 (2017).
47. Ott, P.A. et al. An immunogenic personal neoantigen vaccine for patients with melanoma. *Nature* **547**, 217-221 (2017).
48. Khong, H. & Overwijk, W.W. Adjuvants for peptide-based cancer vaccines. *J Immunother Cancer* **4**, 56 (2016).
49. Kantoff, P.W. et al. Sipuleucel-T immunotherapy for castration-resistant prostate cancer. *N Engl J Med* **363**, 411-422 (2010).
50. Butterfield, L.H. et al. Adenovirus MART-1-engineered autologous dendritic cell vaccine for metastatic melanoma. *J Immunother* **31**, 294-309 (2008).
51. Kranz, L.M. et al. Systemic RNA delivery to dendritic cells exploits antiviral defence for cancer immunotherapy. *Nature* **534**, 396-401 (2016).
52. Trimble, C.L. et al. Safety, efficacy, and immunogenicity of VGX-3100, a therapeutic synthetic DNA vaccine targeting human papillomavirus 16 and 18 E6 and E7 proteins for cervical intraepithelial neoplasia 2/3: a randomised, double-blind, placebo-controlled phase 2b trial. *Lancet* **386**, 2078-2088 (2015).
53. Chiocca, E.A. & Rabkin, S.D. Oncolytic viruses and their application to cancer immunotherapy. *Cancer Immunol Res* **2**, 295-300 (2014).
54. Harrington, K., Freeman, D.J., Kelly, B., Harper, J. & Soria, J.C. Optimizing oncolytic virotherapy in cancer treatment. *Nat Rev Drug Discov* **18**, 689-706 (2019).
55. Maroun, J. et al. Designing and building oncolytic viruses. *Future Virol* **12**, 193-213 (2017).
56. Sauthoff, H. et al. Impact of E1a modifications on tumor-selective adenoviral replication and toxicity. *Mol Ther* **10**, 749-757 (2004).
57. Simpson, G.R. et al. Combination of a fusogenic glycoprotein, prodrug activation, and oncolytic herpes simplex virus for enhanced local tumor control. *Cancer research* **66**, 4835-4842 (2006).
58. Moesta, A.K. et al. Local Delivery of OncoVEX(mGM-CSF) Generates Systemic Antitumor Immune Responses Enhanced by Cytotoxic T-Lymphocyte-Associated Protein Blockade. *Clin Cancer Res* **23**, 6190-6202 (2017).
59. Bartee, M.Y., Dunlap, K.M. & Bartee, E. Tumor-Localized Secretion of Soluble PD1 Enhances Oncolytic Virotherapy. *Cancer research* **77**, 2952-2963 (2017).
60. Fajardo, C.A. et al. Oncolytic Adenoviral Delivery of an EGFR-Targeting T-cell Engager Improves Antitumor Efficacy. *Cancer research* **77**, 2052-2063 (2017).
61. Kaufman, H.L. et al. Systemic versus local responses in melanoma patients treated with talimogene laherparepvec from a multi-institutional phase II study. *J Immunother Cancer* **4**, 12 (2016).
62. Andtbacka, R.H. et al. Talimogene Laherparepvec Improves Durable Response Rate in Patients With Advanced Melanoma. *J Clin Oncol* **33**, 2780-2788 (2015).
63. Rezvani, K. Adoptive cell therapy using engineered natural killer cells. *Bone Marrow Transplant* **54**, 785-788 (2019).
64. Tay, R.E., Richardson, E.K. & Toh, H.C. Revisiting the role of CD4(+) T cells in cancer immunotherapy-new insights into old paradigms. *Cancer Gene Ther* (2020).
65. Prlic, M., Williams, M.A. & Bevan, M.J. Requirements for CD8 T-cell priming, memory generation and maintenance. *Current opinion in immunology* **19**, 315-319 (2007).
66. Gattinoni, L., Speiser, D.E., Lichterfeld, M. & Bonini, C. T memory stem cells in health and disease. *Nature medicine* **23**, 18-27 (2017).
67. Park, C.O. & Kupper, T.S. The emerging role of resident memory T cells in protective immunity and inflammatory disease. *Nature medicine* **21**, 688-697 (2015).

68. Park, S.L., Gebhardt, T. & Mackay, L.K. Tissue-Resident Memory T Cells in Cancer Immunosurveillance. *Trends Immunol* **40**, 735-747 (2019).
69. Ahmed, R., Bevan, M.J., Reiner, S.L. & Fearon, D.T. The precursors of memory: models and controversies. *Nat Rev Immunol* **9**, 662-668 (2009).
70. Liu, Q., Sun, Z. & Chen, L. Memory T cells: strategies for optimizing tumor immunotherapy. *Protein Cell* **11**, 549-564 (2020).
71. Sallusto, F. & Lanzavecchia, A. Memory in disguise. *Nature medicine* **17**, 1182-1183 (2011).
72. Lanzavecchia, A. & Sallusto, F. Progressive differentiation and selection of the fittest in the immune response. *Nat Rev Immunol* **2**, 982-987 (2002).
73. Restifo, N.P. & Gattinoni, L. Lineage relationship of effector and memory T cells. *Current opinion in immunology* **25**, 556-563 (2013).
74. Sallusto, F., Lenig, D., Forster, R., Lipp, M. & Lanzavecchia, A. Two subsets of memory T lymphocytes with distinct homing potentials and effector functions. *Nature* **401**, 708-712 (1999).
75. Gattinoni, L., Klebanoff, C.A. & Restifo, N.P. Paths to stemness: building the ultimate antitumour T cell. *Nat Rev Cancer* **12**, 671-684 (2012).
76. Voskoboinik, I., Whisstock, J.C. & Trapani, J.A. Perforin and granzymes: function, dysfunction and human pathology. *Nat Rev Immunol* **15**, 388-400 (2015).
77. Mitchison, N.A. Studies on the immunological response to foreign tumor transplants in the mouse. I. The role of lymph node cells in conferring immunity by adoptive transfer. *The Journal of experimental medicine* **102**, 157-177 (1955).
78. Mule, J.J., Shu, S., Schwarz, S.L. & Rosenberg, S.A. Adoptive immunotherapy of established pulmonary metastases with LAK cells and recombinant interleukin-2. *Science (New York, N.Y.)* **225**, 1487-1489 (1984).
79. Spiess, P.J., Yang, J.C. & Rosenberg, S.A. In vivo antitumor activity of tumor-infiltrating lymphocytes expanded in recombinant interleukin-2. *Journal of the National Cancer Institute* **79**, 1067-1075 (1987).
80. Rosenberg, S.A. et al. Use of tumor-infiltrating lymphocytes and interleukin-2 in the immunotherapy of patients with metastatic melanoma. A preliminary report. *N Engl J Med* **319**, 1676-1680 (1988).
81. Rosenberg, S.A. et al. Treatment of patients with metastatic melanoma with autologous tumor-infiltrating lymphocytes and interleukin 2. *Journal of the National Cancer Institute* **86**, 1159-1166 (1994).
82. Rosenberg, S.A. & Restifo, N.P. Adoptive cell transfer as personalized immunotherapy for human cancer. *Science (New York, N.Y.)* **348**, 62-68 (2015).
83. Dudley, M.E. et al. Cancer regression and autoimmunity in patients after clonal repopulation with antitumor lymphocytes. *Science (New York, N.Y.)* **298**, 850-854 (2002).
84. Dudley, M.E. et al. Adoptive cell therapy for patients with metastatic melanoma: evaluation of intensive myeloablative chemoradiation preparative regimens. *J Clin Oncol* **26**, 5233-5239 (2008).
85. Rosenberg, S.A. et al. Durable complete responses in heavily pretreated patients with metastatic melanoma using T-cell transfer immunotherapy. *Clin Cancer Res* **17**, 4550-4557 (2011).
86. Dafni, U. et al. Efficacy of adoptive therapy with tumor-infiltrating lymphocytes and recombinant interleukin-2 in advanced cutaneous melanoma: a systematic review and meta-analysis. *Ann Oncol* **30**, 1902-1913 (2019).

87. Dudley, M.E., Wunderlich, J.R., Shelton, T.E., Even, J. & Rosenberg, S.A. Generation of tumor-infiltrating lymphocyte cultures for use in adoptive transfer therapy for melanoma patients. *J Immunother* **26**, 332-342 (2003).
88. Lee, S. & Margolin, K. Tumor-infiltrating lymphocytes in melanoma. *Curr Oncol Rep* **14**, 468-474 (2012).
89. Radvanyi, L.G. Tumor-Infiltrating Lymphocyte Therapy: Addressing Prevailing Questions. *Cancer J* **21**, 450-464 (2015).
90. Lawrence, M.S. et al. Mutational heterogeneity in cancer and the search for new cancer-associated genes. *Nature* **499**, 214-218 (2013).
91. Wolfel, T. et al. A p16INK4a-insensitive CDK4 mutant targeted by cytolytic T lymphocytes in a human melanoma. *Science (New York, N.Y.)* **269**, 1281-1284 (1995).
92. Lu, Y.C. et al. Efficient identification of mutated cancer antigens recognized by T cells associated with durable tumor regressions. *Clin Cancer Res* **20**, 3401-3410 (2014).
93. Stevanovic, S. et al. Complete regression of metastatic cervical cancer after treatment with human papillomavirus-targeted tumor-infiltrating T cells. *J Clin Oncol* **33**, 1543-1550 (2015).
94. Tran, E. et al. Cancer immunotherapy based on mutation-specific CD4+ T cells in a patient with epithelial cancer. *Science (New York, N.Y.)* **344**, 641-645 (2014).
95. Tran, E. et al. T-Cell Transfer Therapy Targeting Mutant KRAS in Cancer. *N Engl J Med* **375**, 2255-2262 (2016).
96. Zacharakis, N. et al. Immune recognition of somatic mutations leading to complete durable regression in metastatic breast cancer. *Nature medicine* **24**, 724-730 (2018).
97. Scheper, W. et al. Low and variable tumor reactivity of the intratumoral TCR repertoire in human cancers. *Nature medicine* **25**, 89-94 (2019).
98. Thommen, D.S. & Schumacher, T.N. T Cell Dysfunction in Cancer. *Cancer Cell* **33**, 547-562 (2018).
99. Klebanoff, C.A., Gattinoni, L. & Restifo, N.P. Sorting through subsets: which T-cell populations mediate highly effective adoptive immunotherapy? *J Immunother* **35**, 651-660 (2012).
100. Gross, G., Waks, T. & Eshhar, Z. Expression of immunoglobulin-T-cell receptor chimeric molecules as functional receptors with antibody-type specificity. *Proc Natl Acad Sci U S A* **86**, 10024-10028 (1989).
101. Schuster, S.J. et al. Tisagenlecleucel in Adult Relapsed or Refractory Diffuse Large B-Cell Lymphoma. *N Engl J Med* **380**, 45-56 (2019).
102. Itzhaki, O. et al. Head-to-head comparison of in-house produced CD19 CAR-T cell in ALL and NHL patients. *J Immunother Cancer* **8** (2020).
103. Ceppi, F. et al. Lymphocyte apheresis for chimeric antigen receptor T-cell manufacturing in children and young adults with leukemia and neuroblastoma. *Transfusion* **58**, 1414-1420 (2018).
104. Hay, K.A. & Turtle, C.J. Chimeric Antigen Receptor (CAR) T Cells: Lessons Learned from Targeting of CD19 in B-Cell Malignancies. *Drugs* **77**, 237-245 (2017).
105. Park, J.H., Geyer, M.B. & Brentjens, R.J. CD19-targeted CAR T-cell therapeutics for hematologic malignancies: interpreting clinical outcomes to date. *Blood* **127**, 3312-3320 (2016).
106. Maude, S.L. et al. Tisagenlecleucel in Children and Young Adults with B-Cell Lymphoblastic Leukemia. *N Engl J Med* **378**, 439-448 (2018).
107. Neelapu, S.S. et al. Axicabtagene Ciloleucel CAR T-Cell Therapy in Refractory Large B-Cell Lymphoma. *N Engl J Med* **377**, 2531-2544 (2017).
108. Wang, M. et al. KTE-X19 CAR T-Cell Therapy in Relapsed or Refractory Mantle-Cell Lymphoma. *N Engl J Med* **382**, 1331-1342 (2020).

109. Yanez, L., Sanchez-Escamilla, M. & Perales, M.A. CAR T Cell Toxicity: Current Management and Future Directions. *Hemasphere* **3**, e186 (2019).
110. Parker, K.R. et al. Single-Cell Analyses Identify Brain Mural Cells Expressing CD19 as Potential Off-Tumor Targets for CAR-T Immunotherapies. *Cell* **183**, 126-142 e117 (2020).
111. Cartellieri, M. et al. Unicar: A Novel Modular Retargeting Platform Technology for CAR T Cells. *Blood* **126**, 5549-5549 (2015).
112. Kim, M.S. et al. Redirection of genetically engineered CAR-T cells using bifunctional small molecules. *J Am Chem Soc* **137**, 2832-2835 (2015).
113. Han, X., Wang, Y., Wei, J. & Han, W. Multi-antigen-targeted chimeric antigen receptor T cells for cancer therapy. *J Hematol Oncol* **12**, 128 (2019).
114. Johnson, L.A. et al. Gene transfer of tumor-reactive TCR confers both high avidity and tumor reactivity to nonreactive peripheral blood mononuclear cells and tumor-infiltrating lymphocytes. *J Immunol* **177**, 6548-6559 (2006).
115. Chandran, S.S. & Klebanoff, C.A. T cell receptor-based cancer immunotherapy: Emerging efficacy and pathways of resistance. *Immunol Rev* **290**, 127-147 (2019).
116. Rath, J.A. & Arber, C. Engineering Strategies to Enhance TCR-Based Adoptive T Cell Therapy. *Cells* **9** (2020).
117. Robbins, P.F. et al. A pilot trial using lymphocytes genetically engineered with an NY-ESO-1-reactive T-cell receptor: long-term follow-up and correlates with response. *Clin Cancer Res* **21**, 1019-1027 (2015).
118. Robbins, P.F. et al. Tumor regression in patients with metastatic synovial cell sarcoma and melanoma using genetically engineered lymphocytes reactive with NY-ESO-1. *J Clin Oncol* **29**, 917-924 (2011).
119. D'Angelo, S.P. et al. Antitumor Activity Associated with Prolonged Persistence of Adoptively Transferred NY-ESO-1 (c259)T Cells in Synovial Sarcoma. *Cancer Discov* **8**, 944-957 (2018).
120. Martin, M., Wei, H. & Lu, T. Targeting microenvironment in cancer therapeutics. *Oncotarget* **7**, 52575-52583 (2016).
121. Berraondo, P. et al. Cytokines in clinical cancer immunotherapy. *Br J Cancer* **120**, 6-15 (2019).
122. Belardelli, F., Ferrantini, M., Proietti, E. & Kirkwood, J.M. Interferon-alpha in tumor immunity and immunotherapy. *Cytokine Growth Factor Rev* **13**, 119-134 (2002).
123. Verhoef, C. et al. Isolated limb perfusion with melphalan and TNF-alpha in the treatment of extremity sarcoma. *Curr Treat Options Oncol* **8**, 417-427 (2007).
124. Neri, D. Antibody-Cytokine Fusions: Versatile Products for the Modulation of Anticancer Immunity. *Cancer Immunol Res* **7**, 348-354 (2019).
125. Mach, J. et al. Use of radiolabelled monoclonal anti-CEA antibodies for the detection of human carcinomas by external photoscanning and tomoscintigraphy. *Immunology today* **2 12**, 239-249 (1981).
126. Van Hal, N.L. et al. Monoclonal antibody U36, a suitable candidate for clinical immunotherapy of squamous-cell carcinoma, recognizes a CD44 isoform. *International journal of cancer* **68**, 520-527 (1996).
127. Stillebroer, A.B., Mulders, P.F., Boerman, O.C., Oyen, W.J. & Oosterwijk, E. Carbonic anhydrase IX in renal cell carcinoma: implications for prognosis, diagnosis, and therapy. *Eur Urol* **58**, 75-83 (2010).
128. Varki, N.M., Reisfeld, R.A. & Walker, L.E. Antigens associated with a human lung adenocarcinoma defined by monoclonal antibodies. *Cancer research* **44**, 681-687 (1984).

129. Feugier, P. A review of rituximab, the first anti-CD20 monoclonal antibody used in the treatment of B non-Hodgkin's lymphomas. *Future Oncol* **11**, 1327-1342 (2015).
130. Carter, P. et al. Humanization of an anti-p185HER2 antibody for human cancer therapy. *Proc Natl Acad Sci U S A* **89**, 4285-4289 (1992).
131. Mueller, B.M., Romerdahl, C.A., Gillies, S.D. & Reisfeld, R.A. Enhancement of antibody-dependent cytotoxicity with a chimeric anti-GD2 antibody. *The Journal of Immunology* **144**, 1382-1386 (1990).
132. Chen, S. et al. Pivotal study of iodine-131-labeled chimeric tumor necrosis treatment radioimmunotherapy in patients with advanced lung cancer. *J Clin Oncol* **23**, 1538-1547 (2005).
133. Schwager, K. et al. A comparative immunofluorescence analysis of three clinical-stage antibodies in head and neck cancer. *Head Neck Oncol* **3**, 25 (2011).
134. Santimaria, M. et al. Immunoscintigraphic detection of the ED-B domain of fibronectin, a marker of angiogenesis, in patients with cancer. *Clin Cancer Res* **9**, 571-579 (2003).
135. Schwager, K. et al. Preclinical characterization of DEKAVIL (F8-IL10), a novel clinical-stage immunocytokine which inhibits the progression of collagen-induced arthritis. *Arthritis Res Ther* **11**, R142 (2009).
136. Murer, P. & Neri, D. Antibody-cytokine fusion proteins: A novel class of biopharmaceuticals for the therapy of cancer and of chronic inflammation. *N Biotechnol* **52**, 42-53 (2019).
137. Kuo, T.T. & Aveson, V.G. Neonatal Fc receptor and IgG-based therapeutics. *MAbs* **3**, 422-430 (2011).
138. Ward, E.S. et al. From sorting endosomes to exocytosis: association of Rab4 and Rab11 GTPases with the Fc receptor, FcRn, during recycling. *Mol Biol Cell* **16**, 2028-2038 (2005).
139. Jain, R.K. & Baxter, L.T. Mechanisms of heterogeneous distribution of monoclonal antibodies and other macromolecules in tumors: significance of elevated interstitial pressure. *Cancer research* **48**, 7022-7032 (1988).
140. Borsi, L. et al. Selective targeting of tumoral vasculature: comparison of different formats of an antibody (L19) to the ED-B domain of fibronectin. *International journal of cancer* **102**, 75-85 (2002).
141. Wu, A.M. et al. Tumor localization of anti-CEA single-chain Fvs: improved targeting by non-covalent dimers. *Immunotechnology* **2**, 21-36 (1996).
142. Margolin, K. et al. Phase I Trial of ALT-803, A Novel Recombinant IL15 Complex, in Patients with Advanced Solid Tumors. *Clin Cancer Res* **24**, 5552-5561 (2018).
143. Genentech Investigational Therapies (https://www.genentechoncology.com/pipeline-molecules.html). (2020).
144. Aggarwal, B.B. Signalling pathways of the TNF superfamily: a double-edged sword. *Nat Rev Immunol* **3**, 745-756 (2003).
145. Burmester, G.R. et al. Long-Term Safety of Adalimumab in 29,967 Adult Patients From Global Clinical Trials Across Multiple Indications: An Updated Analysis. *Adv Ther* **37**, 364-380 (2020).
146. Urquhart, L. Top product forecasts for 2020. *Nat Rev Drug Discov* **19**, 86 (2020).
147. Cai, G. & Freeman, G.J. The CD160, BTLA, LIGHT/HVEM pathway: a bidirectional switch regulating T-cell activation. *Immunol Rev* **229**, 244-258 (2009).
148. Hsieh, S.L. & Lin, W.W. Decoy receptor 3: an endogenous immunomodulator in cancer growth and inflammatory reactions. *J Biomed Sci* **24**, 39 (2017).
149. del Rio, M.L., Schneider, P., Fernandez-Renedo, C., Perez-Simon, J.A. & Rodriguez-Barbosa, J.I. LIGHT/HVEM/LTbetaR interaction as a target for the modulation of the allogeneic immune response in transplantation. *Am J Transplant* **13**, 541-551 (2013).

150. Lu, T.T. & Browning, J.L. Role of the Lymphotoxin/LIGHT System in the Development and Maintenance of Reticular Networks and Vasculature in Lymphoid Tissues. *Frontiers in immunology* **5**, 47 (2014).
151. Ngo, V.N. et al. Lymphotoxin alpha/beta and tumor necrosis factor are required for stromal cell expression of homing chemokines in B and T cell areas of the spleen. *The Journal of experimental medicine* **189**, 403-412 (1999).
152. Lee, Y. et al. Recruitment and activation of naive T cells in the islets by lymphotoxin beta receptor-dependent tertiary lymphoid structure. *Immunity* **25**, 499-509 (2006).
153. Munoz-Erazo, L., Rhodes, J.L., Marion, V.C. & Kemp, R.A. Tertiary lymphoid structures in cancer - considerations for patient prognosis. *Cell Mol Immunol* **17**, 570-575 (2020).
154. Yu, P. et al. Priming of naive T cells inside tumors leads to eradication of established tumors. *Nature immunology* **5**, 141-149 (2004).
155. Qiao, G. et al. LIGHT Elevation Enhances Immune Eradication of Colon Cancer Metastases. *Cancer research* **77**, 1880-1891 (2017).
156. He, B. et al. Vascular targeting of LIGHT normalizes blood vessels in primary brain cancer and induces intratumoural high endothelial venules. *J Pathol* **245**, 209-221 (2018).
157. He, B. et al. Remodeling of Metastatic Vasculature Reduces Lung Colonization and Sensitizes Overt Metastases to Immunotherapy. *Cell Rep* **30**, 714-724 e715 (2020).
158. Johansson-Percival, A. et al. De novo induction of intratumoral lymphoid structures and vessel normalization enhances immunotherapy in resistant tumors. *Nature immunology* **18**, 1207-1217 (2017).
159. Yu, P. et al. Targeting the primary tumor to generate CTL for the effective eradication of spontaneous metastases. *J Immunol* **179**, 1960-1968 (2007).
160. Zou, W. et al. LIGHT delivery to tumors by mesenchymal stem cells mobilizes an effective antitumor immune response. *Cancer research* **72**, 2980-2989 (2012).
161. Loeffler, M., Le'Negrate, G., Krajewska, M. & Reed, J.C. Attenuated Salmonella engineered to produce human cytokine LIGHT inhibit tumor growth. *Proc Natl Acad Sci U S A* **104**, 12879-12883 (2007).
162. Tang, H. et al. Facilitating T Cell Infiltration in Tumor Microenvironment Overcomes Resistance to PD-L1 Blockade. *Cancer Cell* **30**, 500 (2016).
163. Bossen, C. et al. Interactions of tumor necrosis factor (TNF) and TNF receptor family members in the mouse and human. *J Biol Chem* **281**, 13964-13971 (2006).
164. del Rio, M.L., Lucas, C.L., Buhler, L., Rayat, G. & Rodriguez-Barbosa, J.I. HVEM/LIGHT/BTLA/CD160 cosignaling pathways as targets for immune regulation. *J Leukoc Biol* **87**, 223-235 (2010).
165. D'Aloia, M.M., Zizzari, I.G., Sacchetti, B., Pierelli, L. & Alimandi, M. CAR-T cells: the long and winding road to solid tumors. *Cell Death Dis* **9**, 282 (2018).
166. Lundh, S., Maji, S. & Melenhorst, J.J. Next-generation CAR T cells to overcome current drawbacks. *Int J Hematol* (2020).
167. Wu, R. et al. Adoptive T-cell therapy using autologous tumor-infiltrating lymphocytes for metastatic melanoma: current status and future outlook. *Cancer J* **18**, 160-175 (2012).
168. Park, Y.J., Kuen, D.S. & Chung, Y. Future prospects of immune checkpoint blockade in cancer: from response prediction to overcoming resistance. *Exp Mol Med* **50**, 109 (2018).
169. Herbst, R.S. et al. Predictive correlates of response to the anti-PD-L1 antibody MPDL3280A in cancer patients. *Nature* **515**, 563-567 (2014).

170. Skeate, J.G. et al. TNFSF14: LIGHTing the Way for Effective Cancer Immunotherapy. *Frontiers in immunology* **11**, 922 (2020).
171. Hutmacher, C., Gonzalo Nunez, N., Liuzzi, A.R., Becher, B. & Neri, D. Targeted Delivery of IL2 to the Tumor Stroma Potentiates the Action of Immune Checkpoint Inhibitors by Preferential Activation of NK and CD8(+) T Cells. *Cancer Immunol Res* **7**, 572-583 (2019).
172. Hemmerle, T. et al. The antibody-based targeted delivery of TNF in combination with doxorubicin eradicates sarcomas in mice and confers protective immunity. *Br J Cancer* **109**, 1206-1213 (2013).
173. Halin, C. et al. Enhancement of the antitumor activity of interleukin-12 by targeted delivery to neovasculature. *Nat Biotechnol* **20**, 264-269 (2002).
174. Probst, P. et al. Sarcoma Eradication by Doxorubicin and Targeted TNF Relies upon CD8(+) T-cell Recognition of a Retroviral Antigen. *Cancer research* **77**, 3644-3654 (2017).
175. Puca, E. et al. The antibody-based delivery of interleukin-12 to solid tumors boosts NK and CD8(+) T cell activity and synergizes with immune checkpoint inhibitors. *International journal of cancer* **146**, 2518-2530 (2020).
176. Huang, A.Y. et al. The immunodominant major histocompatibility complex class I-restricted antigen of a murine colon tumor derives from an endogenous retroviral gene product. *Proc Natl Acad Sci U S A* **93**, 9730-9735 (1996).
177. Probst, P., Stringhini, M., Ritz, D., Fugmann, T. & Neri, D. Antibody-based Delivery of TNF to the Tumor Neovasculature Potentiates the Therapeutic Activity of a Peptide Anticancer Vaccine. *Clin Cancer Res* **25**, 698-709 (2019).
178. Schachter, J. et al. Pembrolizumab versus ipilimumab for advanced melanoma: final overall survival results of a multicentre, randomised, open-label phase 3 study (KEYNOTE-006). *The Lancet* **390**, 1853-1862 (2017).
179. Fyfe, G. et al. Results of treatment of 255 patients with metastatic renal cell carcinoma who received high-dose recombinant interleukin-2 therapy. *J Clin Oncol* **13**, 688-696 (1995).
180. Atkins, M.B. et al. High-dose recombinant interleukin 2 therapy for patients with metastatic melanoma: analysis of 270 patients treated between 1985 and 1993. *J Clin Oncol* **17**, 2105-2116 (1999).
181. Reading, J.L. et al. The function and dysfunction of memory CD8(+) T cells in tumor immunity. *Immunol Rev* **283**, 194-212 (2018).
182. Schumacher, T.N. & Schreiber, R.D. Neoantigens in cancer immunotherapy. *Science* **348**, 69-74 (2015).
183. Van Allen, E.M. et al. Genomic correlates of response to CTLA-4 blockade in metastatic melanoma. *Science* **350**, 207-211 (2015).
184. Laumont, C.M. et al. Noncoding regions are the main source of targetable tumor-specific antigens. *Sci Transl Med* **10** (2018).
185. Jenkins, N.A., Copeland, N.G., Taylor, B.A. & Lee, B.K. Organization, distribution, and stability of endogenous ecotropic murine leukemia virus DNA sequences in chromosomes of Mus musculus. *Journal of Virology* **43**, 26-36 (1982).
186. Huang, A.Y. et al. The immunodominant major histocompatibility complex class I-restricted antigen of a murine colon tumor derives from an endogenous retroviral gene product. *Proceedings of the National Academy of Sciences, USA* **93**, 9730-9735 (1996).
187. Miller, C.T., Graham, L.J. & Bear, H.D. Adoptive immunotherapy (AIT) of established tumors with tumor antigen peptide-sensitized T cells. *Cancer Research* **64**, 1264-1264 (2004).

188. Rudqvist, N.P. et al. Radiotherapy and CTLA-4 Blockade Shape the TCR Repertoire of Tumor-Infiltrating T Cells. *Cancer Immunol Res* **6**, 139-150 (2018).
189. Villa, A. et al. A high-affinity human monoclonal antibody specific to the alternatively spliced EDA domain of fibronectin efficiently targets tumor neo-vasculature in vivo. *International journal of cancer* **122**, 2405-2413 (2008).
190. Tarli, L. et al. A high-affinity human antibody that targets tumoral blood vessels. *Blood* **94**, 192-198 (1999).
191. Pasche, N. & Neri, D. Immunocytokines: a novel class of potent armed antibodies. *Drug Discov Today* **17**, 583-590 (2012).
192. Murphy, K. & Weaver, C. Janeway's immunobiology, Edn. 9th edition. (Garland Science/Taylor & Francis Group, LLC, New York, NY; 2016).
193. Probst, P., Stringhini, M., Ritz, D., Fugmann, T. & Neri, D. Antibody-based Delivery of TNF to the Tumor Neovasculature Potentiates the Therapeutic Activity of a Peptide Anticancer Vaccine. *Clinical Cancer Research* **25**, 698-709 (2019).
194. Pesu, M., Muul, L., Kanno, Y. & O'Shea, J.J. Proprotein convertase furin is preferentially expressed in T helper 1 cells and regulates interferon gamma. *Blood* **108**, 983-985 (2006).
195. Murray, T. et al. Very Late Antigen-1 Marks Functional Tumor-Resident CD8 T Cells and Correlates with Survival of Melanoma Patients. *Frontiers in immunology* **7**, 573 (2016).
196. Yang, Y. Cancer immunotherapy: harnessing the immune system to battle cancer. *J Clin Invest* **125**, 3335-3337 (2015).
197. Garon, E.B. et al. Pembrolizumab for the treatment of non-small-cell lung cancer. *N Engl J Med* **372**, 2018-2028 (2015).
198. Ansell, S.M. et al. PD-1 blockade with nivolumab in relapsed or refractory Hodgkin's lymphoma. *N Engl J Med* **372**, 311-319 (2015).
199. Golomb, H.M. et al. Alpha-2 interferon therapy of hairy-cell leukemia: a multicenter study of 64 patients. *J Clin Oncol* **4**, 900-905 (1986).
200. Solal-Celigny, P. et al. Recombinant interferon alfa-2b combined with a regimen containing doxorubicin in patients with advanced follicular lymphoma. Groupe d'Etude des Lymphomes de l'Adulte. *N Engl J Med* **329**, 1608-1614 (1993).
201. Neri, D. & Sondel, P.M. Immunocytokines for cancer treatment: past, present and future. *Current opinion in immunology* **40**, 96-102 (2016).
202. Amsen, D., van Gisbergen, K., Hombrink, P. & van Lier, R.A.W. Tissue-resident memory T cells at the center of immunity to solid tumors. *Nature immunology* **19**, 538-546 (2018).
203. Hemmerle, T. & Neri, D. The antibody-based targeted delivery of interleukin-4 and 12 to the tumor neovasculature eradicates tumors in three mouse models of cancer. *International journal of cancer* **134**, 467-477 (2014).
204. Tzeng, A., Kwan, B.H., Opel, C.F., Navaratna, T. & Wittrup, K.D. Antigen specificity can be irrelevant to immunocytokine efficacy and biodistribution. *Proc Natl Acad Sci U S A* **112**, 3320-3325 (2015).
205. Carnemolla, B. et al. Enhancement of the antitumor properties of interleukin-2 by its targeted delivery to the tumor blood vessel extracellular matrix. *Blood* **99**, 1659-1665 (2002).
206. Lode, H.N. et al. Tumor-targeted IL-2 amplifies T cell-mediated immune response induced by gene therapy with single-chain IL-12. *Proc Natl Acad Sci U S A* **96**, 8591-8596 (1999).
207. Yoo, E.M. et al. Anti-CD138-targeted interferon is a potent therapeutic against multiple myeloma. *J Interferon Cytokine Res* **35**, 281-291 (2015).

208. Zhang, N. et al. Targeted and untargeted CD137L fusion proteins for the immunotherapy of experimental solid tumors. *Clin Cancer Res* **13**, 2758-2767 (2007).
209. Tamada, K. et al. LIGHT, a TNF-like molecule, costimulates T cell proliferation and is required for dendritic cell-mediated allogeneic T cell response. *J Immunol* **164**, 4105-4110 (2000).
210. Mauri, D.N. et al. LIGHT, a new member of the TNF superfamily, and lymphotoxin alpha are ligands for herpesvirus entry mediator. *Immunity* **8**, 21-30 (1998).
211. Hemmerle, T., Hess, C., Venetz, D. & Neri, D. Tumor targeting properties of antibody fusion proteins based on different members of the murine tumor necrosis superfamily. *Journal of biotechnology* **172**, 73-76 (2014).
212. Fellermeier, S. et al. Advancing targeted co-stimulation with antibody-fusion proteins by introducing TNF superfamily members in a single-chain format. *Oncoimmunology* **5**, e1238540 (2016).
213. Richards, D.M. et al. HERA-GITRL activates T cells and promotes anti-tumor efficacy independent of FcgammaR-binding functionality. *J Immunother Cancer* **7**, 191 (2019).
214. Venetz, D., Hess, C., Lin, C.W., Aebi, M. & Neri, D. Glycosylation profiles determine extravasation and disease-targeting properties of armed antibodies. *Proc Natl Acad Sci U S A* **112**, 2000-2005 (2015).
215. Muthing, J. et al. Effects of buffering conditions and culture pH on production rates and glycosylation of clinical phase I anti-melanoma mouse IgG3 monoclonal antibody R24. *Biotechnol Bioeng* **83**, 321-334 (2003).
216. Lechner, M.G. et al. Immunogenicity of murine solid tumor models as a defining feature of in vivo behavior and response to immunotherapy. *J Immunother* **36**, 477-489 (2013).
217. Mosely, S.I. et al. Rational Selection of Syngeneic Preclinical Tumor Models for Immunotherapeutic Drug Discovery. *Cancer Immunol Res* **5**, 29-41 (2017).
218. Tang, H. et al. Facilitating T Cell Infiltration in Tumor Microenvironment Overcomes Resistance to PD-L1 Blockade. *Cancer Cell* **29**, 285-296 (2016).
219. Fan, Z. et al. NK-cell activation by LIGHT triggers tumor-specific CD8+ T-cell immunity to reject established tumors. *Blood* **107**, 1342-1351 (2006).
220. Hutt, M. et al. Targeting scFv-Fc-scTRAIL fusion proteins to tumor cells. *Oncotarget* **9**, 11322-11335 (2018).
221. Pasche, N., Wulhfard, S., Pretto, F., Carugati, E. & Neri, D. The antibody-based delivery of interleukin-12 to the tumor neovasculature eradicates murine models of cancer in combination with paclitaxel. *Clin Cancer Res* **18**, 4092-4103 (2012).
222. Kaspar, M., Trachsel, E. & Neri, D. The antibody-mediated targeted delivery of interleukin-15 and GM-CSF to the tumor neovasculature inhibits tumor growth and metastasis. *Cancer research* **67**, 4940-4948 (2007).
223. Rybak, J.N., Roesli, C., Kaspar, M., Villa, A. & Neri, D. The extra-domain A of fibronectin is a vascular marker of solid tumors and metastases. *Cancer research* **67**, 10948-10957 (2007).
224. Schliemann, C. et al. Three clinical-stage tumor targeting antibodies reveal differential expression of oncofetal fibronectin and tenascin-C isoforms in human lymphoma. *Leuk Res* **33**, 1718-1722 (2009).
225. Rohaan, M.W., Wilgenhof, S. & Haanen, J. Adoptive cellular therapies: the current landscape. *Virchows Arch* **474**, 449-461 (2019).
226. Li, D. et al. Genetically engineered T cells for cancer immunotherapy. *Signal Transduct Target Ther* **4**, 35 (2019).
227. Yu, S., Yi, M., Qin, S. & Wu, K. Next generation chimeric antigen receptor T cells: safety strategies to overcome toxicity. *Mol Cancer* **18**, 125 (2019).

228. Dersh, D., Holly, J. & Yewdell, J.W. A few good peptides: MHC class I-based cancer immunosurveillance and immunoevasion. *Nat Rev Immunol* (2020).
229. Rohaan, M.W., van den Berg, J.H., Kvistborg, P. & Haanen, J. Adoptive transfer of tumor-infiltrating lymphocytes in melanoma: a viable treatment option. *J Immunother Cancer* **6**, 102 (2018).
230. Hanson, H.L. et al. Eradication of established tumors by CD8+ T cell adoptive immunotherapy. *Immunity* **13**, 265-276 (2000).
231. Leisegang, M. et al. Eradication of Large Solid Tumors by Gene Therapy with a T-Cell Receptor Targeting a Single Cancer-Specific Point Mutation. *Clin Cancer Res* **22**, 2734-2743 (2016).
232. Hanada, K.I., Yu, Z., Chappell, G.R., Park, A.S. & Restifo, N.P. An effective mouse model for adoptive cancer immunotherapy targeting neoantigens. *JCI Insight* **4** (2019).
233. Stringhini, M., Probst, P. & Neri, D. Immunotherapy of CT26 murine tumors is characterized by an oligoclonal response of tissue-resident memory T cells against the AH1 rejection antigen. *European journal of immunology* (2020).
234. Bouet-Toussaint, F. et al. Interleukin-2 expanded lymphocytes from lymph node and tumor biopsies of human renal cell carcinoma, breast and ovarian cancer. *Eur Cytokine Netw* **11**, 217-224 (2000).
235. Teague, R.M. et al. Interleukin-15 rescues tolerant CD8+ T cells for use in adoptive immunotherapy of established tumors. *Nature medicine* **12**, 335-341 (2006).
236. Muranski, P. et al. Increased intensity lymphodepletion and adoptive immunotherapy--how far can we go? *Nat Clin Pract Oncol* **3**, 668-681 (2006).
237. Lai, J.Z., Zhu, Y.Y., Ruan, M., Chen, L. & Zhang, Q.Y. Local Irradiation Sensitized Tumors to Adoptive T Cell Therapy via Enhancing the Cross-Priming, Homing, and Cytotoxicity of Antigen-Specific CD8 T Cells. *Frontiers in immunology* **10**, 2857 (2019).
238. Fisher, B. et al. Tumor localization of adoptively transferred indium-111 labeled tumor infiltrating lymphocytes in patients with metastatic melanoma. *J Clin Oncol* **7**, 250-261 (1989).
239. Youniss, F.M. et al. Near-infrared imaging of adoptive immune cell therapy in breast cancer model using cell membrane labeling. *PLoS One* **9**, e109162 (2014).
240. Slaney, C.Y., Kershaw, M.H. & Darcy, P.K. Trafficking of T cells into tumors. *Cancer research* **74**, 7168-7174 (2014).
241. Gattinoni, L. et al. Wnt signaling arrests effector T cell differentiation and generates CD8+ memory stem cells. *Nature medicine* **15**, 808-813 (2009).
242. Gurusamy, D. et al. Multi-phenotype CRISPR-Cas9 Screen Identifies p38 Kinase as a Target for Adoptive Immunotherapies. *Cancer Cell* **37**, 818-833 e819 (2020).
243. Kondo, T. et al. Notch-mediated conversion of activated T cells into stem cell memory-like T cells for adoptive immunotherapy. *Nat Commun* **8**, 15338 (2017).
244. Matsui, K., O'Mara, L.A. & Allen, P.M. Successful elimination of large established tumors and avoidance of antigen-loss variants by aggressive adoptive T cell immunotherapy. *Int Immunol* **15**, 797-805 (2003).
245. Crompton, J.G., Sukumar, M. & Restifo, N.P. Uncoupling T-cell expansion from effector differentiation in cell-based immunotherapy. *Immunol Rev* **257**, 264-276 (2014).
246. Pilipow, K. et al. Antioxidant metabolism regulates CD8+ T memory stem cell formation and antitumor immunity. *JCI Insight* **3** (2018).
247. Scrimieri, F. et al. Murine leukemia virus envelope gp70 is a shared biomarker for the high-sensitivity quantification of murine tumor burden. *Oncoimmunology* **2**, e26889 (2013).

248. Attermann, A.S., Bjerregaard, A.M., Saini, S.K., Gronbaek, K. & Hadrup, S.R. Human endogenous retroviruses and their implication for immunotherapeutics of cancer. *Ann Oncol* **29**, 2183-2191 (2018).
249. Zhao, Q. et al. Proteogenomics Uncovers a Vast Repertoire of Shared Tumor-Specific Antigens in Ovarian Cancer. *Cancer Immunol Res* **8**, 544-555 (2020).
250. Morishige, T. et al. Creation of a LIGHT mutant with the capacity to evade the decoy receptor for cancer therapy. *Biomaterials* **31**, 3357-3363 (2010).
251. Rosenberg, S.A. (22nd Annual Meeting, American Society of Gene & Cell Therapy, Washington D.C.; 2019).
252. Dash, P. et al. Paired analysis of TCRα and TCRβ chains at the single-cell level in mice. *The Journal of Clinical Investigation* **121**, 288-295 (2011).
253. Picelli, S. et al. Full-length RNA-seq from single cells using Smart-seq2. *Nat Protoc* **9**, 171-181 (2014).
254. Probst, P. et al. Sarcoma Eradication by Doxorubicin and Targeted TNF Relies upon CD8+ T-cell Recognition of a Retroviral Antigen. *Cancer Research* **77**, 3644-3654 (2017).
255. Kitaura, K., Shini, T., Matsutani, T. & Suzuki, R. A new high-throughput sequencing method for determining diversity and similarity of T cell receptor (TCR) α and β repertoires and identifying potential new invariant TCR α chains. *BMC Immunology* **17**, 38 (2016).
256. Bolger, A.M., Lohse, M. & Usadel, B. Trimmomatic: a flexible trimmer for Illumina sequence data. *Bioinformatics* **30**, 2114-2120 (2014).
257. Bray, N.L., Pimentel, H., Melsted, P. & Pachter, L. Near-optimal probabilistic RNA-seq quantification. *Nat Biotechnol* **34**, 525-527 (2016).
258. Dobin, A. et al. STAR: ultrafast universal RNA-seq aligner. *Bioinformatics* **29**, 15-21 (2013).
259. Robinson, M.D., McCarthy, D.J. & Smyth, G.K. edgeR: a Bioconductor package for differential expression analysis of digital gene expression data. *Bioinformatics* **26**, 139-140 (2010).
260. Putelli, A., Kiefer, J.D., Zadory, M., Matasci, M. & Neri, D. A fibrin-specific monoclonal antibody from a designed phage display library inhibits clot formation and localizes to tumors in vivo. *J Mol Biol* **426**, 3606-3618 (2014).
261. Pasche, N. et al. Cloning and characterization of novel tumor-targeting immunocytokines based on murine IL7. *Journal of biotechnology* **154**, 84-92 (2011).
262. Rajendra, Y., Kiseljak, D., Baldi, L., Hacker, D.L. & Wurm, F.M. A simple high-yielding process for transient gene expression in CHO cells. *Journal of biotechnology* **153**, 22-26 (2011).
263. Zhang, M.C., Liu, H.P., Demchik, L.L., Zhai, Y.F. & Yang, D.J. LIGHT sensitizes IFN-gamma-mediated apoptosis of HT-29 human carcinoma cells through both death receptor and mitochondria pathways. *Cell Res* **14**, 117-124 (2004).
264. Schmidt, J. et al. Reversible major histocompatibility complex I-peptide multimers containing Ni(2+)-nitrilotriacetic acid peptides and histidine tags improve analysis and sorting of CD8(+) T cells. *J Biol Chem* **286**, 41723-41735 (2011).